Project #24

DOE/BETC/2215–1
Distribution Category UC-92a

METHODS FOR DETERMINING VENTED VOLUMES DURING GAS WELL BLOWOUTS

By

Murray F. Hawkins, Jr., *Principal Investigator*
Zaki Bassiouni
William J. Bernard
Adam T. Bourgoyne
Michael J. Veazey
Walter R. Whitehead

Coastal Petroleum Associates, Inc.
P.O. Drawer 16450-B
Baton Rouge, Louisiana 70893
504/769-1321

C. Ray Williams, *Technical Project Officer*
U.S. Department of Energy
Bartlesville Energy Technology Center
P.O. Box 1398
Bartlesville, Oklahoma 74003
918/336-2400, Ext. 359

Prepared for the U.S. Department of Energy
Under P.O. No. P-B-9-2215 and
Funded by USGS/OCS Oil and Gas Operations

Date Submitted–July 1980
Date Published–October 1980

U.S. DEPARTMENT OF ENERGY

FOREWORD

When hydrocarbons are lost from a well during a blowout, methods for estimating the lost volumes are often needed by both industry and government. This publication provides the currently accepted calculation methods for gas blowouts and proposes some methods which need further definition.

This work was funded by the Research and Development Program for Outer Continental Shelf Oil and Gas Operations of the U.S. Geological Survey in cooperation with Bartlesville Energy Technology Center (BETC) of the U.S. Department of Energy. BETC provided contracting, monitoring and technology transfer through its Drilling Technology Program.

A similar work effort is being performed by the same contractor to assess the technology for estimating liquid hydrocarbon volumes lost during blowouts.

John B. Gregory
Research Program Manager
OCS Oil and Gas Operations
U.S.G.S., Reston, VA

C. Ray Williams
Project Manager
Drilling and Offshore Technology
Bartlesville Energy Technology Center
U. S. Department of Energy
Bartlesville, OK

ABSTRACT

Several methods are presented for determining vented volumes during gas well blowouts. The methods described apply to gas production in which no liquids phase(s), hydrocarbon and/or water, are present in the gas. Each method is illustrated with a numerical example. Sensitivity analyses provide estimates of probable errors. The method of crossplotting formation and flow string resistances is the only one which does not require special measurements. It is therefore applicable to cratered wells and underwater blowouts. The report includes several suggestions for investigations which might lead to better methods.

CONTENTS

SECTION 1
INDUSTRY SURVEY

1.1 Introduction

A survey of several major oil companies, independents and companies which service the petroleum industry reveals no standard method for estimating amounts of gas lost during blowouts. Discussions during the survey made it apparent that, owing to the varied conditions of blowouts, there can not be a standard method. The methods reported in current use can be broadly categorized as:

1.2 Guesstimates
1.3 Engineering Calculations
1.4 Direct Measurements
1.5 Extrapolations

Each of these methods has its advantages and limitations. They are briefly described in this section and treated in detail in other sections of this report.

1.2 Guesstimates

The widest margin of error probably occurs with techniques based mainly on intuition or experience, assisted only by crude measurements with no associated calculations which are usually influenced consciously or unconsciously by parameters such as height of the flame, noise level, deflection of a sledge hammer handle placed in the gas flow stream, etc. These are classified as guesstimates. The purpose of guesstimates is usually to establish an order of magnitude and not to provide precise values for engineering or economic determinations. They are used primarily to size equipment to be used in bringing the well under control and are certainly subject to considerable error.

The technique, which is highly individualized and in some cases surprisingly accurate, depends mainly on the experience and background of the guesser. In times past when flaring was more prevalent and regulations more lax, many people developed a good intuitive feeling for blowout flow rates by comparison with past jets or flares of reasonably well known rates. However, the passing of time and the scarcity of intentional flaring has diminished this intuitive feeling substantially within the industry. Although it is conceivable that they exist, no calibration curves relating vented volume with such things as flare height, noise level, heat intensity or hammer handle deflection were uncovered in

the literature or during the industry survey.

Depending on circumstances, surface conditions, personal danger, and the ability to position measuring equipment into the flow stream, a guesstimate may be the only approach to obtain vented volumes. However, under certain conditions, more accurate estimates may be made. The details of some of these techniques outlined below are further discussed in other sections of this report.

1.3 Engineering Calculations

If certain data are available or can be reasonably estimated, fluid flow calculations can bracket the vented flow rates between maximum and minimum values. Of course, where more is known about the several parameters, particularly the more sensitive ones, the bracket range is reduced.

For the reservoir, the more important data include static reservoir pressure, productive stratum thickness, permeability, gas viscosity and reservoir temperature. For the flow string, the more important data include the geometry of the well bore flow path, e.g., through drill pipe or through the annulus, depth, gas specific gravity, reservoir temperature, and surface well head pressure. From these and other data it is possible to calculate separately the pressure losses in the formation (Section 7) and in the flow string (Section 8). A simultaneous consideration of these yields a value of the uncertainties in the several variables and the manner in which they enter into the calculations provides a measure of the uncertainty in the estimated flow rate.

In some cases, where there is an appreciable decline in reservoir pressure during the blowout, the material balance method can be used to estimate the volume of vented gas. The use and limitations of this method are presented in Section 2.

1.4 Direct Measurement

The most accurate technique of estimating vented gas is that of making measurements of the gas flow rate during the blowout. There are however, several obvious limitations. First, it is necessary to have the proper surface facilities to allow measurements to be made, i.e., diverter line and pressure taps; and a reasonably safe condition must exist to allow personnel to make the measurements. In many cases the choke lines, diverter lines and other surface facilities are destroyed

or rendered unusable by the blowout or a subsequent fire and measurements are impossible. In many of the remaining cases, it is just too dangerous to approach the well to make the necessary measurements.

In the Arkoma Basin, where wells are commonly drilled with air, many prolific gas zones are drilled into with no mud in the hole thereby creating a condition of uncontrolled blowout for some period until the well is filled with mud. It is standard practice there to gauge the gas being vented by placing a Pitot tube in the flow stream for higher flow rate wells and by using a portable orifice tester for the lower rate wells. A discussion of the pitot tube and other direct measurement techniques is included in Sections 3 and 4.

1.5 Extrapolations

In some cases, the blowout is partially contained and emergency gas sales are made while steps are taken to bring the well completely under control. It usually takes considerable time to accomplish this during which a reasonable decline curve may be established. This decline curve may be extrapolated back to the initial time of the blowout to approximate initial flow rate. The amount of gas lost is then mathematically estimated by formulas such as:

$$Q = \frac{q_i - q_t}{a} \qquad (1.1)$$

where:

Q = gas volume produced between q_i and q_t, SCF
q_i = initial gas flow rate, SCF/day
q_t = gas flow rate at time t, SCF/day
a = decline factor, t^{-1}, $days^{-1}$

The extrapolation method will be discussed in more detail in Section 5 and followed by a discussion of limitations and error ranges.

SECTION 2
MATERIAL BALANCE METHODS

2.1 Introduction

For gas blowouts in which there is an appreciable drop in reservoir pressure during the blowout, the material balance method can in some instances be used to estimate the volume of vented gas. The pressure drop during the blowout should be a minimum of about five per cent of the initial pressure. Also, use of the material balance method is generally, but not exclusively, limited to volumetric gas reservoirs, i.e., those without water drive.

The principle underlying the material balance method for gas reservoirs is quite simple. For ideal gas behavior and reservoirs with no pressure support mechanizms, e.g., water influx, the fraction of the reservoir gas produced and/or lost during a blowout is equal to the fractional loss in reservoir pressure. In its application, however, there are a number of complex aspects which should be carefully considered. Where the gas in place at start of blowout is determined by the volumetric method, consideration should be given to the accuracy of the several data required.

2.2 Theory and Formulas

Application of the material balance method to determine vented gas requires first a determination of the reservoir gas in place at the start of blowout. Where there is sufficient pressure production history for the reservoir, the material balance method may be used. The following formula, Eq. (1.30) of Ref. 2.1 is a form of the material balance for gas reservoirs which have no water influx and from which no formation water is produced.

$$\frac{p_{sc} G_p}{T_{sc}} = \frac{p_i V}{z_i T_r} - \frac{p_f V}{z_f T_r} \qquad (2.1)$$

in which

p_{sc} & T_{sc} = standard temperature and pressure, degrees Rankine and psia.
G_p = standard cubic feet of gas produced during reservoir pressure drop $(p_i - p_f)$.
p_i, p_f = initial and final average reservoir pressures, psia.

T_r = reservoir temperature, degrees Rankine.
z_i, z_f = gas deviation factors at temperature T_r and pressures p_i and p_f, dimensionless.
V = reservoir hydrocarbon pore volume HCPV, cubic feet.

The hydrocarbon pore volume can also be determined by the volumetric method where the necessary data are available. The following formula applies.

$$V = 43{,}560 \times V_b \times \phi \times (1-S_w) \qquad (2.2)$$

where V = hydrocarbon pore volume, cubic feet
V_b = reservoir bulk volume, acre-feet.
ϕ = average reservoir porosity, fraction of pore volume.
S_w = average connate water saturation, fraction of pore volume.

Once the hydrocarbon pore volume has been obtained by either method, the gas in place at any pressure can be found using the following formula:

$$G = V \times \frac{p \times T_{sc}}{z \times T_r \times p_{sc}} \qquad (2.3)$$

where G = standard cubic feet, SCF of gas in the reservoir at pressure p
V = hydrocarbon pore volume, cubic feet
p = average reservoir pressure, psia
T = reservoir temperature, degrees Rankine
z = gas deviation factor at p and T_r.
T_{sc}, p_{sc} = standard temperature and pressure, degrees Rankine and psia.

Finally, then, the vented gas volume is calculated as the difference between the gas in place G_i at start of blowout when reservoir pressure was p_i, and the gas in place G_f at end of blowout when pressure is p_f, less any produced gas G_p by other wells during the blowout, or,

$$G_p(\text{blowout}) = G_i - G_f - G_p \qquad (2.4)$$

2.3 Example Using the Material Balance Method

To illustrate the use of the material balance method, example 2.1 considers a gas reservoir with no water drive in which the discovery well Smith No. 1 had been producing long enough prior to the blowout in Smith No. 2 so that the material balance method could

be used to determine the reservoir's hydrocarbon pore volume, using Eq. (2.1). Data were also available to make an independent determination of the hydrocarbon pore volume using Eq. (2.2). Using both of these determinations, the volumes of vented gas during the 61 day blowout in Smith No. 2 are calculated, making allowance for the continued production from Smith No. 1 during the blowout.

Example 2.1

Data

9,000 psia----------Initial reservoir pressure, measured in Smith No. 1 producing well
8,000 psia----------Reservoir pressure at start of blowout, based on pressure history of Smith No. 1
7,400 psia----------Reservoir pressure at end of blowout, measured in Smith No. 1
240°F---------------700°R, reservoir temperature
1.29 @ 9,000 psia
1.23 @ 8,000 psia---Gas deviation factors at 240°F
1.19 @ 7,400 psia
14.7 psia & 60°F----Standard Conditions used
12×10^9 SCF----------Smith No. 1 production to start of blowout
61 days-------------Duration of blowout
720×10^9 SCF---------Smith No. 1 production during blowout
Zero----------------Smith No. 1 formation water production
Zero----------------Estimated reservoir water influx
76,700 acre-feet----Bulk reservoir volume, isopach map
25 per cent---------Average porosity
30 per cent---------Average connate water
13,000 feet---------Reservoir depth
12.1 lb/gal---------Mud weight in Smith No. 2 at time of blowout

Calculations

A-1 Hydrocarbon pore volume (HCPV) calculated by material balance using Smith No. 1 data, using Eq. (2.1):

$$\frac{14.7 \times 12 \times 10^9}{520} = \frac{9{,}000\ V_{HCPV}}{1.29 \times 700} - \frac{8{,}000\ V_{HCPV}}{1.23 \times 700}$$

$$V_{HCPV} = \underline{0.503 \times 10^9 ft^3}$$

A-2 Gas in place at start of blowout (t=0).
Using Eq. (2.3):

$$G(t=0) = 0.503\times10^{9}\times\frac{8,000\times520}{1.23\times700\times14.7}$$

$$= \underline{165.3\times10^{9}\text{SCF}}$$

A-3 Gas in place at end of blowout (t=61 days)
Using Eq. (2.3):

$$G(t=61) = 0.503\times10^{9}\times\frac{7,400\times520}{1.19\times700\times14.7}$$

$$= \underline{158.1\times10^{9}\text{SCF}}$$

A-4 Vented blowout gas from Smith No. 2 using Eq. (2.4):

$$G_p(\text{blowout}) = G(t=0) - G(t=61) - G_p(\text{Smith No. 1})$$

$$= 165.3\times10^{9} - 158.1\times10^{9} - 0.720\times10^{9}$$

$$= \underline{6.48\times10^{9}\text{SCF}}$$

A-5 Average Smith No. 2 blowout rate

$$q_{sc} = \frac{6.48\times10^{9}\text{SCF}}{61\text{ days}} = \underline{106\text{ MMSCF/D}}$$

B-1 HCPV by Volumetric Method, using Eq. (2.2):

$$V_{HCPV} = 43,560\times A(\text{ac-ft})\times\phi\times(1-S_w)$$

$$= 43,560\times76,700\times0.25\times(1-0.30)$$

$$= \underline{0.584\times10^{9}\text{ft}}$$

B-2 Gas in place at start of blowout (t=0)
Using Eq. (2.3):

$$G(t=0) = 0.584\times10^{9}\times\frac{8,000\times520}{1.23\times700\times14.7}$$

$$= \underline{191.9\times10^{9}\text{SCF}}$$

B-3 Gas in place at end of blowout (t=61 days)
Using Eq. (2.3):

$$G(t=61) = 0.584\times10^{9}\times\frac{7,400\times520}{1.19\times700\times14.7}$$

$$= \underline{183.6\times10^{9}\text{SCF}}$$

B-4 Vented blowout gas from Smith No. 2

$$G_p(\text{blowout}) = G(t=0) - G(t=61) - G_p(\text{Smith No. 1})$$

$$= 191.9\times10^{9}-183.6\times10^{9}-0.720\times10^{9}$$

$$= \underline{7.58\times10^{9}\text{SCF}}$$

B-5 Average Smith No. 2 blowout rate

$$q_{sc} = \frac{7.58\times10^{9}}{61 \text{ days}} = \underline{124 \text{ MMSCF/D}}$$

C-1 Reservoir pressure at start of blowout calculated from Smith No. 2 mud weight

$$p = 0.052(\text{psi/ft/ppg})\times W(\text{ppg})\times D(\text{feet})$$

$$= 0.052\times12.1\times13,000$$

$$= 8180 \text{ psia}$$

2.4 Critique of the Example and the Method

If the pressure production data from Smith No. 1 had been inadequate for using a material balance, or if Smith No. 2 had been the discovery and blowout well, the material balance method could not have been used to determine the hydrocarbon pore volume. It could only be determined if adequate data for the volumetric method, Eq. (2.2), were available. In the absence of pressure data from Smith No. 1 and/or if Smith No. 2 had been the discovery well, reservoir pressure at start of blowout could only be inferred from the mud weight (density) and depth as in Part C-1 of Example 2.1. A pressure at the end of the blowout would also be needed.

Pressures obtained from mud weight and depth are subject to considerable error. The reservoir pressure may be higher or lower than that calculated from the mud weight and depth. If the blowout occurs during

drilling, then the reservoir pressure is greater than the sum of the hydrostatic mud column pressure and the annular friction loss. Where blowouts occur during tripping operations, the reservoir pressure is less than the hydrostatic pressure of the mud column, owing to a reduction of well pressure below the bit by the swabbing action as the drill string is hoisted. Where the blowout is caused by failure to keep the hole full of mud, the reservoir pressure is lower than that calculated from mud weight and depth. In many blowouts, good values of reservoir pressures are available when the blowout preventers are closed, i.e., the sum of the surface pressure gauge reading and the pressure of the hydrostatic column of mud in the drill pipe.

The main uncertainty in determining the hydrocarbon pore volume by the material balance method, Eq. (2.1), derives from uncertainties in the pressures. From Eq. (2.1) it is seen that the hydrocarbon pore volume is inversely proportional to the difference $(p_i/z_i - p_f/z_f)$. For the example this difference is

$$\frac{9000}{1.29} - \frac{8000}{1.23} = 6976-6504 = 472$$

Suppose owing to one of several causes, the pressure at start of blowout was really 8100 psia. Then

$$\frac{9000}{1.29} - \frac{8100}{1.23} = 6976-6585 = 391$$

and the resultant value of the hydrocarbon pore volume using 8100 would be $0.607 \times 10^9 ft^3$, or 17 per cent larger than the value calculated using 8000 psia. As the gas deviation factor at 8100 is a little larger than 1.23, the error would be a little bit larger than 17 per cent. A major cause for pressure errors is that the pressure measured in wells may not be the true average pressure of the reservoir, owing to differential delpetion of areas of the reservoir.

Error analysis for the volumetric estimate of the hydrocarbon pore volume is straightforward. As the ranges of porosity and connate water are somewhat limited, the major source of error arises from the estimate of the bulk reservoir volume. Where the reservoir thickness is reasonably uniform, the bulk volume estimate is essentially an estimate of the productive area. In other cases the bulk volume is determined from isopach maps whose validity depends upon the number of control wells available and geological interpretation.

Assuming the estimate of bulk reservoir volume contains the major uncertainty, the per cent error in the hydrocarbon pore volume is that of the uncertainty in the estimate of bulk reservoir volume.

In the event Eq. (2.1) is used where there is water influx, calculated hydrocarbon pore volumes will be larger than the actual, and so will calculated volumes of gas in place. Thus, the calculated volumes of blowout gas will be larger than actual. Use of Eq. (2.1) therefore sets a maximum value to the vented gas volumes. Reference 2.2 contains a fuller discussion of the use of the volumetric and material balance methods on gas reservoirs.

SECTION 3
FLOW RATE MEASUREMENTS WITH PITOT TUBES

3.1 Introduction

The Pitot tube can be used to measure gas flow rates from wells under open flow conditions (Refs. 3.1 and 3.2). It is used to sense the difference between the dynamic and static pressures in a moving gas stream. This pressure differential is equal to the velocity head and is measured by a suitable device. The velocity is then determined and used to evaluate gas flow rates. Although less sophisticated than other gas flow measurement devices, it is the best suited device for gas flow measurements during gas well blowouts, except where a diverter or bleed line has been installed. As the Pitot tube has been widely and successfully employed to obtain "Back-Pressure" test data on gas wells, many operators are familiar with its use.

3.2 Description of the Pitot Tube

A sketch of the simple pitot tube, invented by H. Pitot, is shown in Fig. 3.1. This is sometimes called an impact tube or stagnation tube. The Pitot tube in principle is made by bending one leg of a manometer so that the opening is pointing exactly against the direction of gas flow. If one end of the manometer is left open to the atmosphere, the instrument indicates dynamic head, which is the sum of the static pressure and the pressure exerted by the velocity of the gas. The static pressure is measured by tapping the side of the line and measuring the pressure perpendicular to the line of flow.

A sketch of a combined Pitot and static tube device is also shown in Fig. 3.1. By this arrangement the static head is automatically subtracted from the dynamic head so that the manometer reading is a measure of the velocity head.

In open flow measurements the Pitot tube is located at the open end of the casing as shown also in Fig. 3.1. Where the other end of the manometer is left open to the atmosphere, the manometer reading is a measure of the velocity head. For small velocity heads the manometer liquid is water and for larger heads, mercury. For heads above 20 psi, Bourdon or dead weight gauges are used.

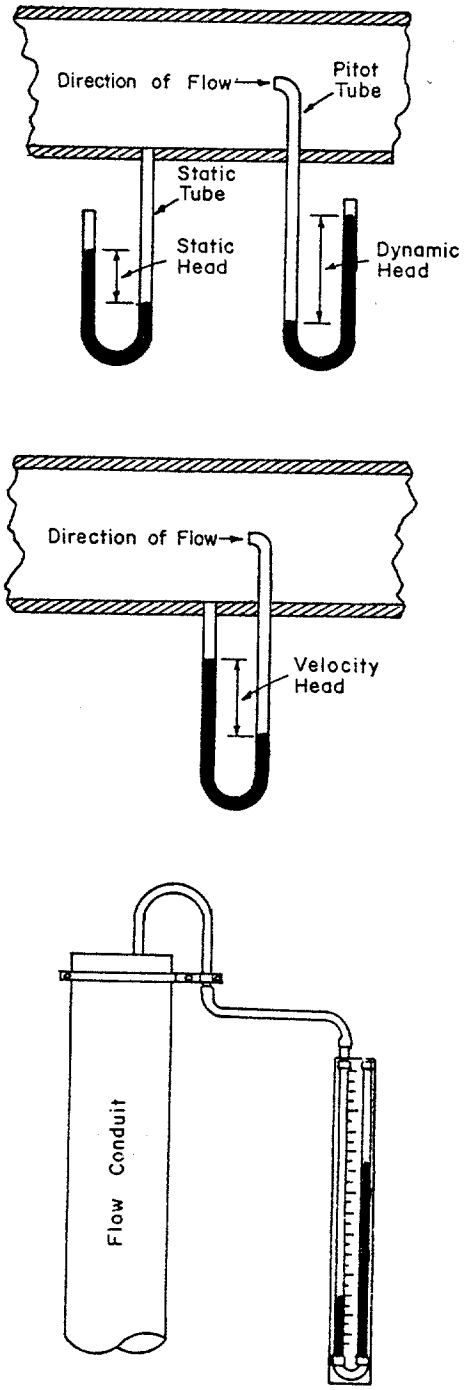

Fig. 3.1 Pitot tubes: Simple Pitot and static tubes (upper); combined Pitot and static tubes (middle); and open flow Pitot tube (lower)

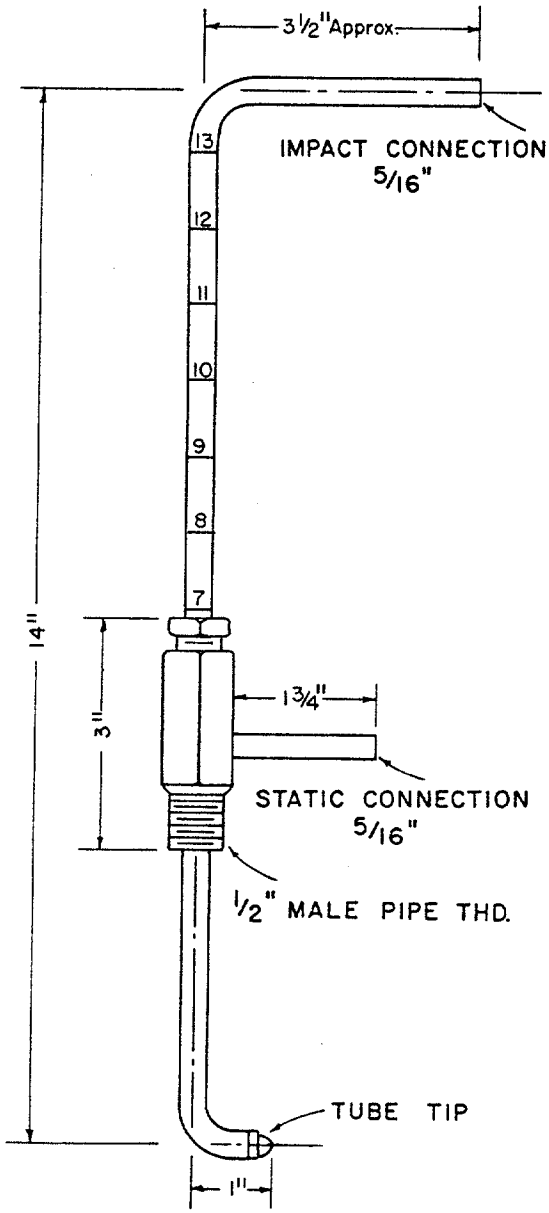

Fig. 3.2 Drawing of a commercially available Pitot tube (Ref. 3.3). (Courtesy Chandler Engineering Company.)

Figure 3.2 is a drawing of a Pitot tube which is available commercially (Ref. 3.3). It may be used for either open or closed flow. For high velocities and large diameter gas streams the tube shown would need to be strengthened and provided with a substantial support to position it in the stream.

3.3 Pitot Tube Formula

For all velocities between zero and sonic velocity it can be reasonably assumed that the part of the main stream which is stopped by the impact tube is stopped isentropically. Under these conditions it has been shown (Ref. 3.1) that the stream velocity at the impact tube is given by:

$$v = 58.58\ E \left\{\frac{n}{n-1}\ \frac{T}{G}\ \left[(p_i/p_a)^{\frac{n-1}{n}} - 1\right]\right\}^{0.5} \qquad (3.1)$$

where

v = velocity at Pitot tube, ft/sec

n = ratio of specific heats of the gas

p_i = impact pressure indicated by the tube, psia

p_a = static pressure which is atmospheric pressure in open subsonic flow, psia

T = flowing temperature, ^0R

G = gas gravity, (air=1)

E = efficiency factor which is the ratio between theoretical and actual velocities.

3.4 Flow Rate Determination

The velocity of gas through a circular pipe or annuli is not uniformly distributed (Ref. 3.4). Consequently, to determine the quantity of gas flowing, an average value for the gas velocity must be obtained. For approximate work involving circular flow cross section, the pitot tube can be located at the center of the pipe where the maximum velocity exists. The ratio of the average velocity and the maximum velocity may be assumed to be 0.862 (Ref. 3.5). The Pitot tube can also be placed at a point in the circular pipe where the actual velocity is equal to the average velocity of the entire cross section. This point is usually assumed to be on the circumference of a circle whose radius is 74 per cent of the radius of the pipe and concentric with the pipe (Ref. 3.6).

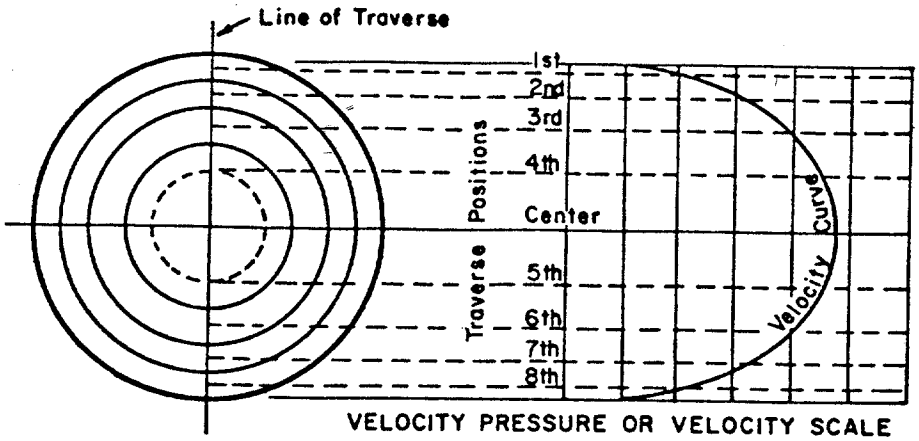

Fig. 3.3. Traverse positions for four equal areas.

Table I

Distances in Per Cent from Inside Surface to Point of Traverse

Number of Equal Areas	1st	2nd	3rd	4th	5th	6th	7th	8th	9th	10th
1	14.6	85.4								
2	6.7	25.0	75.0	93.3						
3	4.5	14.7	29.6	70.4	85.3	95.5				
4	3.4	10.6	19.5	32.3	67.7	80.5	89.4	96.6		
5	2.6	8.3	14.7	22.8	34.2	65.8	77.2	85.3	91.7	97.4

For more accurate work it is better to make a traverse of the pipe. A traverse is the only recommended method in annular flow as the position of maximum velocity or the mean velocity is hard to predict. To run a traverse, the pipe is first divided into a number of equal areas, a circle at the center and annular rings around it, as illustrated by Fig. 3.3. Mean diameters are determined for the annular rings, and where these cut the line of traverse, points are determined in which positions the Pitot tube is placed and a reading made. The two points in the inner circle are located where the circumference of the circle, having one-half the area of inner circle, cuts the line of traverse. Table I gives the distances in per cent from the inside surface of the pipe to the various positions of the traverse.

The velocity at each reading position is calculated using Eq. (3.1). The arithmetic mean of these readings is the average velocity.

In case the above method of running a traverse is impractical or if the flow is annular, several readings have to be taken on a diameter. The velocity at each position is calculated and a velocity distribution plot is constructed. The average velocity is then determined graphically.

Where velocities are varying, several readings should be taken over a period of time to obtain average values. As the Pitot tube reading is correct only when the tube is exactly parallel to the current of flow (Ref. 3.4), it may be necessary to rotate the tube with respect to the pipe axis until a maximum reading is obtained.

The quantity q of gas flowing through a duct is obtained as a product of the average velocity v_a and the duct area A. For a circular duct with inside diameter D:

$$q = 0.471\ D^2 v_a \frac{p\ T_{sc}}{p_{sc}\ T} \qquad (3.2)$$

where:

q = flow rate, MSCF/D
D = inside diameter, inches
v_a = average velocity, ft/sec
p = pressure of flowing gas, psia
T = temperature of flowing gas, ^0R
p_{sc} = standard pressure, psia
T_{sc} = standard temperature, ^0R

3.5 Illustrative Example with Error Analysis

The following example illustrates the use of Pitot tube measurements to calculate the gas flow rate where gas is blowing out to the atmosphere through 10-3/4 inch casing. Following the example, error analysis is applied to evaluate the precision of the measurement.

Example 3.1

Data:

Casing diameter (I.D.).....9.85 in
Gas specific gravity (Air=1).....0.665
Flowing temperature.....85°F
Barometric pressure.....14.65 psia

Standard temperature.....60°F
Standard pressure.....14.7 psia

Pitot tube measurements:

No.	% Diameter (Table I)	Inches From Inner Wall	Readings psig
1	4.5	0.44	3.0
2	14.7	1.45	6.0
3	29.6	2.92	8.0
4	70.4	6.93	9.0
5	85.3	8.40	6.0
6	95.5	9.41	2.0

Solution

For n=1.28, n/(n-1)=1.28/(1.28-1)=4.57 and (n-1)/n=0.219. Assuming E=1.00, for a Pitot reading of 3.0 psig, by Eq. (3.1) the velocity is

$$v = 58.58 \times 1.00\{4.57 \times \frac{545}{0.665}[(\frac{3.0}{14.65})^{0.219}-1]\}^{0.5}$$

$$v = \underline{734 \text{ ft/sec}}$$

For p_i=6.0, 8.0, 9.0, 6.0 and 2.0, the respective velocities are 1002, 1137, 1195, 1002, and 606 ft/sec. The average velocity is therefore,

$$v_a = \frac{734+1002+1137+1195+1002+606}{6}$$

$$v_a = \underline{946 \text{ ft/sec}}$$

Now using Eq. (3.2) to find the flow rate:

$$q = 0.471 \times 9.85^2 \times 9.46 \times \frac{14.65}{14.70} \times \frac{520}{545}$$

$$q = \underline{41{,}000 \text{ MSCF/D}}$$

In Table II maximum probable errors are assigned to the parameters of Eqs. (3.1) and (3.2) for Example 3.1. The probable error introduced into the flow rate by each of these was calculated as shown in the last column.

The maximum probable error in the flow rate resulting from the worst combination of the individual errors assigned to the parameters is -28% or +11%. The calculated flowrate for Example 3.1 is 41,000 MSCF/D bracketed between the extremes of 30,000 and 45,000 MSCF/D.

Table II

Parameter	Probable Error in Parameter	Probable Error In Flow Rate
E	-10%	-10%
n	±10%	± 3%
G	±10%	∓ 5%
T	±50%	∓ 4%
p	±10%	±10%

3.6 Limitation of the Pitot Tube Application

The Pitot tube application is limited to subsonic velocity. If the flow is sonic the static pressure is no longer atmospheric. The value of the static pressure is then unavailable unless the side of the pipe is tapped which is a remote possibility.

The sonic velocity v_s is expressed in Ref. 3.5 by:

$$v_s = 41.44 \left[\frac{nzT}{G}\right]^{0.5} \text{ ft/sec} \qquad (3.3)$$

where z is the gas deviation factor. Substituting in Eq. (3.2)

$$q_s = 19.52 \frac{D^2 p_{atm} T_{sc}}{p_{sc} T} \left[\frac{nzT}{G}\right]^{0.5} \text{ MSCF/day} \qquad (3.4)$$

where q_s is the maximum flow rate which could be accurately determined by the Pitot tube.

For the following average flow conditions and gas properties:

p_{atm} = 14.7 psia T_{sc} = 60°F n = 1.28 z = 1.00

p_{sc} = 14.7 psia T = 60°F G = 0.65

Equation (3.4) becomes:

$$q_s = 625D^2 \qquad (3.5)$$

Equation (3.5) is shown as a plot in Fig. 3.4. It indicates that where gas is vented to the atmosphere through 10 inch diameter casing, as in Example 3.1,

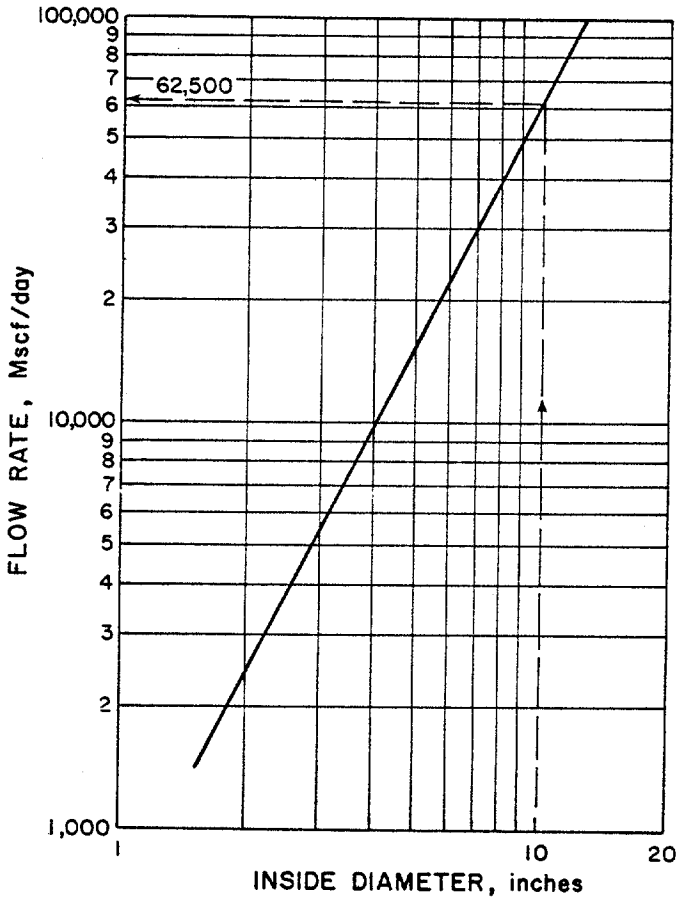

Fig. 3.4. Limits of flow rate for using Pitot tubes.

sonic velocity is reached at a flow rate of 62,500 MMSCF/D. As this is far above the 41,000 MSCF/D calculated in Example 3.1, the use of the Pitot formulas are valid.

SECTION 4
MEASUREMENTS IN BLEED LINES

4.1 Introduction

Figures 4.1–4.3 are diagrams of typical choke manifold assemblies recommended by the American Petroleum Institute, Ref. 4.1, for various working pressures. In addition to two or three vent lines through which flow is controlled by manual and/or remotely operated adjustable chokes, these systems contain bleed lines through which well fluids may be allowed to flow unrestricted to the atmosphere.

Bleed lines are usually straight runs of horizontal pipe, fifty to one hundred feet long and of a diameter at least that of the choke lines. The upstream end of the bleed line contains one or two plug or gate valves and a pressure gauge. The downstream end is open to the atmosphere. Where wells are vented or blowing out through bleed lines, it is possible to calculate the flow rate from pressure gauge readings and the length and diameter of the bleed line. This method of calculating flow rate can also be applied to diverter or blooie lines where the lines are equipped with pressure gauges.

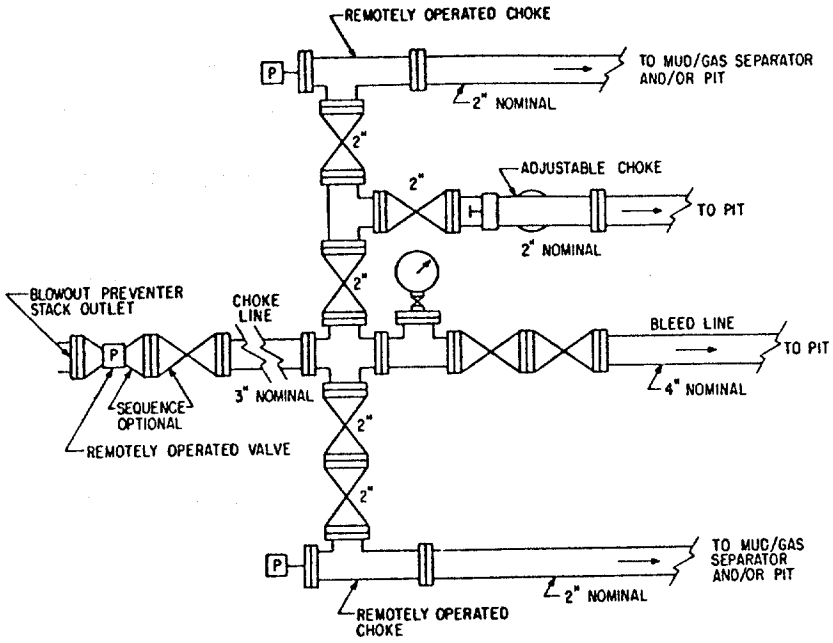

Fig.4.1.Typical choke manifold assembly for 10,000 and 15,000 psi rated working pressure service. Courtesy American Petroleum Institute, Ref. 4.1.

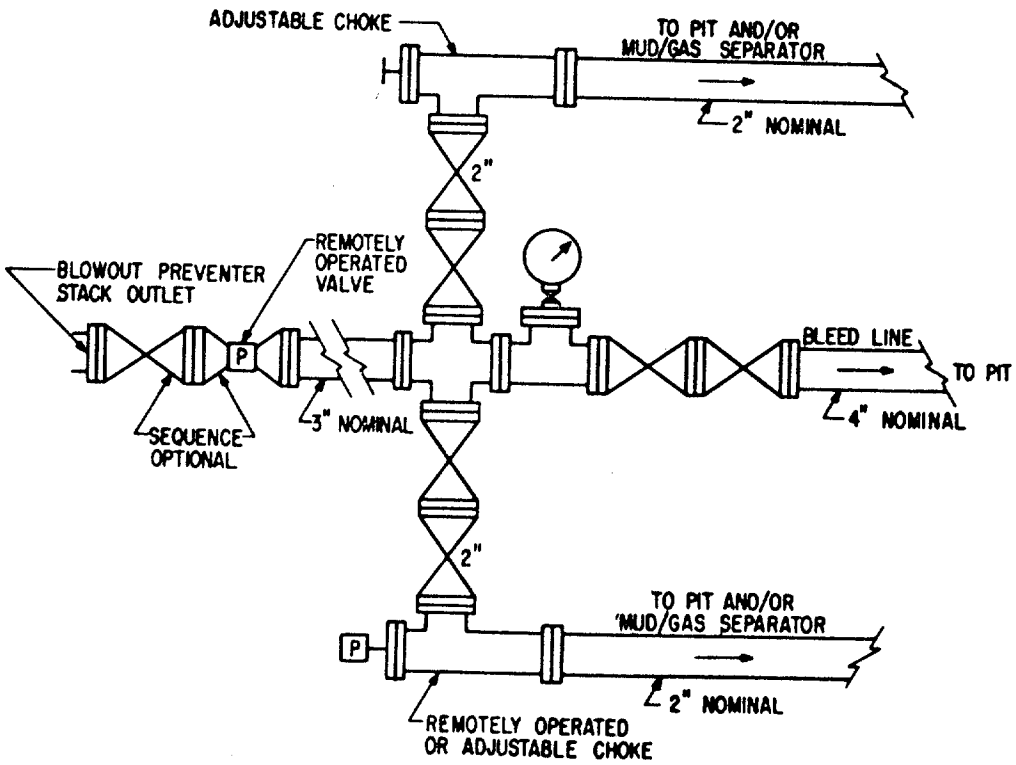

Fig.. 4.2. Typical choke manifold assembly for 5000 psi rated working pressure service. Courtesy American Pet. Institute, Ref. 4.1.

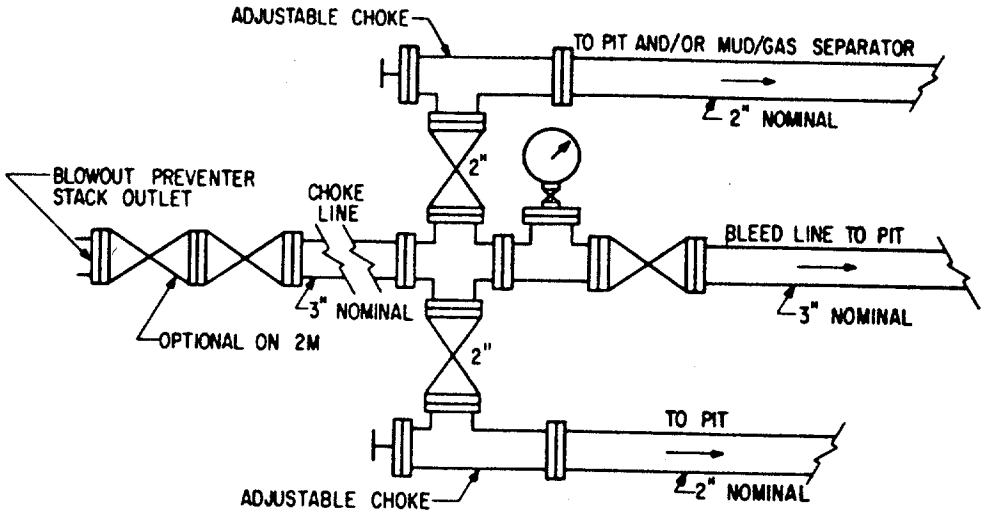

Fig.4.3.Typical choke manifold assembly for 2000 and 3000 psi rated working pressure service. Courtesy American Petroleum Institute, Ref. 4.1.

4.2 Bleed Line FLow Calculations

In compressible fluid flow in pipe lines of uniform cross section, the effect of friction is to increase the velocity and to decrease the pressure of the stream. If the pressure drop is sufficiently high, which is the case in well blowouts through small diameter pipes, the exit velocity reaches sonic velocity. Although the line discharges to atmospheric pressure, the outlet pressure is significantly higher.

The sonic velocity v_s at the pipe outlet is expressed in Ref. 4.2 as:

$$v_s = \left[\frac{k\, z_o\, R\, T_o}{W}\right]^{0.5} \qquad (4.1)$$

where

k = ratio of the specific heats
R = universal gas constant
W = gas molecular weight
z_o = gas compressibility factor at <u>outlet</u> temperature T_o and pressure p_o

Expressing W in terms of gas specific gravity G, the absolute temperature T_o in ^0R, and replacing R by its numerical value, Eq.(4.1) yields for the velocity in feet per second:

$$v_s = 41.44\left[\frac{k\, z_o\, T_o}{G}\right]^{0.5} \qquad (4.2)$$

Hence the flow rate q_o in MCF/D at outlet pressure and temperature

$$q_o = 19.53\, D^2 \left[\frac{k\, z_o\, T_o}{G}\right]^{0.5} \qquad (4.3)$$

where D is the line inside diameter in inches.

The flow rate q_o can also be expressed using the Clinedinst equation, Ref. 4.3, as:

$$q_o = 7.965 \frac{p_c\, D^5 T_o}{p_o\, GLf} \left(\int_o^{p_{ri}} \frac{p_r}{z}\, dp_r - \int_o^{p_{ro}} \frac{p_r}{z}\, dp_r \right) \qquad (4.4)$$

where

p_o = outlet pressure, psia
p_c = pseudocritical pressure, psia
f = friction factor
L = pipe length, ft
p_i = inlet pressure, psia, recorded by the gauge.

The integral function

$$\int_0^{p_r} \frac{p_r}{z}\, dp_r$$

has been evaluated by Nisle and Poettmann, Ref. 4.4, and are given in Table 4.1.

Equations (4.3) and (4.4) contain two unknown parameters q_o and p_o. The other parameters can be measured or estimated. The pipe inside diameter D and pipe roughness e are usually known. Complete turbulence can be assumed and the friction factor f obtained from Fig. 4.4, Ref. 4.5. If the temperature T_o of the exiting gas stream can not be measured it must be estimated. The gas gravity G is likewise estimated or measured if a gas sample has been obtained.

The equivalent length of valves, if present, is added to the axial length of the line before substituting for L in Eq. (4.4). The valves usually used are full bore gate or plug valves. The friction losses across these valves when fully open are small and can be predicted with fair accuracy. The equivalent lengths of valves are available in the literature, e.g., Ref. 4.6, or from the manufacturer.

Equations (4.3) and (4.4) are used to construct a plot of flow rate versus inlet pressure, measured by the gauge, using a range of assumed values of outlet pressure p_o which are unmeasured. Values of G and T_o in Eq. (4.3) must be estimated or measured. From these and the assumed values of p_o the gas deviation factor z_o and the ratio of the specific heats can be determined using Figs. 4.5 (Ref. 4.7), 4.6 (Ref. 4.8) and 4.7 (Ref. 4.9). Placing these in Eq. (4.3) values of q_o are obtained.

These values of q_o are placed in Eq. (4.4) together with values of p_c, p_o, D, L, and f. The values of the second integral in Eq. (4.4) are evaluated using Table 4.1, leaving only the values of the first integral to be solved for. Entering Table 4.1 with the values of these integrals, the values of the upper limits p_{ri} are obtained, and finally the values of p_i.

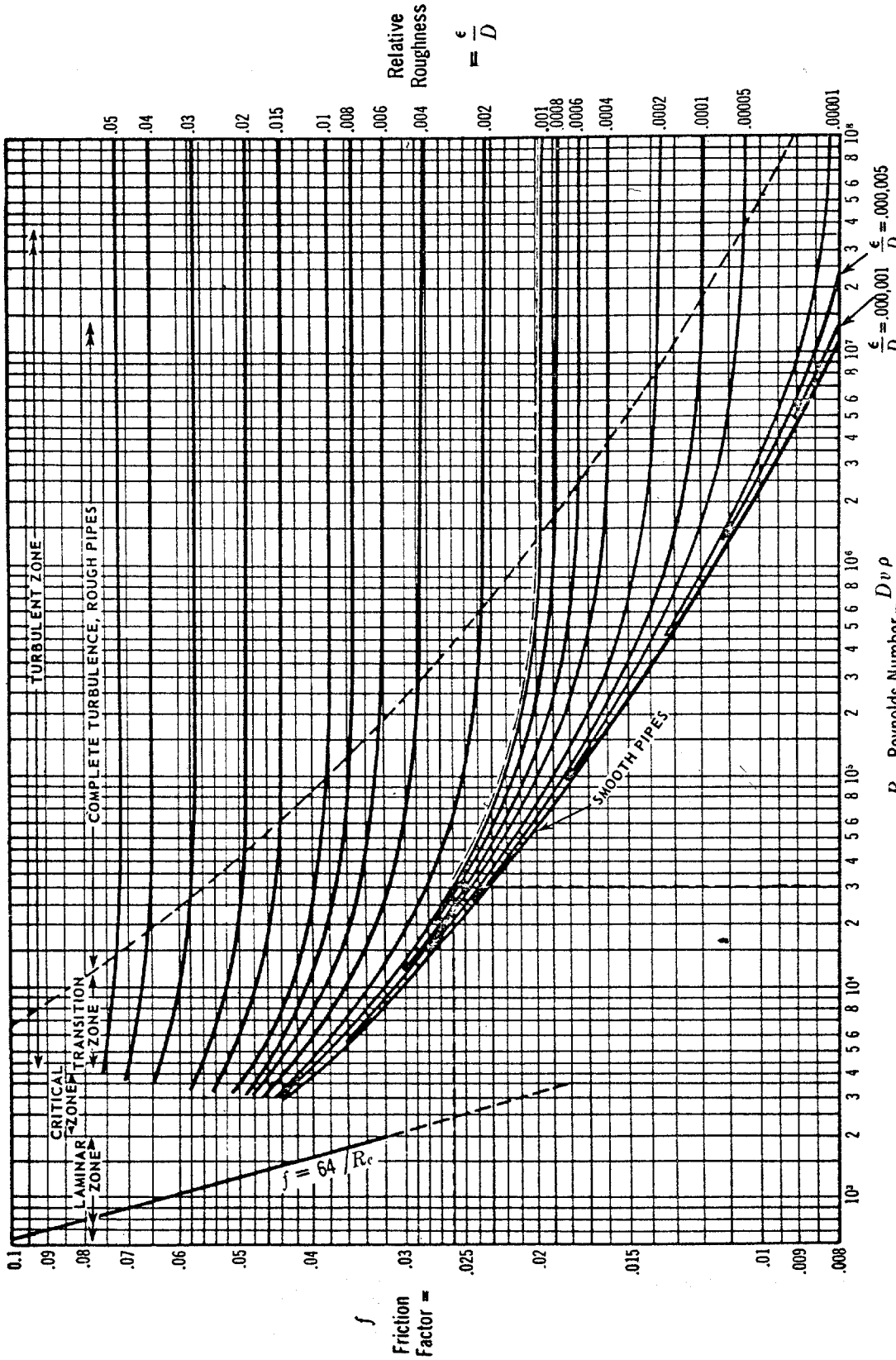

Fig. 4.4. Friction factors for pipe flow. (Courtesy Crane, Ref. 4.5.)

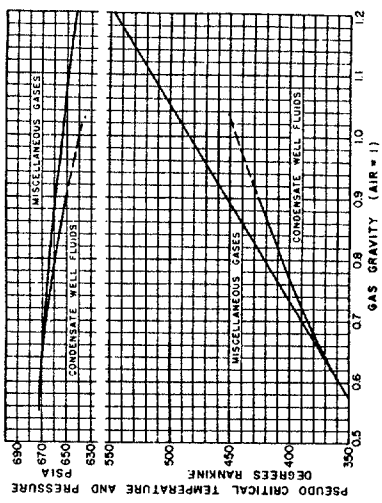

Fig. 4.6. Pseudoreduced pressure and temperature vs gas gravity. (Courtesy Natural Gasoline Association of America, Ref. 4.8.)

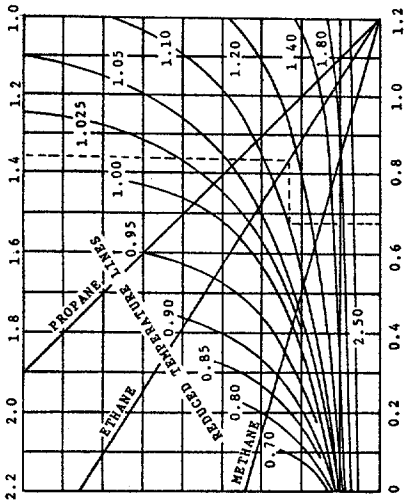

Fig. 4.7. Ratio of specific heats for hydrocarbons as functions of reduced pressure and temperature. (After Edmister, Ref. 4.9, Courtesy Petroleum Engineer.)

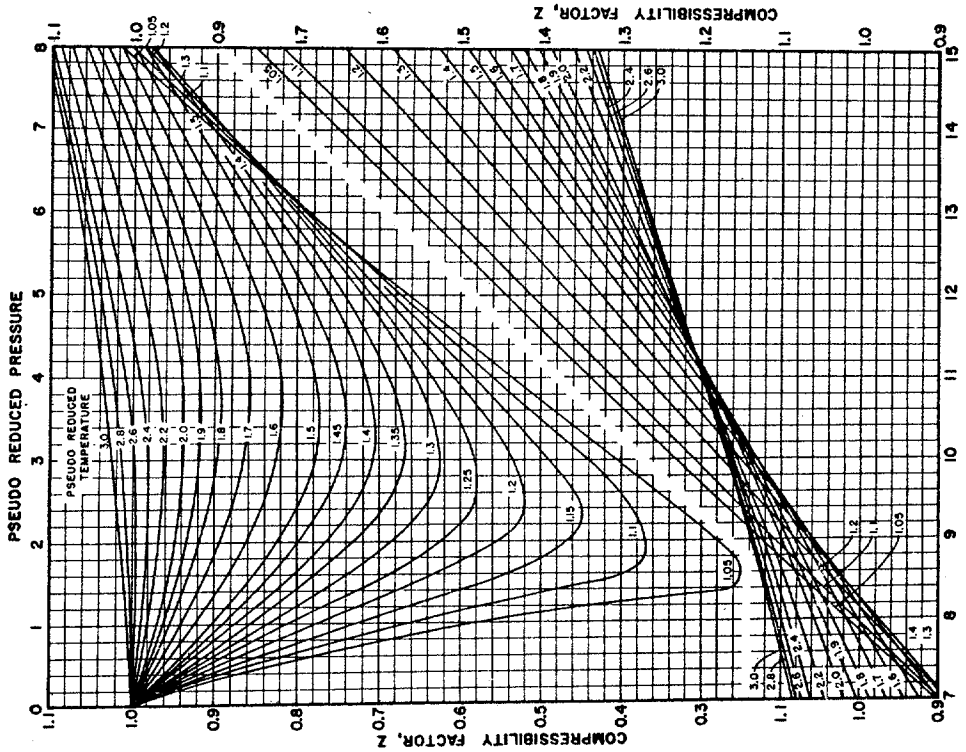

Fig. 4.5. Gas compressibility factor vs reduced pressure and temperature. (After Standing and Katz, Trans. AIME, Ref. 4.7.)

As a final step, the values of q_o are reduced to standard conditions using

$$q_{sc} = q_o \frac{p_o \, T_{sc}}{p_{sc} \, T_o} \qquad (4.5)$$

Now a plot can be made of the flow rate q_{sc} versus the inlet pressure p_i as measured by the gauge on the bleed line. From this plot values for the flow rate are obtained for any value of inlet pressure. If the outlet velocity is subsonic, p_o will be atmospheric, and Eq. (4.4) may be used alone to find the relation between p_i and q_o, and using Eq. (4.5) to reduce q_o values to standard conditions.

4.3 Illustrative Example

A gas well was vented through two fully-opened gate valves and a 50 ft, 4 inch schedule 160 bleed line. A pressure gauge upstream from the valves initially recorded 1005 psig and 886 psig six days later when it was brought under control. The method described in the previous section will be used to calculate the initial and final flow rates and the gas vented during the six day blowout. Additional data needed to perform the calculation include:

Pipe absolute roughness = 0.0018 inch
Line inside diameter = 3.438 inch
Gas gravity = 0.60
Flow temperature = 77^0F
Barometric pressure = 14.62 psia
Standard temperature = 60^0F
Standard pressure = 14.7 psia

Solution

(1) Adjusted bleed line length for two valves.

L = 50+2x13x(3.438/12)
L = 57.45 ft.

(2) Gas deviation factor and ratio of specific heats.

Find P_c = 672 psia and T_c = 358^0R from Fig. 4.6 for G = 0.60. For T_o = 77 F, T_r = (77+460)/358 = 1.50. For p_o = 400 psia, for example, P_r = 400/672 = 0.60. From Fig. 4.5 z_o = 0.94. From Fig. 4.7, k = 1.3.

(3) Friction factor

Relative pipe roughness = 0.0018/3.438 = 0.00052.

From Fig. 4.4, for complete turbulence, f = 0.017.

(4) Flow rate

By Eq. (4.3)

$$q_o = 19.53x(3.438)^2(1.3x0.94x537/0.60)^{0.5}$$

$$q_o = 7634 \text{ ft}^3/\text{day at 400 psi and } 77^0\text{F}$$

By Eq. (4.5)

$$q_{sc} = 7634 \times \frac{400}{14.7} \times \frac{520}{537}$$

$$= 201{,}000 \text{ MSCF/D}$$

$$= 201.0 \text{ MMSCF/D (Table 4.2 and Fig. 4.7)}$$

(5) Value of inlet pressure

Substitute q_o from (4) and solve for the first integral of Eq. (4.4). For p_o = 400 psia p_{ro} = 400/672 = 0.60. From Table 4.1 for T_{ro} = 1.50, for p_{ro} = 0.60 the value of the second integral of Eq. (4.4) is 0.18. Note that values in Table 4.1 are to be multiplied by 1000. Equation (4.4) becomes

$$7634 = 7.965 \times \frac{672x3.438^5x537}{400x0.60x57.45x0.017} \text{ (A—0.18)}$$

where A is the value of the first integral, which from the above

$$A = 1.040$$

Enter Table 4.1 with A = 1.040, for T_{ro} = 1.50 by interpolation find p_{ri} = 1.388. Then

$$p_i = p_{ri} x p_c = 1.388x672 = 932 \text{ psia}$$

(6) Repeat the above for a range of assumed values of outlet pressure p_o. Table 4.2 summarizes the intermediate values and provides the data from with the flow rate at standard condition in plotted versus inlet pressure as shown in Fig. 4.8.

Using Fig. 4.8 the flow rates at 1005 psig (1019.7 psia) and 886 psig (900.7 psia) are, respectively, 235

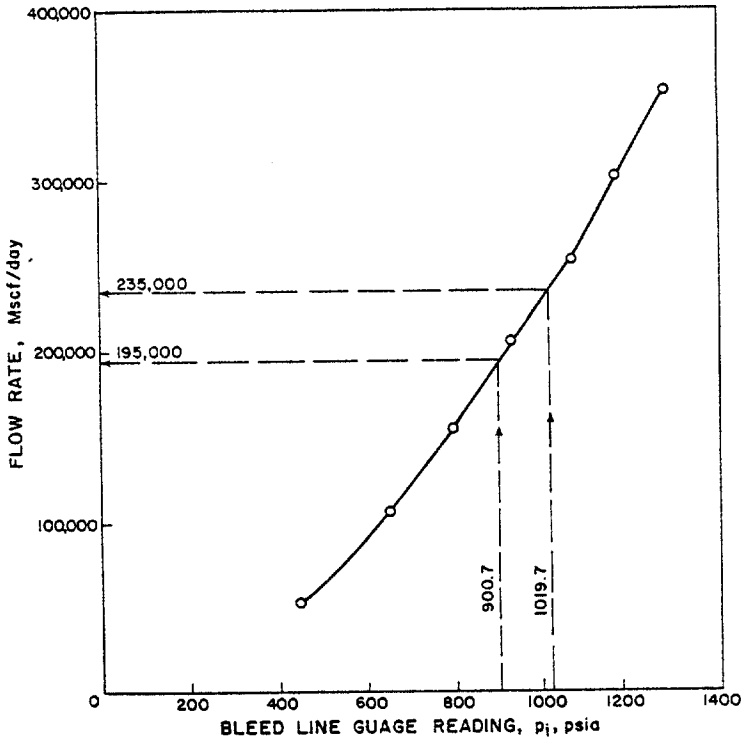

Fig. 4.8. Flow rate versus inlet pressure.

Table 4.2

p_o	100	200	300	400	500	600	700
p_{ro}	0.149	0.298	0.446	0.595	0.744	0.893	1.042
z_o	0.99	0.97	0.95	0.94	0.92	0.91	0.90
q_o	7835	7755	7675	7634	7552	7511	7470
$\int_o^{p_{ro}}$	0	0.04	0.09	0.18	0.28	0.42	0.57
$\int_o^{p_{ri}}$	0.221	0.477	0.739	1.040	1.344	1.690	2.034
p_{ri}	0.664	0.976	1.178	1.388	1.602	1.745	1.905
p_i	446	650	792	932	1076	1173	1280
q_{sc}*	52.6	101.4	154.6	201.0	253.5	302.6	351.1

*q_{sc} in MMSCF/D.

and 195 MMSCF/D. Assuming a linear decline in flow rate for the six day period the vented gas volume is

$$Q = \frac{235+195}{2} \times 6 = 1,290 \text{ MMSCF}$$

4.4 Limitations and Accuracy of Bleed Line Flow Calculations

The above calculations are limited to the case of a line of uniform cross section with no area restriction. This should usually be the case except when a valve is partially closed. A partially closed valve creates a throat. With a limited length of the line it is possible that the flow may be choked at the throat. The situation becomes somewhat more complex as supersonic flow might occur at the throat exit. Also with the valve partially closed it is hard to predict the friction losses across the valve, the cross section of the flow and the flow temperature and pressure at the throat. However, flow rates calculated assuming fully open valves are maximum estimates.

In the case of uniform lines, the calculated flow rate accuracy is sensitive to the flow temperature, the gas gravity and the friction factor as determined by the pipe roughness. Considering the above numerical example, let the flow temperature be 177^0F instead of 77^0F. The flow rate corresponding to p_i of 1019.7 psig would be 256 MMSCF/day instead of 235 MMSCF/day. An error of 100 degrees in determining the flow temperature will only result in an error less than 10 per cent in the flowrate. This is relatively small because only the absolute temperature raised to the power of 0.5 appears in the calculations.

If we cut the pipe roughness down by half, say to 0.0009 inch, the relative roughness and friction factors are then 0.00026 and 0.0145 respectively, resulting in a flow rate of 255 MMSCF/day. A 50 per cent error in the pipe roughness will result in an error in flow rate less than 10 per cent.

The gas gravity can usually be estimated within 0.1. Should the gas gravity be 0.7 instead of 0.6, a flow rate of 216 MMSCF/day is calculated. This again represents an error in flow rate less than 10 per cent.

The flow temperature, gas gravity and pipe roughness can usually be estimated with accuracy at least equal to that used in the above discussion. The flow rate calculated with this method is fairly accurate.

Table 4.1. Values of $\int_0^{P_r} (p_r/z)dp_r$.

(After Nisle and Poettman, Ref. 4.4. Courtesy The Petroleum Engineer.)

CAUTION Multiply all values given in the table by 1000, e.g., 0.00228 is actually 2.28.

Pseudo reduced pressure P_r	Pseudo reduced temperature T_r																			
	1.05	1.10	1.15	1.20	1.25	1.30	1.35	1.40	1.45	1.50	1.60	1.70	1.80	1.90	2.00	2.20	2.40	2.60	2.80	3.00
.05	00000	00000	00000	00000	00000	00000	00000	00000	00000	00000	00000	00000	00000	00000	00000	00000	00000	00000	00000	00000
.10	00000	00000	00000	00000	00000	00000	00000	00000	00000	00000	00000	00000	00000	00000	00000	00000	00000	00000	00000	00000
.15	00001	00001	00001	00001	00001	00001	00001	00001	00001	00001	00001	00001	00001	00001	00001	00001	00001	00001	00001	00001
.20	00001	00001	00001	00001	00001	00001	00001	00001	00001	00001	00001	00001	00001	00001	00001	00002	00002	00002	00002	00002
.25	00003	00003	00003	00003	00003	00002	00002	00002	00002	00002	00002	00002	00002	00002	00002	00002	00002	00002	00002	00002
.30	00004	00004	00004	00004	00004	00004	00004	00004	00004	00004	00004	00004	00004	00004	00004	00004	00004	00004	00004	00004
.35	00006	00006	00006	00006	00006	00006	00006	00005	00005	00005	00005	00005	00005	00005	00005	00005	00005	00005	00005	00005
.40	00008	00008	00008	00008	00008	00007	00007	00007	00007	00007	00007	00007	00007	00007	00007	00007	00007	00007	00007	00007
.45	00010	00010	00010	00010	00010	00010	00010	00010	00010	00010	00009	00009	00009	00009	00009	00009	00009	00009	00009	00009
.50	00013	00013	00013	00013	00012	00012	00012	00012	00012	00012	00012	00012	00012	00012	00012	00012	00012	00012	00012	00012
.55	00016	00016	00016	00015	00015	00015	00015	00015	00015	00015	00015	00014	00014	00014	00014	00014	00014	00014	00014	00014
.60	00020	00019	00019	00019	00019	00018	00018	00018	00018	00018	00018	00017	00017	00017	00017	00017	00017	00017	00017	00017
.65	00024	00023	00023	00022	00022	00021	00021	00021	00021	00021	00021	00021	00020	00020	00020	00020	00020	00020	00020	00020
.70	00028	00027	00027	00026	00026	00025	00025	00025	00025	00025	00024	00024	00024	00024	00024	00024	00023	00023	00023	00023
.75	00033	00032	00031	00030	00030	00029	00029	00029	00029	00028	00028	00028	00028	00028	00027	00027	00027	00027	00027	00027
.80	00039	00037	00036	00035	00034	00034	00033	00033	00033	00033	00032	00032	00032	00031	00031	00031	00031	00031	00031	00031
.85	00045	00042	00041	00040	00039	00038	00038	00038	00037	00037	00037	00036	00036	00036	00035	00035	00035	00035	00035	00035
.90	00051	00048	00047	00045	00044	00043	00043	00042	00042	00042	00041	00041	00040	00040	00040	00040	00039	00039	00039	00039
.95	00059	00055	00053	00051	00050	00049	00048	00048	00047	00047	00046	00045	00045	00045	00045	00044	00044	00044	00044	00044
1.00	00067	00062	00059	00057	00056	00053	00054	00053	00053	00052	00051	00051	00050	00050	00050	00049	00049	00049	00049	00048
1.05	00075	00070	00066	00064	00062	00061	00060	00059	00058	00058	00057	00056	00055	00055	00055	00054	00054	00054	00054	00053
1.10	00085	00078	00074	00071	00069	00067	00066	00065	00064	00064	00063	00062	00061	00061	00060	00060	00059	00059	00059	00059
1.15	00097	00087	00082	00078	00076	00074	00073	00072	00071	00070	00069	00068	00067	00067	00066	00065	00065	00065	00065	00064
1.20	00109	00097	00090	00086	00083	00081	00080	00078	00077	00077	00075	00074	00073	00073	00072	00071	00071	00070	00070	00070
1.25	00124	00108	00099	00095	00091	00089	00087	00086	00084	00084	00082	00080	00080	00079	00078	00078	00077	00076	00076	00076
1.30	00141	00120	00109	00104	00100	00097	00095	00093	00092	00091	00089	00087	00086	00086	00085	00084	00084	00083	00083	00082
1.35	00161	00132	00120	00113	00109	00105	00103	00101	00099	00098	00096	00094	00093	00093	00092	00091	00090	00089	00089	00089
1.40	00185	00146	00131	00123	00118	00114	00112	00109	00107	00106	00104	00102	00101	00100	00099	00098	00097	00096	00096	00096
1.45	00212	00161	00143	00133	00128	00123	00121	00118	00116	00114	00112	00109	00108	00107	00106	00105	00104	00103	00103	00103
1.50	00241	00178	00155	00145	00138	00133	00130	00127	00124	00123	00120	00117	00116	00115	00114	00113	00112	00111	00111	00110
1.55	00271	00196	00169	00156	00149	00143	00139	00136	00133	00132	00128	00126	00124	00123	00122	00120	00119	00118	00118	00117
1.60	00302	00216	00183	00169	00160	00153	00149	00146	00143	00141	00137	00134	00132	00131	00130	00128	00127	00126	00126	00125
1.65	00334	00237	00198	00181	00172	00164	00160	00156	00153	00150	00146	00143	00141	00140	00138	00137	00136	00134	00134	00133
1.70	00368	00259	00214	00195	00184	00176	00171	00166	00163	00160	00156	00152	00150	00149	00147	00145	00144	00143	00142	00141
1.75	00402	00282	00231	00209	00197	00188	00182	00177	00173	00170	00166	00162	00159	00158	00156	00154	00153	00151	00151	00150
1.80	00436	00305	00249	00224	00210	00200	00193	00188	00184	00181	00176	00172	00169	00167	00165	00163	00162	00160	00160	00158
1.85	00471	00330	00267	00239	00224	00213	00206	00200	00195	00192	00186	00182	00179	00177	00175	00173	00171	00169	00169	00168
1.90	00506	00355	00286	00256	00239	00226	00218	00212	00207	00203	00197	00193	00189	00187	00185	00182	00180	00179	00178	00177
1.95	00541	00381	00307	00273	00254	00240	00231	00224	00219	00215	00208	00203	00199	00197	00195	00192	00190	00188	00187	00186
2.00	00576	00408	00327	00290	00270	00254	00244	00237	00231	00227	00219	00214	00210	00208	00205	00202	00200	00198	00197	00196

Table 4.1, page 2.

Pseudo reduced pressure P_r	Pseudo reduced temperature T_r																		
	1.05	1.10	1.15	1.20	1.25	1.30	1.35	1.40	1.45	1.50	1.60	1.70	1.80	1.90	2.00	2.20	2.40	2.60	2.80	3.00
2.05	00612	00435	00349	00308	00286	00269	00258	00250	00244	00239	00231	00225	00221	00218	00216	00213	00211	00208	00207	00206
2.10	00648	00463	00372	00328	00303	00284	00272	00264	00257	00251	00243	00237	00232	00229	00227	00223	00221	00219	00218	00216
2.15	00684	00492	00395	00347	00320	00300	00287	00278	00270	00264	00256	00249	00244	00241	00238	00234	00232	00229	00228	00226
2.20	00720	00521	00419	00368	00338	00316	00302	00292	00284	00278	00268	00261	00256	00252	00250	00245	00243	00240	00239	00237
2.25	00756	00550	00444	00389	00356	00333	00318	00307	00298	00291	00281	00273	00268	00264	00261	00257	00254	00251	00250	00248
2.30	00792	00580	00469	00411	00375	00350	00334	00323	00312	00306	00295	00288	00281	00277	00273	00269	00268	00263	00261	00259
2.35	00828	00610	00495	00433	00395	00368	00351	00338	00327	00320	00308	00299	00293	00289	00286	00281	00278	00274	00272	00271
2.40	00865	00641	00521	00456	00415	00387	00368	00354	00343	00335	00322	00313	00306	00302	00298	00293	00290	00286	00284	00282
2.45	00901	00672	00548	00479	00436	00405	00385	00371	00358	00350	00337	00327	00320	00315	00311	00305	00302	00298	00296	00294
2.50	00937	00704	00576	00503	00457	00425	00403	00388	00374	00365	00351	00341	00333	00328	00324	00318	00315	00311	00308	00306
2.55	00974	00736	00603	00527	00479	00444	00421	00405	00391	00381	00366	00355	00347	00342	00337	00331	00327	00323	00321	00318
2.60	01010	00768	00632	00552	00501	00465	00440	00423	00408	00397	00382	00370	00361	00356	00351	00345	00340	00336	00334	00331
2.65	01047	00800	00660	00577	00523	00485	00459	00441	00425	00414	00397	00385	00376	00370	00365	00358	00354	00349	00347	00344
2.70	01083	00833	00689	00602	00546	00507	00479	00460	00443	00431	00413	00400	00391	00384	00379	00372	00367	00363	00360	00357
2.75	01120	00866	00718	00628	00570	00526	00499	00479	00461	00448	00429	00416	00406	00399	00394	00386	00381	00376	00373	00370
2.80	01157	00899	00748	00655	00594	00550	00519	00498	00479	00466	00446	00432	00421	00414	00408	00401	00395	00390	00387	00384
2.85	01193	00933	00778	00682	00618	00573	00540	00518	00498	00484	00463	00448	00437	00429	00423	00415	00410	00404	00401	00398
2.90	01230	00966	00808	00709	00643	00596	00562	00538	00517	00502	00480	00464	00453	00445	00439	00430	00424	00419	00415	00412
2.95	01267	01000	00838	00736	00668	00619	00584	00559	00536	00521	00498	00481	00469	00461	00454	00445	00439	00433	00429	00426
3.00	01304	01034	00868	00764	00694	00643	00606	00580	00556	00540	00516	00498	00486	00477	00470	00461	00454	00448	00444	00440
3.05	01340	01068	00899	00792	00720	00667	00628	00601	00577	00559	00534	00516	00502	00493	00486	00476	00470	00463	00459	00455
3.10	01377	01103	00930	00821	00746	00692	00651	00623	00597	00579	00553	00533	00519	00510	00502	00492	00485	00479	00474	00470
3.15	01414	01137	00961	00850	00773	00717	00675	00645	00618	00599	00572	00552	00537	00527	00519	00508	00501	00494	00489	00485
3.20	01451	01171	00992	00879	00800	00742	00698	00667	00640	00620	00591	00570	00555	00544	00536	00525	00517	00510	00505	00501
3.25	01488	01206	01024	00908	00827	00768	00722	00690	00661	00641	00611	00589	00573	00562	00553	00542	00534	00526	00521	00516
3.30	01525	01241	01056	00938	00855	00794	00747	00713	00683	00662	00631	00608	00591	00580	00571	00559	00550	00543	00537	00532
3.35	01562	01275	01088	00968	00883	00820	00772	00737	00706	00683	00651	00627	00609	00598	00588	00576	00567	00559	00553	00548
3.40	01599	01310	01120	00998	00911	00847	00797	00761	00729	00705	00671	00647	00628	00616	00606	00593	00584	00576	00570	00565
3.45	01636	01345	01152	01029	00940	00874	00822	00785	00752	00727	00692	00666	00647	00635	00624	00611	00602	00593	00587	00581
3.50	01674	01380	01185	01059	00969	00901	00848	00810	00775	00750	00714	00687	00667	00654	00643	00629	00619	00611	00604	00598
3.55	01711	01415	01218	01090	00998	00929	00874	00835	00799	00772	00735	00707	00687	00673	00662	00647	00637	00628	00621	00615
3.60	01748	01450	01251	01122	01027	00957	00901	00860	00823	00796	00757	00728	00707	00692	00681	00666	00655	00646	00639	00632
3.65	01785	01485	01284	01153	01057	00985	00928	00886	00848	00819	00779	00749	00727	00712	00700	00685	00674	00664	00656	00650
3.70	01822	01520	01317	01185	01087	01014	00955	00912	00872	00843	00802	00770	00747	00732	00720	00704	00692	00682	00674	00668
3.75	01859	01556	01351	01217	01117	01043	00982	00938	00897	00867	00824	00792	00768	00753	00739	00723	00711	00701	00692	00686
3.80	01897	01591	01384	01249	01148	01072	01010	00965	00923	00891	00847	00814	00789	00773	00760	00742	00730	00720	00711	00704
3.85	01934	01627	01418	01281	01178	01102	01038	00991	00949	00916	00871	00836	00811	00794	00780	00762	00750	00739	00730	00722
3.90	01971	01663	01452	01313	01209	01132	01066	01019	00975	00941	00895	00859	00833	00815	00801	00782	00769	00758	00749	00741
3.95	02009	01698	01486	01346	01240	01162	01095	01046	01001	00966	00919	00882	00855	00836	00821	00802	00789	00777	00768	00760
4.00	02046	01734	01520	01379	01272	01192	01124	01074	01027	00992	00943	00908	00877	00858	00843	00823	00809	00797	00787	00779
4.05	02083	01770	01555	01412	01304	01223	01153	01102	01054	01018	00967	00929	00899	00880	00864	00844	00829	00817	00807	00799
4.10	02121	01805	01589	01445	01335	01254	01183	01130	01082	01044	00992	00952	00922	00902	00886	00865	00850	00837	00827	00818
4.15	02158	01841	01624	01478	01368	01285	01212	01159	01109	01070	01017	00976	00945	00925	00907	00886	00870	00858	00847	00838
4.20	02196	01878	01659	01512	01400	01317	01242	01188	01137	01097	01043	01001	00968	00947	00930	00907	00891	00878	00867	00858
4.25	02233	01914	01694	01545	01432	01348	01272	01217	01165	01124	01068	01025	00992	00970	00952	00929	00913	00899	00888	00879
4.30	02271	01950	01729	01579	01465	01380	01303	01246	01193	01151	01094	01050	01016	00993	00975	00951	00934	00920	00908	00899
4.35	02308	01986	01764	01613	01498	01412	01334	01276	01222	01179	01120	01075	01040	01017	00998	00973	00956	00941	00929	00920
4.40	02346	02022	01799	01648	01531	01445	01365	01306	01250	01207	01147	01100	01064	01040	01021	00995	00978	00963	00951	00941
4.45	02383	02059	01835	01682	01564	01477	01396	01336	01280	01235	01173	01126	01089	01064	01044	01018	01000	00985	00972	00962
4.50	02421	02095	01870	01716	01598	01510	01427	01367	01309	01263	01200	01152	01113	01089	01068	01041	01022	01007	00994	00984
4.55	02458	02132	01906	01751	01631	01543	01459	01397	01338	01291	01228	01178	01139	01113	01092	01064	01045	01029	01016	01005
4.60	02496	02168	01942	01786	01665	01576	01491	01428	01368	01320	01255	01204	01164	01138	01116	01088	01067	01051	01038	01027
4.56	02533	02205	01978	01821	01699	01609	01523	01460	01398	01349	01283	01231	01189	01163	01140	01111	01090	01074	01060	01049
4.70	02571	02242	02014	01856	01733	01643	01555	01491	01429	01379	01311	01258	01215	01188	01165	01135	01114	01097	01083	01072
4.75	02609	02279	02050	01891	01768	01677	01588	01523	01459	01408	01339	01285	01241	01213	01190	01159	01137	01120	01105	01094
4.80	02646	02316	02086	01926	01802	01710	01621	01555	01490	01438	01368	01312	01268	01239	01215	01183	01161	01143	01128	01117
4.85	02684	02352	02122	01962	01837	01745	01654	01587	01521	01466	01396	01340	01294	01265	01240	01208	01185	01167	01152	01140
4.90	02722	02389	02159	01998	01872	01779	01687	01619	01552	01498	01425	01368	01321	01291	01266	01232	01209	01191	01173	01163
4.95	02759	02427	02195	02033	01907	01813	01720	01652	01583	01529	01454	01396	01348	01317	01292	01257	01233	01215	01199	01187
5.00	02797	02464	02232	02069	01942	01848	01754	01685	01615	01559	01484	01424	01375	01344	01318	01283	01258	01239	01223	01210
5.05	02835	02501	02268	02105	01977	01883	01787	01717	01647	01590	01513	01453	01403	01371	01344	01308	01283	01263	01247	01234
5.10	02873	02538	02305	02141	02012	01918	01821	01751	01679	01621	01543	01481	01430	01398	01370	01334	01308	01288	01271	01258
5.15	02910	02575	02342	02178	02048	01953	01855	01784	01711	01653	01573	01510	01458	01428	01397	01359	01333	01313	01296	01283
5.20	02948	02613	02379	02214	02084	01988	01890	01817	01743	01684	01604	01540	01486	01453	01424	01385	01358	01338	01320	01307
5.25	02986	02650	02416	02251	02120	02023	01924	01851	01776	01716	01634	01569	01515	01480	01451	01412	01384	01363	01345	01332

Table 4.1, page 3.

Pseudo reduced pressure P_r	Pseudo reduced temperature T_r																			
	1.05	1.10	1.15	1.20	1.25	1.30	1.35	1.40	1.45	1.50	1.60	1.70	1.80	1.90	2.00	2.20	2.40	2.60	2.80	3.00
5.30	03024	02688	02453	02287	02156	02059	01959	01885	01809	01748	01665	01599	01543	01508	01478	01433	01410	01388	01371	01357
5.35	03061	02725	02490	02324	02192	02095	01994	01919	01842	01780	01696	01629	01572	01536	01506	01465	01436	01414	01396	01382
5.40	03099	02763	02527	02361	02228	02130	02029	01953	01875	01813	01727	01659	01601	01565	01534	01492	01462	01440	01422	01408
5.45	03137	02800	02565	02398	02264	02168	02064	01988	01908	01845	01758	01689	01630	01593	01562	01519	01489	01466	01447	01433
5.50	03175	02838	02602	02435	02301	02203	02099	02022	01942	01878	01790	01720	01660	01622	01590	01546	01515	01492	01474	01459
5.55	03213	02876	02639	02472	02338	02239	02135	02057	01976	01911	01821	01750	01690	01651	01618	01574	01542	01519	01500	01485
5.60	03250	02913	02677	02509	02374	02275	02170	02092	02010	01944	01853	01781	01720	01680	01647	01602	01569	01546	01526	01512
5.65	03288	02951	02715	02546	02411	02312	02206	02127	02044	01978	01886	01812	01750	01710	01676	01630	01597	01573	01553	01538
5.70	03326	02989	02752	02584	02448	02348	02242	02162	02078	02011	01918	01844	01780	01740	01705	01658	01624	01600	01580	01565
5.75	03364	03027	02790	02621	02485	02385	02278	02198	02113	02045	01951	01875	01810	01770	01734	01686	01652	01627	01607	01592
5.80	03402	03065	02828	02659	02522	02422	02314	02233	02147	02079	01983	01907	01841	01800	01764	01715	01680	01656	01634	01619
5.85	03440	03103	02866	02697	02560	02459	02350	02269	02182	02113	02016	01939	01872	01830	01794	01744	01708	01683	01662	01646
5.90	03478	03141	02904	02734	02597	02496	02387	02305	02217	02147	02049	01971	01903	01860	01824	01773	01737	01711	01690	01674
5.95	03516	03179	02942	02772	02635	02533	02423	02341	02253	02182	02083	02004	01935	01891	01854	01802	01765	01739	01718	01702
6.00	03554	03217	02980	02810	02672	02570	02460	02377	02288	02216	02116	02036	01966	01922	01884	01831	01794	01767	01746	01730
6.05	03592	03256	03018	02848	02710	02608	02497	02413	02323	02251	02150	02069	01998	01953	01914	01861	01823	01796	01774	01758
6.10	03630	03294	03056	02886	02748	02645	02534	02450	02359	02286	02184	02102	02030	01984	01945	01891	01852	01825	01803	01786
6.15	03668	03332	03094	02924	02786	02683	02571	02486	02395	02321	02218	02135	02062	02016	01976	01921	01882	01854	01832	01815
6.20	03706	03371	03133	02963	02824	02721	02608	02523	02431	02357	02252	02168	02095	02048	02007	01951	01911	01883	01861	01844
6.25	03745	03409	03171	03001	02862	02758	02646	02560	02467	02392	02286	02202	02127	02080	02038	01982	01941	01912	01890	01873
6.30	03783	03447	03210	03039	02900	02796	02683	02597	02503	02428	02321	02235	02160	02112	02070	02012	01971	01942	01919	01902
6.35	03821	03486	03248	03078	02938	02834	02721	02634	02540	02464	02356	02269	02193	02144	02102	02043	02001	01972	01949	01931
6.40	03860	03524	03287	03116	02977	02872	02758	02671	02577	02500	02391	02303	02226	02176	02134	02074	02032	02002	01979	01961
6.45	03898	03563	03325	03155	03015	02911	02796	02708	02613	02536	02426	02338	02259	02209	02166	02106	02062	02032	02009	01991
6.50	03936	03601	03364	03193	03053	02949	02834	02746	02650	02572	02461	02372	02293	02242	02198	02137	02093	02063	02039	02021
6.55	03974	03640	03403	03232	03092	02987	02872	02783	02687	02609	02497	02407	02326	02275	02230	02169	02124	02094	02069	02051
6.60	04013	03679	03441	03271	03131	03026	02910	02821	02724	02645	02532	02441	02360	02308	02263	02201	02155	02124	02100	02082
6.65	04051	03717	03480	03309	03170	03064	02948	02859	02762	02682	02568	02476	02394	02342	02296	02233	02187	02156	02131	02113
6.70	04090	03756	03519	03348	03208	03103	02987	02897	02799	02719	02604	02511	02429	02375	02329	02265	02218	02187	02162	02144
6.75	04128	03795	03558	03387	03247	03142	03025	02935	02837	02756	02640	02547	02463	02409	02362	02297	02250	02218	02193	02175
6.80	04167	03834	03597	03426	03286	03181	03064	02973	02875	02793	02677	02582	02498	02443	02395	02330	02282	02250	02224	02206
6.85	04205	03873	03636	03465	03325	03220	03102	03012	02912	02831	02713	02618	02532	02477	02429	02363	02314	02282	02256	02237
6.90	04244	03912	03675	03504	03364	03259	03141	03050	02950	02868	02750	02654	02567	02512	02463	02396	02347	02314	02288	02269
6.95	04283	03951	03714	03543	03404	03298	03180	03089	02988	02906	02786	02690	02603	02548	02497	02429	02379	02346	02320	02301
7.00	04321	03990	03763	03582	03443	03337	03219	03127	03027	02944	02823	02726	02638	02581	02531	02462	02412	02379	02352	02333
7.05	04360	04029	03793	03622	03482	03377	03258	03166	03065	02982	02861	02762	02673	02616	02565	02496	02445	02411	02384	02365
7.10	04399	04068	03832	03661	03522	03416	03297	03205	03104	03020	02898	02799	02709	02651	02600	02530	02478	02444	02417	02398
7.15	04437	04107	03871	03701	03561	03456	03336	03244	03142	03058	02935	02835	02745	02686	02635	02564	02512	02477	02450	02431
7.20	04476	04146	03911	03740	03601	03495	03376	03283	03181	03097	02973	02872	02781	02722	02669	02598	02545	02510	02483	02464
7.25	04515	04185	03950	03780	03640	03535	03415	03322	03220	03135	03010	02909	02817	02757	02705	02632	02579	02544	02516	02497
7.30	04554	04224	03989	03819	03680	03575	03455	03362	03259	03174	03048	02946	02853	02793	02740	02667	02613	02577	02549	02530
7.35	04593	04264	04029	03859	03720	03615	03495	03401	03298	03212	03086	02983	02890	02829	02775	02701	02647	02611	02583	02563
7.40	04632	04303	04069	03899	03760	03655	03534	03441	03337	03251	03124	03021	02926	02865	02811	02736	02682	02645	02617	02597
7.45	04671	04342	04108	03938	03800	03695	03574	03481	03376	03290	03163	03058	02963	02901	02847	02771	02716	02679	02651	02631
7.50	04710	04382	04148	03978	03840	03735	03614	03520	03416	03329	03201	03096	03000	02938	02883	02807	02751	02714	02685	02665
7.55	04749	04421	04188	04018	03880	03775	03654	03560	03455	03368	03240	03134	03037	02974	02919	02842	02786	02748	02719	02699
7.60	04788	04461	04227	04058	03920	03815	03695	03600	03495	03408	03278	03172	03075	03011	02955	02878	02821	02783	02754	02733
7.65	04826	04500	04267	04098	03960	03856	03735	03640	03535	03447	03317	03210	03112	03048	02992	02913	02856	02818	02789	02768
7.70	04865	04540	04307	04138	04000	03896	03775	03681	03575	03487	03356	03248	03150	03085	03028	02949	02891	02853	02823	02803
7.75	04904	04579	04347	04178	04041	03937	03816	03721	03615	03527	03395	03287	03188	03122	03063	02985	02927	02888	02859	02838
7.80	04944	04619	04387	04219	04081	03977	03856	03761	03655	03567	03433	03326	03228	03160	03102	03022	02963	02924	02894	02873
7.85	04983	04659	04427	04259	04122	04018	03897	03802	03695	03607	03474	03364	03264	03198	03139	03058	02999	02960	02929	02908
7.90	05022	04698	04467	04299	04162	04059	03937	03842	03736	03647	03513	03403	03302	03235	03176	03095	03035	02995	02965	02944
7.95	05061	04738	04507	04340	04203	04100	03978	03883	03776	03687	03553	03442	03340	03273	03214	03132	03071	03031	03001	02979
8.00	05101	04778	04548	04380	04244	04140	04019	03924	03817	03727	03593	03482	03379	03311	03251	03169	03108	03068	03037	03015
8.05	05140	04818	04588	04421	04285	04181	04060	03964	03857	03768	03633	03521	03418	03350	03289	03206	03145	03104	03073	03051
8.10	05179	04857	04628	04461	04328	04222	04101	04005	03898	03808	03673	03560	03457	03388	03327	03243	03182	03141	03110	03088
8.15	05219	04897	04668	04502	04367	04263	04142	04046	03939	03849	03713	03600	03496	03427	03365	03281	03219	03177	03146	03126
8.20	05258	04937	04708	04542	04408	04304	04184	04087	03980	03889	03754	03640	03535	03465	03404	03318	03256	03214	03183	03161
8.25	05298	04977	04749	04583	04449	04346	04225	04129	04021	03930	03794	03680	03574	03504	03442	03356	03293	03252	03220	03198
8.30	05337	05017	04789	04624	04490	04387	04266	04170	04062	03971	03835	03720	03614	03543	03481	03394	03331	03289	03257	03235
8.35	05377	05057	04830	04664	04531	04428	04308	04211	04103	04012	03875	03760	03653	03582	03520	03433	03369	03326	03294	03272
8.40	05416	05097	04870	04705	04573	04470	04349	04253	04144	04054	03916	03800	03693	03622	03559	03471	03407	03364	03332	03309
8.45	05456	05137	04911	04746	04614	04511	04391	04294	04186	04095	03957	03841	03732	03661	03598	03509	03445	03402	03369	03347
8.50	05496	05177	04951	04787	04656	04553	04433	04336	04227	04136	03998	03881	03773	03701	03637	03548	03483	03440	03407	03384

Table 4.1, page4.

Pseudo reduced pressure	Pseudo reduced temperature T_r																			
P_r	1.05	1.10	1.15	1.20	1.25	1.30	1.35	1.40	1.45	1.50	1.60	1.70	1.80	1.90	2.00	2.20	2.40	2.60	2.80	3.00
8.55	05535	05217	04992	04828	04697	04594	04474	04378	04269	04178	04039	03922	03813	03741	03677	03587	03522	03478	03445	03422
8.60	05575	05257	05032	04869	04739	04636	04516	04419	04310	04219	04081	03963	03854	03780	03716	03628	03560	03516	03483	03460
8.65	05614	05298	05073	04910	04780	04678	04558	04461	04352	04261	04122	04004	03894	03821	03756	03665	03599	03555	03522	03499
8.70	05654	05338	05114	04952	04822	04719	04600	04503	04394	04303	04163	04045	03935	03861	03796	03705	03638	03594	03560	03537
8.75	05694	05378	05155	04993	04863	04761	04642	04545	04436	04345	04205	04086	03976	03901	03836	03744	03677	03633	03599	03576
8.80	05734	05419	05195	05034	04905	04803	04684	04587	04478	04387	04247	04128	04017	03942	03876	03784	03717	03672	03638	03614
8.85	05774	05459	05236	05076	04947	04845	04726	04629	04520	04429	04289	04169	04058	03982	03917	03824	03756	03711	03677	03653
8.90	05814	05499	05277	05117	04989	04887	04768	04671	04562	04471	04331	04211	04099	04023	03957	03864	03796	03750	03716	03692
8.95	05854	05540	05318	05159	05030	04929	04810	04714	04604	04513	04373	04252	04140	04064	03998	03904	03836	03790	03756	03732
9.00	05894	05580	05359	05200	05072	04972	04852	04756	04647	04556	04415	04294	04181	04105	04039	03944	03876	03830	03795	03771
9.05	05934	05621	05400	05242	05114	05014	04895	04798	04689	04598	04457	04336	04223	04146	04079	03985	03916	03869	03833	03811
9.10	05974	05662	05441	05283	05156	05056	04937	04841	04732	04641	04500	04378	04265	04188	04121	04025	03956	03910	03875	03850
9.15	06014	05702	05483	05325	05198	05099	04980	04884	04774	04683	04542	04421	04307	04229	04162	04066	03996	03950	03915	03890
9.20	06054	05743	05524	05367	05241	05141	05023	04926	04817	04726	04585	04463	04348	04271	04203	04107	04037	03990	03955	03930
9.25	06094	05784	05565	05408	05283	05184	05065	04969	04860	04769	04628	04505	04391	04313	04245	04148	04078	04031	03995	03971
9.30	06134	05825	05606	05450	05325	05226	05108	05012	04903	04812	04670	04548	04433	04355	04286	04189	04119	04071	04036	04011
9.35	06174	05865	05648	05492	05367	05269	05151	05055	04946	04855	04713	04591	04475	04397	04328	04230	04160	04112	04077	04052
9.40	06215	05906	05689	05534	05410	05311	05194	05098	04989	04898	04756	04633	04518	04439	04370	04272	04201	04153	04118	04093
9.45	06255	05947	05731	05576	05452	05354	05237	05141	05032	04941	04799	04676	04560	04481	04412	04314	04242	04195	04159	04133
9.50	06295	05988	05772	05618	05494	05397	05280	05184	05075	04984	04843	04719	04603	04524	04454	04355	04284	04238	04200	04175
9.55	06335	06029	05814	05660	05537	05440	05323	05227	05118	05028	04886	04762	04646	04566	04497	04397	04325	04277	04241	04216
9.60	06376	06070	05855	05702	05579	05483	05366	05270	05162	05071	04929	04806	04689	04609	04539	04439	04367	04319	04283	04257
9.65	06416	06111	05897	05744	05622	05526	05409	05314	05205	05115	04973	04849	04732	04652	04582	04481	04409	04361	04324	04299
9.70	06456	06152	05938	05786	05665	05569	05452	05357	05249	05158	05016	04893	04775	04695	04625	04524	04451	04403	04366	04341
9.75	06497	06193	05980	05829	05707	05612	05495	05400	05292	05202	05060	04936	04818	04738	04668	04566	04493	04445	04408	04383
9.80	06537	06234	06022	05871	05750	05655	05539	05444	05336	05246	05104	04980	04862	04781	04711	04609	04536	04487	04450	04425
9.85	06578	06276	06063	05913	05793	05698	05582	05488	05380	05290	05148	05024	04905	04824	04754	04652	04578	04530	04493	04467
9.90	06618	06317	06105	05956	05835	05741	05626	05531	05424	05334	05192	05068	04949	04868	04797	04694	04621	04572	04533	04509
9.95	06659	06358	06147	05998	05878	05784	05669	05575	05467	05378	05236	05112	04993	04912	04841	04737	04664	04615	04578	04552
10.00	06699	06399	06189	06040	05921	05828	05713	05619	05511	05422	05280	05156	05037	04955	04884	04780	04707	04658	04621	04595
10.05	06740	06441	06231	06083	05964	05871	05756	05662	05556	05466	05324	05200	05081	04999	04928	04824	04750	04701	04664	04637
10.10	06780	06482	06273	06126	06007	05915	05800	05706	05600	05510	05369	05244	05125	05043	04972	04867	04793	04744	04707	04680
10.15	06821	06523	06315	06168	06050	05958	05844	05750	05644	05555	05413	05289	05169	05087	05016	04911	04837	04787	04750	04724
10.20	06862	06565	06357	06211	06093	06002	05888	05794	05688	05599	05457	05333	05214	05131	05060	04954	04880	04831	04793	04767
10.25	06902	06606	06399	06253	06136	06045	05932	05839	05733	05644	05502	05378	05258	05176	05104	04998	04924	04875	04837	04811
10.30	06943	06648	06441	06296	06179	06089	05976	05883	05777	05688	05547	05422	05303	05220	95148	05042	04968	04918	04881	04854
10.35	06984	06689	06483	06339	06223	06133	06020	05927	05821	05733	05592	05467	05347	05265	05193	05088	05012	04962	04925	04898
10.40	07025	06731	06525	06382	06266	06176	06064	05971	05866	05778	05636	05512	05392	05310	05237	05131	05056	05006	04969	04942
10.45	07065	06772	06567	06425	06309	06220	06108	06016	05911	05823	05681	05557	05437	05354	05282	05175	05100	05051	05013	04986
10.50	07106	06814	06610	06467	06353	06264	06152	06060	05955	05868	05727	05602	05482	05399	05327	05219	05145	05095	05057	05030
10.55	07147	06855	06652	06510	06396	06308	06196	06105	06000	05912	05772	05647	05527	05444	05372	05264	05189	05140	05102	05075
10.60	07188	06897	06694	06553	06440	06352	06240	06149	06045	05957	05817	05693	05573	05490	05417	05309	05234	05184	05146	05119
10.65	07229	06939	06736	06596	06483	06396	06285	06194	06090	06003	05862	05738	05618	05535	05462	95354	05279	05229	05191	05164
10.70	07270	06980	06779	06639	06527	06440	06329	06239	06135	06048	05908	05784	05664	05580	05507	05399	05324	05274	05236	05209
10.75	07310	07022	06821	06682	06570	06484	06374	06283	06180	06093	05953	05829	05709	05626	05553	05444	05369	05319	05281	05254
10.80	07351	07064	06864	06726	06614	06528	06418	06328	06225	06138	05999	05875	05755	05671	05598	05489	05414	05364	05326	05299
10.85	07392	07106	06906	06769	06658	06572	06463	06373	06270	06184	06045	05921	05801	05717	05644	05535	05459	05410	05372	05344
10.90	07433	07148	06949	06812	06701	06616	06507	06418	06316	06229	06090	05967	05847	05763	05690	05580	05505	05455	05417	05390
10.95	07474	07190	06991	06855	06745	06661	06552	06463	06361	06275	06136	06013	05893	05809	05735	05626	05551	05501	05463	05435
11.00	07515	07231	07034	06898	06789	06705	06597	06508	06406	06320	06182	06059	05939	05855	05781	05672	05597	05547	05509	05481
11.05	07556	07273	07077	06942	06833	06749	06642	06553	06452	06366	06228	06105	05985	05901	05827	05718	05643	05593	05555	06527
11.10	07597	07315	07119	06985	06877	06794	06686	06599	06497	06412	06274	06151	06031	05947	05873	05764	05689	05639	05601	06573
11.15	07638	07357	07162	07028	06921	06838	06731	06644	06543	06458	06320	06197	06078	05993	05920	05810	05735	05685	05647	06619
11.20	07680	07399	07205	07072	06965	06882	06776	06689	06589	06503	06366	06244	06124	06040	05966	05857	05781	06731	05693	06665
11.25	07721	07441	07247	07115	07009	06927	06821	06735	06634	06549	06413	06290	06171	06086	06013	05903	05828	05778	05740	06712
11.30	07762	07483	07290	07158	07053	06972	06866	06780	06680	06595	06459	06337	06217	06133	06059	05950	05874	05825	05786	06758
11.35	07803	07525	07333	07202	07097	07016	06911	06826	06726	06642	06505	06383	06264	06180	06106	05998	05921	05871	05833	06806
11.40	07844	07568	07376	07245	07141	07061	06956	06871	06772	06688	06552	06430	06311	06227	06153	06043	05968	05918	05880	06853
11.45	07885	07610	07419	07289	07185	07106	07002	06917	06818	06734	06599	06477	06358	06274	06200	06090	06015	05965	05927	06900
11.50	07927	07652	07462	07332	07229	07150	07047	06962	06864	06780	06645	06524	06405	06321	06247	06137	06062	06012	05974	06947
11.55	07968	07694	07505	07376	07273	07195	07092	07008	06910	06827	06692	06571	06452	06368	06294	06185	06109	06060	06022	06994
11.60	08009	07736	07548	07420	07317	07240	07137	07054	06956	06873	06739	06618	06499	06415	06341	06232	06157	06107	06069	06042
11.65	08051	07779	07591	07463	07362	07285	07183	07100	07002	06919	06785	06665	06547	06463	06389	06279	06204	06154	06117	06089
11.70	08092	07821	07634	07507	07406	07330	07228	07146	07048	06966	06832	06712	06594	06510	06436	06327	06252	06202	06164	06137
11.75	08133	07863	07677	07551	07450	07375	07274	07192	07095	07013	06879	06760	06641	06556	06484	06375	06300	06250	06212	06185

Table 4.1, page 5.

Pseudo reduced pressure P_r	Pseudo reduced temperature T_r									Pseudo reduced Temperature T_r				Pseudo reduced temperature T_r					
	1.05	1.10	1.15	1.20	1.25	1.30	1.35	1.40	1.45	1.50	1.60	1.70	1.80	1.90	2.00	2.20	2.40	2.60	2.80	3.00
11.80	08175	07905	07720	07595	07495	07420	07319	07238	07141	07059	06928	06807	06689	06605	06532	06422	06347	06298	06260	06233
11.85	08216	07948	07763	07638	07539	07465	07365	07284	07188	07106	06974	06854	06737	06653	06579	06470	06395	06346	06308	06281
11.90	08258	07990	07806	07682	07584	07510	07410	07330	07234	07153	07021	06902	06785	06701	06627	06518	06443	06394	06356	06330
11.95	08299	08033	07849	07726	07628	07555	07456	07376	07281	07200	07068	06950	06832	06749	06675	06566	06492	06442	06405	06378
12.00	08341	08075	07892	07770	07673	07600	07502	07422	07327	07246	07115	06997	06880	06797	06723	06615	06540	06491	06453	06427
12.05	08382	08117	07935	07814	07718	07646	07548	07469	07374	07293	07163	07045	06928	06845	06772	06663	06589	06540	06502	06475
12.10	08424	08160	07979	07858	07762	07691	07593	07515	07421	07340	07210	07093	06976	06893	06820	06712	06637	06588	06551	06524
12.15	08465	08202	08022	07902	07807	07736	07639	07561	07468	07387	07258	07141	07025	06942	06868	06760	06686	06637	06600	06573
12.20	08507	08245	08065	07946	07852	07781	07685	07608	07515	07435	07305	07189	07073	06990	06917	06809	06735	06686	06649	06622
12.25	08549	08287	08108	07990	07896	07827	07731	07654	07561	07482	07353	07237	07121	07038	06966	06858	06784	06735	06698	06671
12.30	08590	08330	08152	08034	07941	07872	07777	07701	07608	07529	07401	07285	07170	07087	07015	06907	06833	06785	06747	06721
12.35	08632	08373	08195	08078	07986	07918	07823	07748	07655	07576	07449	07333	07218	07136	07063	06956	06883	06834	06797	06770
12.40	08674	08415	08238	08123	08031	07963	07869	07794	07703	07624	07497	07382	07267	07185	07112	07005	06932	06883	06846	06820
12.45	08715	08458	08282	08167	08076	08009	07916	07841	07750	07671	07544	07430	07316	07233	07162	07055	06981	06933	06896	06870
12.50	08757	08500	08325	08211	08121	08054	07962	07888	07797	07719	07592	07479	07364	07282	07211	07104	07031	06983	06946	06919
12.55	08799	08543	08369	08255	08166	08100	08008	07935	07844	07766	07641	07527	07413	07332	07260	07154	07081	07033	06996	06969
12.60	08840	08586	08412	08300	08211	08145	08054	07981	07891	07814	07689	07576	07462	07381	07309	07204	07131	07083	07046	07020
12.65	08882	08628	08456	08344	08256	08191	08101	08028	07939	07862	07737	07624	07511	07430	07359	07253	07181	07133	07096	07070
12.70	08924	08671	08499	08388	08301	08237	08147	08075	07986	07909	07785	07673	07560	07479	07409	07303	07231	07183	07147	07120
12.75	08966	08714	08543	08433	08346	08282	08194	08122	08034	07957	07833	07722	07609	07529	07458	07353	07281	07234	07197	07171
12.80	09008	08757	08586	08477	08391	08328	08240	08169	08081	08005	07882	07771	07659	07579	07508	07403	07332	07284	07248	07222
12.85	09050	08800	08630	08521	08436	08374	08287	08217	08129	08053	07930	07820	07708	07628	07558	07454	07382	07335	07299	07272
12.90	09091	08842	08673	08566	08481	08420	08333	08264	08176	08101	07979	07869	07758	07678	07608	07504	07433	07386	07349	07323
12.95	09133	08885	08717	08610	08526	08466	08380	08311	08224	08149	08027	07918	07807	07728	07658	07555	07484	07437	07400	07374
13.00	09175	08928	08761	08655	08571	08512	08427	08358	08272	08197	08076	07967	07857	07778	07708	07605	07535	07488	07452	07426
13.05	09217	08971	08804	08699	08617	08557	08473	08406	08319	08245	08125	08017	07906	07828	07758	07656	07586	07539	07503	07477
13.10	09259	09014	08848	08744	08662	08603	08520	08453	08367	08293	08173	08066	07956	07878	07809	07707	07637	07590	07554	07528
13.15	09301	09057	08892	08789	08707	08649	08567	08500	08415	08341	08222	08116	08006	07928	07859	07758	07688	07642	07606	07580
13.20	09343	09100	08935	08833	08753	08696	08614	08548	08463	08390	08271	08165	08056	07978	07910	07809	07739	07693	07658	07632
13.25	09385	09143	08979	08878	08798	08742	08660	08595	08511	08438	08320	08215	08106	08029	07961	07860	07791	07745	07709	07684
13.30	09427	09186	09023	08923	08843	08788	08707	08643	08559	08486	08369	08264	08156	08079	08011	07911	07842	07797	07761	07736
13.35	09470	09229	09067	08967	08889	08834	08754	08690	08607	08535	08418	08314	08206	08130	08062	07963	07894	07849	07813	07788
13.40	09512	09272	09111	09012	08934	08880	08801	08738	08655	08583	08467	08364	08257	08180	08113	08014	07946	07901	07866	07840
13.45	09554	09315	09154	09057	08980	08926	08848	08786	08704	08632	08516	08414	08307	08231	08164	08066	07998	07953	07918	07892
13.50	09596	09358	09198	09102	09025	08973	08895	08833	08752	08681	08566	08464	08357	08282	08215	08117	08050	08006	07970	07945
13.55	09638	09401	09242	09146	09071	09019	08942	08881	08800	08729	08615	08514	08408	08333	08267	08169	08102	08058	08023	07997
13.60	09680	09444	09285	09191	09116	09065	08990	08929	08848	08778	08664	08564	08458	08384	08318	08221	08155	08111	08075	08050
13.65	09723	09487	09330	09236	09162	09112	09037	08977	08897	08827	08714	08614	08509	08435	08369	08273	08207	08163	08128	08103
13.70	09765	09530	09374	09281	09208	09158	09084	09025	08945	08876	08763	08664	08560	08486	08421	08326	08260	08216	08181	08156
13.75	09807	09573	09418	09326	09253	09204	09131	09073	08994	08925	08813	08715	08610	08537	08472	08378	08312	08269	08234	08209
13.80	09849	09616	09462	09371	09299	09251	09179	09121	09042	08974	08862	08765	08661	08588	08524	08430	08365	08322	08287	08262
13.85	09892	09659	09506	09416	09345	09297	09226	09169	09091	09023	08912	08815	08712	08640	08576	08483	08418	08375	08341	08316
13.90	09934	09703	09550	09461	09390	09344	09273	09217	09140	09072	08962	08866	08763	08691	08628	08535	08471	08429	08394	08369
13.95	09976	09746	09594	09506	09436	09391	09321	09265	09188	09121	09011	08916	08814	08743	08680	08588	08525	08482	08447	08423
14.00	10019	09789	09638	09551	09482	09437	09368	09313	09237	09170	09061	08967	08866	08795	08732	08641	08578	08536	08501	08477
14.05	10061	09832	09682	09596	09528	09484	09416	09361	09286	09219	09111	09018	08917	08846	08784	08694	08631	08589	08555	08531
14.10	10103	09875	09727	09641	09574	09530	09463	09409	09335	09268	09161	09069	08968	08898	08836	08747	08685	08643	08609	08585
14.15	10146	09919	09771	09687	09620	09577	09511	09458	09384	09318	09211	09119	09019	08950	08889	08800	08738	08697	08663	08639
14.20	10188	09962	09815	09732	09668	09624	09558	09506	09432	09367	09261	09170	09071	09002	08941	08853	08792	08751	08717	08693
14.25	10231	10005	09859	09777	09712	09671	09606	09554	09481	09417	09311	09221	09122	09054	08994	08907	08846	08805	08771	08747
14.30	10273	10049	09903	09822	09758	09717	09654	09603	09530	09466	09362	09272	09174	09106	09047	08960	08900	08860	08826	08802
14.35	10316	10092	09948	09867	09804	09764	09701	09651	09580	09516	09412	09324	09226	09158	09099	09014	08954	08914	08880	08856
14.40	10358	10135	09992	09913	09850	09811	09749	09700	09629	09565	09462	09375	09277	09211	09152	09068	09008	08969	08935	08911
14.45	10401	10179	10036	09958	09896	09858	09797	09748	09678	09615	09512	09426	09329	09263	09205	09121	09063	09023	08990	08966
14.50	10443	10222	10081	10003	09942	09905	09845	09797	09727	09664	09563	09477	09381	09316	09258	09175	09117	09078	09044	09021
14.55	10486	10266	10125	10049	09988	09952	09892	09846	09776	09714	09613	09529	09433	09368	09311	09229	09172	09133	09099	09076
14.60	10528	10309	10169	10094	10034	09999	09894	09894	09825	09764	09664	09580	09485	09421	09364	09283	09226	09188	09155	09131
14.65	10571	10352	10214	10139	10080	10046	09988	09943	09875	09814	09714	09632	09537	09473	09418	09338	09281	09243	09210	09186
14.70	10614	10396	10258	10183	10126	10093	10036	09992	09924	09864	09765	09683	09589	09526	09471	09392	09336	09298	09265	09242
14.75	10656	10439	10302	10230	10173	10140	10084	10041	09973	09914	09816	09735	09641	09579	09524	09446	09391	09353	09321	09297
14.80	10699	10483	10347	10275	10219	10187	10132	10089	10023	09964	09866	09787	09694	09632	09578	09501	09446	09409	09376	09353
14.85	10742	10526	10391	10321	10265	10234	10180	10138	10072	10014	09917	09838	09746	09685	09632	09556	09501	09464	09432	09409
14.90	10784	10570	10436	10366	10311	10281	10228	10187	10122	10064	09968	09890	09798	09738	09685	09610	09557	09520	09488	09465
14.95	10827	10613	10480	10412	10358	10328	10276	10236	10171	10114	10019	09942	09851	09791	09739	09665	09612	09576	09544	09521
15.00	10870	10657	10525	10457	10404	10375	10324	10285	10221	10164	10070	09994	09904	09845	09793	09720	09668	09632	09600	09577

SECTION 5
EXTRAPOLATION OF MEASURED OPEN FLOW RATES

5.1 Introduction

It is common practice in the petroleum industry to maintain updated graphical records of producing rates plotted versus time, among other possible variables. The producing rates may be on well, lease, reservoir or field bases. Plots of production rate versus time are called "decline curves" even though there may be periods of rate increases. The main use of decline curves is to predict future producing rates and ultimate recovery by extrapolating past producing rate history into the future. In the case of well blowouts, where a period of unmeasured blowout rates is followed by a period of measured blowout rates, it is just as reasonable to extrapolate into the past.

The extrapolation of decline curves, into either the past or the future may be done by drawing a trend line or curve through the data from which the extrapolation is made. Because extrapolation of straight or nearly straight lines is more reliable than extrapolating curved lines, an attempt is usually made to discover a type of plot which produces a straight line, or one nearly straight. These techniques are discussed in Ref. 5.1 , and will not be repeated here.

A more objective approach to extrapolation is by curve fitting in which a variety of mathematical forms relating flow rate and time is explored to find the one which fits the data with the smallest deviation. In this method, as in graphical "eyeball" extrapolation, it is often observed that the earlier and later portions of the data appear to have different trends. In this case, of course, it is reasonable to use the later portion of the data to forcast future rates, and the earlier portion to backcast.

5.2 Diverting Blowouts

Blowout wells are often brought under control by capping. In this procedure a section of pipe containing a full opening valve or valves is positioned over the flow stream so that it flows through the pipe section and valve(s). The pipe section is sealed to the well casing after which closing the valve brings the well under control.

In some cases it is feared that closing the valve will cause an underground blowout, i.e., gas will flow from the blowout formation to another, usually much shallower, formation or to the surface around (outside of) the casing. In other cases it is feared that the casing to which the cap is attached will not withstand the pressure when the valve is closed. In these cases the capping section is provided with side outlets or diverter lines below the valve(s), so that when the valve is closed, the stream is diverted away from the well. Now it is possible to place a rig over the well and using snubbing procedures to get pipe down the well through which heavy mud or cement may be pumped to kill the well or to complete it as a producing well.

A similar situation exists where the blowout preventers are closed and the well blows through diverter or blooie lines, whose valves are not closed, as explained above, for fear of casing rupture, failure of the blowout preventers, and/or underground blowouts. In some cases the diverted gas is flared and in others it is captured for sales. In the former case it is possible under some circumstances to estimate flow rate from the pressure in the diverter or blooie line, as discussed in Section 4. Where the gas is sold, it is of course measured. In both of these cases it may be some time after start of blowout before flow rates are measured, and rates during this period can be estimated using extrapolation techniques.

5.3 Example Illustrating Extrapolation

Many mathematical forms are used to define decline curves: linear, exponential, polynomial, hyperbolic, harmonic, etc. The most commonly used form is the exponential decline, i.e., one in which flow rate declines exponentially with time and therefore plots as a straight line on semilog paper, rate plotted on the log scale. Example 5.1 illustrates the extrapolation of measured blowout rates to estimate rates prior to the installation of measurement devices.

Example 5.1

A diverter installation was completed on a blowing gas well 18 days after start of blowout. During the following 25 days gas was flowed into a pipeline while snubbing operations were in progress to kill the well. Flow rate data was available for only 10 of the last 25 days before the well was brought under control:

DAYS	19	21	24	27	29	32	35	37	41	43
MMSCF/D	48.2	49.1	49.2	42.8	45.0	41.9	39.3	36.2	36.7	35.1

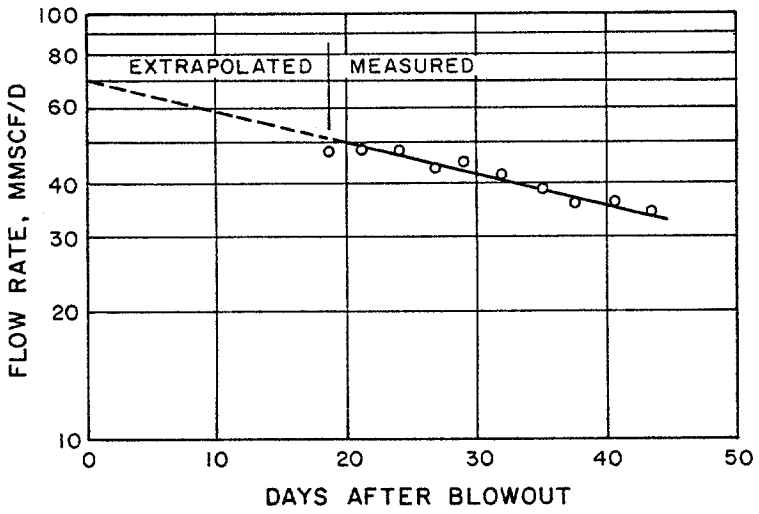

Fig. 5.1. Plot of flow rate data for Example 5.1.

Solution—Graphical

1. Plot the data on semilog paper, Fig. 5.1.
2. Draw a straight line through the data points, and extrapolate to t=0 and t=50.

   Read: q=70.0 MMSCF/D for t=0 days
   q=30.0 MMSCF/D for t=50 days

   Solve for q_o and a in $q = q_o e^{-at}$

   For t = 0, $70 = q_o e^{-a(0)}$ or $q_o = 70$

   For t = 50, $30 = 70e^{-a(50)}$ and $a = 0.017 \text{ days}^{-1}$

3. Vented gas during first 18 days

$$Q = \frac{q_o - q_{18}}{a}$$

$$= \frac{70.0-51.0}{0.017}$$

$$= 1120 \text{ MMSCF}$$

4. Vented gas during last 25 days

$$Q = \frac{q_{18} - q_{43}}{a}$$

$$Q = \frac{51.0-34.0}{0.017}$$

$$Q = 1000 \text{ MMSCF}$$

Solution-Analylical

Use the method of Least Squares to calculate the equation of the straight line (semilog plot) which best fits the data. Using $q=q_o e^{-at}$ as the basic form and $\ln q=\ln q_o+at$ as the linear equivalent, the Least Square equations are:

$$\Sigma \ln q = n \ln q_o + a\Sigma t$$

$$\Sigma t \ln q = \ln q_o \Sigma t + a \Sigma t^2$$

For the example: n=10, $\Sigma \ln q=37.385$; $\Sigma t=308$; and $\Sigma t=10{,}096$. Placing these values in the above equations:

$$37.385 = 10 \ln q_o + 308a$$

$$1142.3 = 308 \ln q_o + 10096a$$

These solve to yield $q_o=67.3$ MMSCF/D and $a=-0.0151$ days^{-1}. Using these values the calculated values of q(18 day)=51.3 MMSCF/D and q(43 days)=35.2 MMSCF/D. Then the gas vented during the first 18 days is calculated as

$$Q = (67.3-51.3)/0.0151 = 1060 \text{ MMSCF}$$

and that during the last 25 days as

$$Q = (51.3-35.2)/0.0151 = 1066 \text{ MMSCF}.$$

5.4 Error Analysis

With data of the quantity and quality of that given in Example 5.1, the calculated vented gas volume during the first 18 days should be within five percent. This assumes that the flow rate is declining during those first 18 days at the same exponential rate as in the later 25 days. There is, of course, no assurance that this is true, although it is a most reasonable assumption. There are factors which could cause the flow rate in the early days to be either higher or lower than the extrapolated values.

The accuracy of the extrapolation may be improved by fitting a curve to the data, using statistical techniques such as the method of Least Squares, as shown in Example 5.1. Such techniques are also useful where there are larger and most erratic fluctuations in the data. They provide an objective calculation of the best fit of a line or curve to the data points as opposed to the "eyeball" method.

Some consideration should be given to the effect of installing a diverter line on the well and to the effect of connecting the diverter line into a pipeline into which the gas must flow against the prevailing pipeline pressure. The calculation methods of Example 8.1 are available for evaluating the effect of these.

Section 6
ESTIMATES FROM BACK PRESSURE TESTS

6.1 Introduction

Extrapolation of back pressure tests of gas wells at low rates is used in regulatory work to determine the open flow capacity (rate). The open flow capacity is the rate at which a well would flow if the flowing bottom hole pressure were atmospheric, i.e., if there were no flow string resistance, only formation resistance. Open flow capacities are therefore estimates of maximum rates during blowouts.

Back pressure testing consist of flowing a well at several successive rates and measuring at each rate the flowing bottom hole pressure, the flowing well head pressure and the flow rate. The static reservoir pressure is also measured or calculated from measured static well head pressures. The theory and practice of back pressure testing is discussed in Refs. 6.1-6.3.

The data from a back pressure test are plotted on log-log paper with flow rate as abscissa versus the differences of the squares of the static and flowing bottom hole absolute pressures. In most cases the data plot as a straight line, and extrapolate to the open flow capacity, i.e., flowing bottom hole pressure equal to atmospheric pressure.

The results of back pressure tests are useful in calculating the rate at which gas wells can flow against any surface (back) pressure. With proper caution, these tests can also be of use in estimating blowout rates; particularly if a test has been made on a well which later blew out, or with less precision on a well using back pressure tests from other wells producing from the same reservoir.

6.2 Back Pressure Test Theory

The formula for the steady-state, radial flow of gases in the reservoir in the laminar regime is basic to most back pressure test theory. It is derived in Ref. 6.2 as

$$q_{sc} = \frac{703\ k\ h\ (p_e^2 - p_w^2)}{\mu\ T\ z\ \ln\ (r_e/r_w)} \qquad (6.1)$$

Equation (6.1) predicts that a plot of flow rate versus the difference of the squares of the pressures on log-log paper will give a straight line whose slope is 45^0. Experience shows that for the data from many wells this is true, particularly at lower flow rates. For other wells and at higher flow rates the slope is usually less than 45^0 and the formula of Eq. (6.1) is modified as

$$q_{sc} = \frac{703\ k\ h\ (p_e^2 - p_w^2)^n}{\mu\ T\ z\ \ln\ (r_e/r_w)} \qquad (6.2)$$

The need for the exponent n in Eq. (6.2) is usually explained by the occurrence of turbulent flow in the formation. At low flow rates the regime is laminar and n = 1. At higher rates turbulent flow begins in the vicinity of the well, where gas velocities are highest. As flow rate is increased, the turbulent zone extends further into the formation, and under open flow conditions a considerable portion of the drainage area is in turbulent flow.

The back pressure formula is therefore written as

$$q_{sc} = C(p_e^2 - p_w^2)^n \qquad (6.3)$$

From Eq. (6.2) the coefficient C is a characteristic of each well and its drainage area, and includes the geometry (h, r_e and r_w), gas characteristics (μ and z), and formation permeability and temperature (k and T). As the values of some of these parameters are difficult to determine individually, they are grouped in the coefficient C.

Taking the logarithm of both sides of Eq. (6.3), it becomes

$$\log q_{sc} = \log C + n \log(p_e^2 - p_w^2) \qquad (6.4)$$

Figure 6.1 is a typical plot of data taken in a back pressure test. For a slope of 40^0, n=tan 40^0=0.839.

Extrapolation from the measured data to a flowing bottom hole pressure of 14.7 psia yields an open flow capacity of 53 MMSCF/D. It should be realized that the open flow capacity is a theoretical figure used for practical purposes, by regulatory bodies to deter-

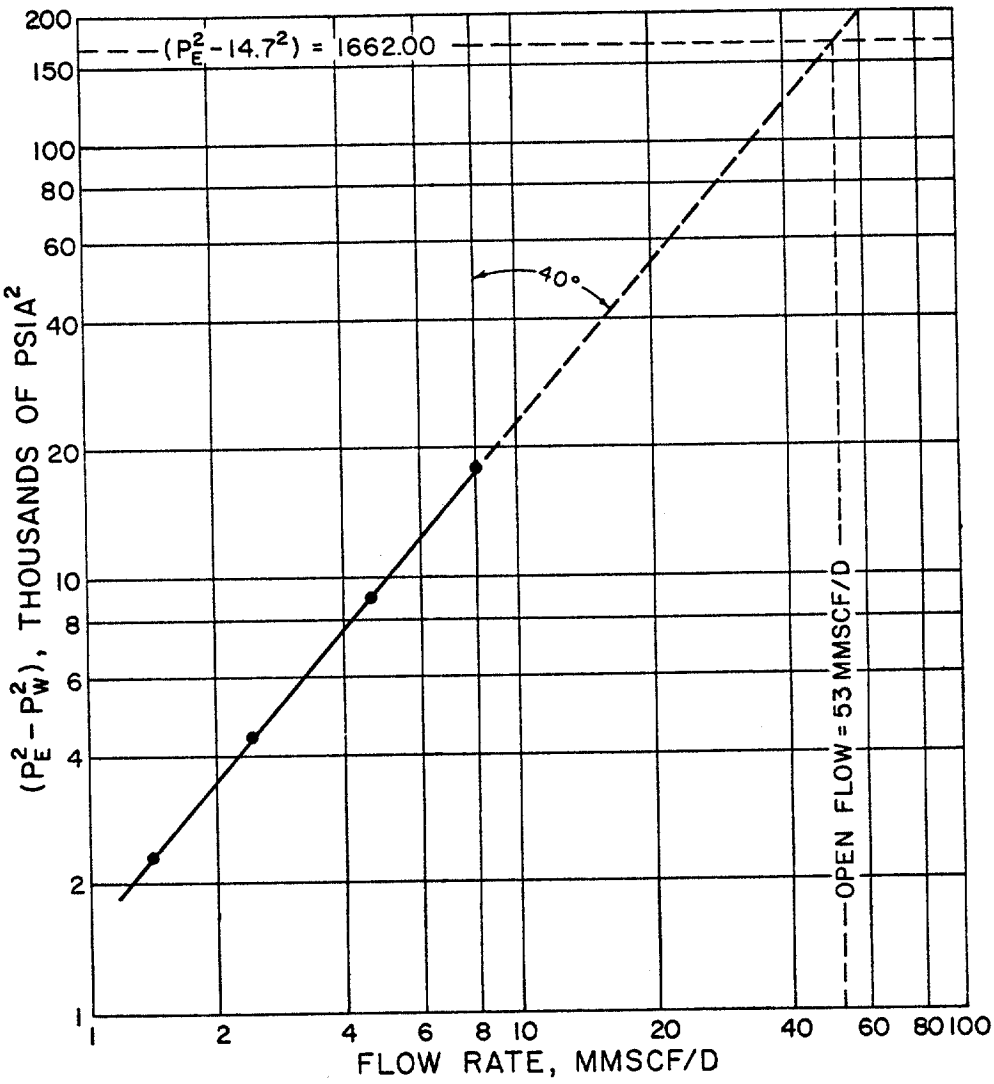

Fig. 6.1. Typical back pressure data plot with extrapolation to find open flow capacity p_e=1290psia.

mine allowables. The extrapolation assumes the constancy of the exponent n, i.e., an unchanging flow regime, and also the constancy of flowing temperature, gas viscosity and gas deviation factor.

In back pressure testing, the flow at a selected rate should be continued long enough for the reservoir to closely approach steady state conditions. Whenever stabilization cannot be reached within a reasonable period of time because of reservoir conditions, or when flow rates of sufficient duration to reach stabilized conditions are impractical, the constant time multipoint test (Refs. 6.5, 6.6 and 6.7) or the isochronal method (Ref. 6.6) should be used. Both methods are devised to give the coefficient C and the exponent n.

6.3 Estimation of Blowout Rate from Back Pressure Tests on the Blowout Well

In the above discussion it was pointed out that the blowout rate of a gas well will be lower, generally much lower, than the open flow capacity of the well because of two factors. One of these is the increasing importance of turbulence at higher flow rates, where test data are usually not taken. The other is the flow string resistance, which is not included in the back pressure test which measures only formation resistance.

Some idea of the importance of these factors can be understood from a theoretical study by Elenbaas and Katz, Ref. 6.3. This study pertained to a well 5000 feet deep with a static reservoir pressure of 2100 psia. Flow was through a casing of 6-5/8 inches I.D. The formation porosity was 26 percent for a Wilcox sand of 48-65 mesh for which permeability and turbulence characteristics were determined by laboratory tests. Calculations were placed on one foot of formation thickness for a gas gravity of 0.65 (Air=1) and a reservoir temperature of 115^0F.

The solid line of Fig. 6.2 is the calculated back pressure plot. Note that in the low flow rate range the slope is 45^0 (n=1.00) and that it increases progressively through the so called transition (partially turbulent) range to the almost fully turbulent range where the slope approaches 60^0 (n=0.5).

At 50 MMSCF/D the friction of the flow string caused the flowing bottom hole pressure to be approximately 1500 psia. Thus, the blowout rate is determined as 50 MMSCF/D and not some considerably higher rate, the open flow capacity, taken where flowing bottom hole pressure is assumed to be atmospheric.

Figure 6.2 also shows the error of extrapolating back pressure data taken in the laminar or laminar-turbulent transition range to estimate either open flow capacities or blowout rates. Although data taken over a limited range of flow rates usually appears to be linear on the log-log plot, over a wide range the data plot as a curve as shown in Fig. 6.2. Table I gives an idea of the overestimation of blowout rates from improper extrapolation.

In some back pressure tests the data do not plot as or near to a straight line on log-log paper. In most of these cases the data are usually erratic, and where four or more data points are available there

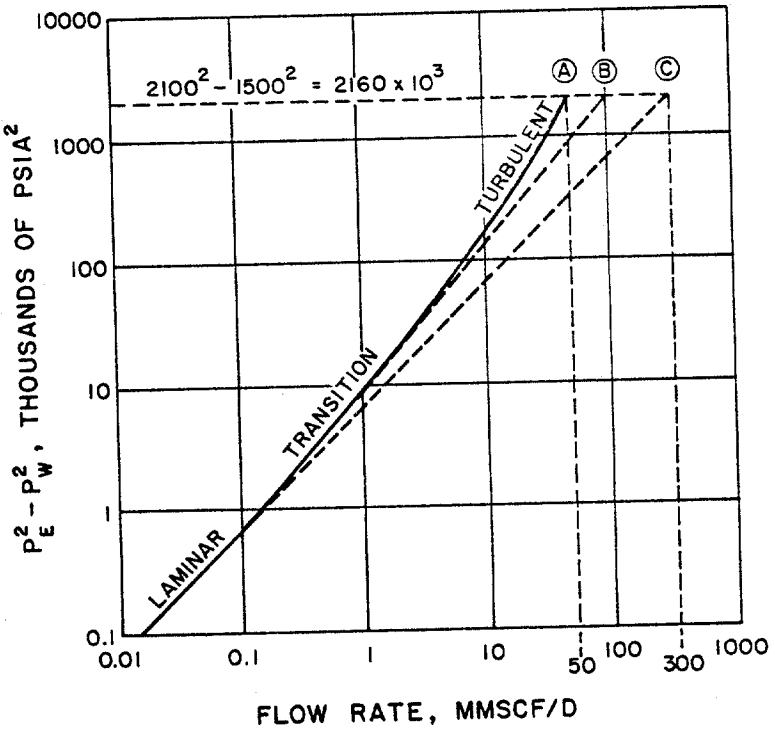

Fig.6.2 Back pressure curve covering laminar through full turbulent flow in the reservoir.

Table I

Line (Fig. 4.2)	A	B	C
Est'd Blowout Rate	50	100	300
Percent Overestimation	0	100	600

is no reasonably smooth trend line which can be drawn through the data. The usual explanation for this behavior is formation damage which varies with flow rate.

Graham and Boyd, Ref. 6.4, have shown that back pressure tests on a number of Gulf Coast wells taken shortly after completion may not be reliable for predicting later flow performance, that both the coefficient C and the exponent n of Eq. (6.3) may change during production. These wells were generally found to have better flow characteristics after weeks or months of production during which the well was cleaned of formation damages during drilling and/or completion.

In view of the foregoing it is obvious that back pressure test data obtained on a well prior to blowout should be used with caution in estimating the well's blowout rate. Use of stabilized back pressure data

without these considerations will generally result in an overestimation of the blowout rate by as much as several hundred percent.

6.4 Use of Back Pressure Tests on Other Wells in the Same Reservoir

Section 6.3 discussed the problems of using back pressure data on the blowout well to estimate its subsequent blowout rate. Let us now consider the additional difficulty of using back pressure data, not from the blowout well, but from other wells completed in the same reservoir.

The flow performance of a gas well depends on several parameters. These parameters are classified into two groups. The first group include parameters which can reasonably be assumed to remain essentially the same at different wells in the same reservoir, such as:

1. shut-in pressure
2. reservoir temperature
3. average gas viscosity
4. gas deviation factor

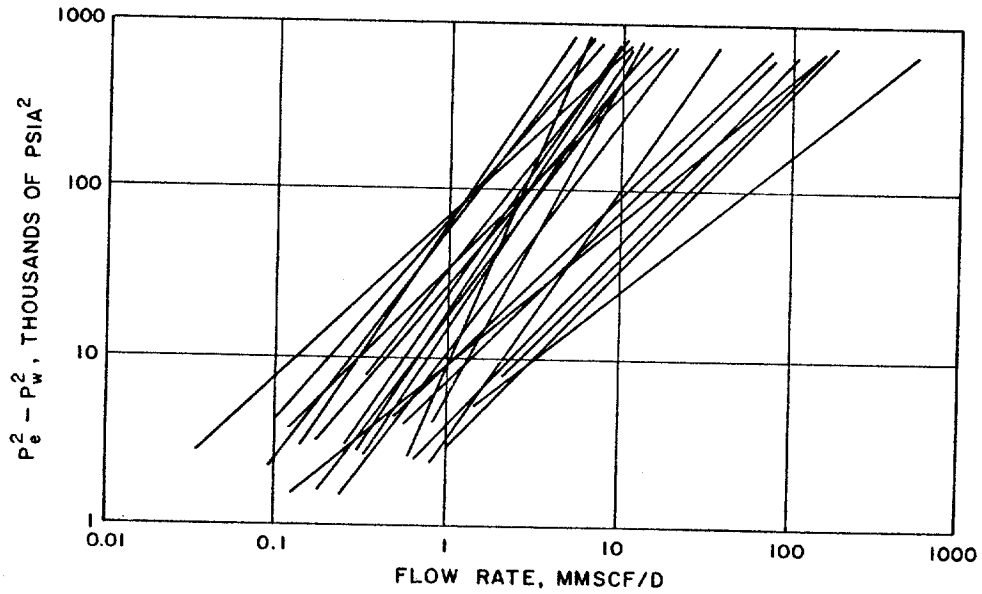

Fig. 6.3. Back pressure data on 23 wells in one field. (After Rawlins and Schellhardt, Ref. 6.1. Courtesy U.S. Bureau of Mines.)

The second group includes parameters that are more likely to vary, sometimes drastically. Some of these parameters are:

1. formation thickness
2. formation permeability
3. formation damage (skin)
4. well stimulation
5. drainage radius
6. effective well radius
7. type of completion

It should be expected, therefore, that wells producing from the same reservoir will exhibit different flow characteristics. Figure 6.3 after Rawlins and Schellhardt (Ref. 6.1), shows the results of back pressure tests on 23 wells in one field, presumably completed in the same reservoir. Although it is likely that a study of the available data would explain some of the differences among the wells, it appears that at least a ten-fold variation exists in the open flow capacity of these wells.

6.5 Illustrative Example

A gas well blew out of control for 10 days. The back pressure equation describing flow in an offset well where sand thickness averaged 38 feet is

$$q = 1.24(p_e^2 - p_w^2)^{0.74}$$

where q is in MSCF/D. Assuming the same value of the exponent for the wild well, its back pressure equation may be written as

$$q = C(p_e^2 - p_w^2)^{0.74}$$

From Eqs (6.2) and (6.3) we may write

$$\frac{C}{h} = \frac{703\ k}{\mu\ T\ z\ \ln(r_e/r_w)}$$

Assuming k, μ, T, z, r_e and r_w are the same for both wells, C for the blowout well will be that for the offset well increased by the ratio of the formation thicknesses at the two wells. As formation thickness at the blowout well was determined to be 57 feet,

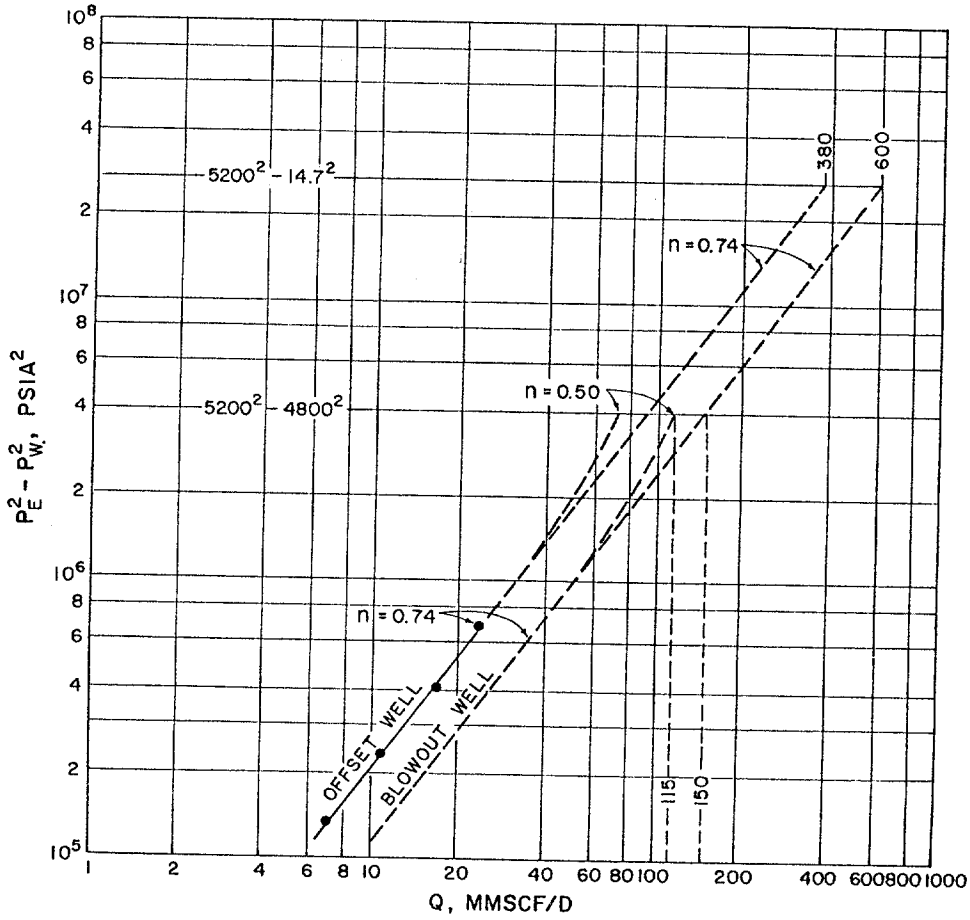

Fig. 6.4. Graphical solution to illustrative example.

C for the blowout well is calculated as

$$C = 1.24 \times \frac{57}{36} = 1.96$$

and the calculated back pressure equation for the wild well is

$$q = 1.96(p_e^2 - p_w^2)^{0.74}$$

Reservoir pressure at the time of blowout was close to 5200 psia and the flowing bottom hole pressure was calculated to be 4800 psia at 150,000 MSCF/D using the methods of Section 8. Thus, the estimated blowout rate is

$$q = 1.96(5200^2 - 4800^2)^{0.74}$$

$$q = 150{,}000 \text{ MSCF/D } (150 \text{ MMSCF/D})$$

Assuming slope of 0.74, at p_w = 14.7 psia the open flow capacity for the blowout well is calculated to be 600 MMSCF/D, and at 4800 psia flowing bottom hole pressure 150 MMSCF/D.

The graphical solutions for the above calculations are shown in Fig. 6.4. Also shown are extrapolations assuming complete turbulence is reached at a flowing bottom hole pressure of 4800 psia, i.e., that n = 0.50. For the blowout well this gives an estimated blowout rate of 115 MMSCF/D. Thus for 10 days the vented gas lies between 11.5 and 15.0 MMSCF. These figures are, of course, subject to large uncertainties. In addition to those introduced in the extrapolation of back pressure data, in this example we have those of adapting back pressure data from another well in the same reservoir. The accuracy of back pressure data is also open to question in some tests. For instance, in the example presented, the pressure drawdown, $p_e - p_w$, was 66 psi at 24 MMSCF/D and only 13 psi at the lowest rate of 7 MMSCF/D. Even where these pressures are measured with subsurface gauges, small uncertainties in the static and flowing pressures can cause large uncertainties in the back pressure curves. For example, had the drawdown at 24 MMSCF/D been 70 psi, rather than 66 psi, the slope between the two highest points would be 0.62 rather than 0.74, the average of all points. Where the pressure is calculated from surface measurements of a static column in an annulus or kill string, additional uncertainties are introduced.

SECTION 7
FORMATION RESISTANCE

7.1 Introduction

Flow string resistance and formation resistance control the amount of escaping gas during a blowout. Formation resistance occurs as gas flows through the small, tortuous pore spaces of the reservoir rock toward the wellbore. Flow string resistance occurs as gas flows up the wellbore toward the surface. These two resistances act in series, and it cannot be said, a priori, which is the more dominant.

Techniques are available to estimate the relationship of the flow rate of the escaping gas to these two resistances. The procedure follows three basic steps:

1. Formation resistance

   Using an appropriate formula for the flow of gas in the reservoir, the flow rates are calculated for a range of flowing bottom hole pressures. A plot of these data such as shown in Fig. 7.1 is an expression of the formation resistance, which involves properties of the reservoir rock and gas. As indicated, maximum flow rate occurs for zero bottom hole pressure, and the rate declines as bottom hole pressure rises.

2. Flow string resistance

   Using appropriate formulas for the flow of gas through pipes, annuli, etc., a flow rate is assumed and using a surface flowing pressure (usually zero psig) the pressure is calculated at the bottom of the flow string. Other bottom hole pressures are calculated for a range of assumed flow rates, the results of which plotted, as in Fig. 7.1, express the resistance of the flow string to the flow of gas.

3. Blowout rate

   The intersection of the formation and flow string resistance curves is the calculated blowout rate, about 55 MMSCF/D for the plots of Fig. 7.1.

Procedures for calculating the formation resistance are investigated in this section and those for flow string resistance in Section 8. In Section 9 the combination

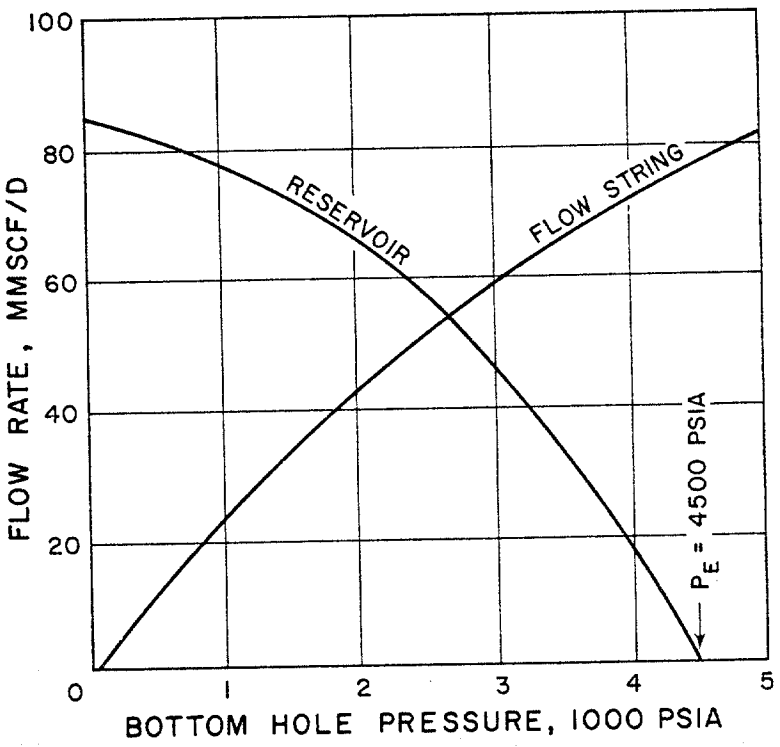

Fig.7.1 Typical formation and flow string resistance curves.

of the two procedures to estimate blowout rate(s) is discussed. Although the calculation techniques are based on established engineering principles and their use is straight forward, the results are strongly influenced by certain pieces of the data, some or all of which may be subject to large uncertainty. Also the calculations are laborious and are most appropriately handled by computers. The computer technique also allows extensive sensitivity analysis to help bracket data uncertainties.

7.2 Reservoir Geometry

The relationship of flow rate to pressure drop experienced by gas as it flows through the reservoir rock is influenced by: reservoir geometry, gas properties, and reservoir rock properties.

All of the calculation procedures used in this report are based on flow systems of radial geometry, such as shown in Fig. 7.2. In this radial system r_w represents the radius of the wellbore, r_e represents the outer or external radial boundary of the reservoir, and h represents the net thickness of the formation. The value of r_w is commonly taken to be the radius of the

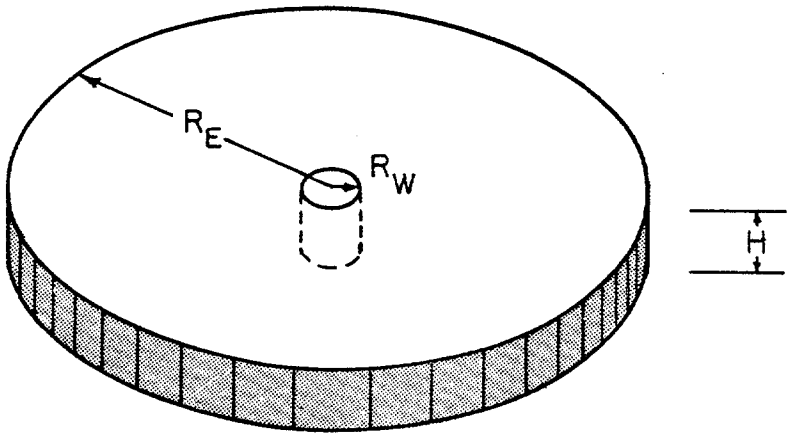

Fig. 7.2. A radial system of thickness h, external radius r_e, and well bore radius r_w.

drill bit if gas is flowing into an open hole and is taken to be the internal radius of the casing if it is flowing through perforated casing. The value of r_e is the radius of the boundary of the reservoir if the reservoir is indeed circular. Since no reservoirs are truly radial in shape and wells may be located off center, an equivalent radius is normally used, defined as the radius of a circle whose area is the same as the reservoir. This procedure has been shown in practice to be a good approximation for most reservoir systems. For the reservoir area A in acres, the equivalent external radius r_e in feet is:

$$r_e = [43{,}560\ A/\pi]^{0.5} \qquad (7.1)$$

For an area of 125 acres, the equivalent external radius is:

$$r_e = [43{,}560 \times 125/3.14]^{0.5} = 1316 \text{ ft.}$$

7.3 Steady State Flow

One formula which relates the gas flow rate q_{sc} and the flowing bottom hole pressure p_w for radial systems is derived as Eq. (6.72) of Ref. 7.1 as:

$$q_{sc} = \frac{703\ kh\ (p_e^2 - p_w^2)}{\mu T z\ \ln(r_e/r_w)} \qquad (7.2)$$

in which

q_{sc} = flow rate in SCF/day at standard conditions of 14.7 psia and 60^0F
k = reservoir permeability, darcies
h = reservoir thickness, feet
p_e = pressure at radius r_e, psia
p_w = wellbore pressure at r_w, psia
μ = average gas viscosity, centipoise
T = reservoir temperature, degrees Rankine
z = average gas deviation factor, dimensionless
r_e/r_w = ratio of external radius to well bore radius, dimensionless.

Equation (7.2) is commonly referred to as a steady state equation. It assumes the maintenance of pressure at a value p_e at the external radius r_e. This would be the case for active water drive gas reservoirs in which reservoir pressure is maintained at p_e, and for which Eq. (7.2) would be applicable except for an initial transient period which is discussed later. The pressure p_e is the reservoir pressure measured or estimated at the time of blowout.

Equation (7.2) may be used as shown in Example 7.1 to calculate a formation resistance such as Fig. 7.1, which shows the relationship between bottom hole pressure and flow rate.

Example 7.1

p_e = 4500 psia; p_w = 3000 psia; k = 0.064 darcy
h = 15 feet; μ = 0.025cp; z = 1.10
r_e = 6000 ft; r_w = 0.333 ft; T = 660^0R

$$q_{sc} = \frac{703 \times 0.064 \times 15 (4500^2 - 3000^2)}{0.025 \times 600 \times 1.10 \times \ln(6000/0.333)}$$

$$q_{sc} = 47.0 \text{ MMSCF/D}$$

For $p_w = 0$, $q_{sc} = 85$ MMSCF/D. These points are included in the reservoir curve shown in Fig. 7.1.

7.4 Error Analysis

The terms in the denominator of Eq. (7.2) can be evaluated much more precisely than those in the numerator. All of which determine the relationship between the flow

rate and the bottom hole pressure. Gas deviation factors and viscosities can be estimated with good precision using the methods of Ref. 7.2. Reservoir temperatures can also be estimated with good precision in nearly all instances.

At first glance, the uncertainty in estimating the external radius r_e might appear to have a large effect on the calculation; but because both it and the wellbore radius, which is also subject to considerable uncertainty, enter the formula as logarithms, the effect of their uncertainty is relatively small. This may be illustrated by considering values of the external radius as twice (12,000 feet) and half (3,000 feet) the 6,000 foot radius used in Example 7.1. As $\ln(12{,}000/0.333) = 10.5$, $\ln(6{,}000/0.333) = 9.8$, and $\ln(3{,}000/0.333) = 9.1$, it is seen that a 100 per cent variation in the estimate of the external radius (or the ratio r_e/r_w) produces less than an 8 per cent variation in the logarithm.

On the other hand, the uncertainty in some of the other variables, particularly formation thickness and permeability, may be quite large, sometimes even in well developed reservoirs whose formation thicknesses and permeabilities vary widely throughout the reservoir and are reflected in varying well productivities. In discovery wells, the reservoir permeability can only be estimated from permeability trends in the area, depth or knowledge about the particular formation. The formation thickness may be obtained from driller's logs, electric or other logs run, but there is uncertainty about how representative the thickness at the well is of the whole drainage area. Also, in some instances the blowout may occur before the producing formation has been fully penetrated. In any event, the uncertainties in permeability and thickness are reflected directly in the calculated values of flow rates for assumed bottom hole pressures. Good estimates of thickness can be obtained from isopach maps in areas having good well control.

The effect of uncertainty in the external pressure p_e, taken to be reservoir pressure at the time of blowout, varies with the absolute values of both the reservoir pressure and the assumed bottom hole pressures. For example, had the external pressure been 4400 psia instead of 4500 psia in Example 7.1, the calculated flow rate would have been 45 MMSCF/D instead of 47 MMSCF/D.

7.5 Semi-Steady State Flow

Where water drive is absent and after an initial transient period as mentioned above, the radial gas flow

formula Eq. (6.81) of Ref. 7.3 applies.

$$q_{sc} = \frac{703\ kh(p_e^2 - p_w^2)}{\mu Tz\ \ln(0.61\ r_e/r_w)} \qquad (7.3)$$

The only difference between Eq. (7.3) and Eq. (7.2) is in the log term. Because of the relative insensitivity of the log term, as discussed in Sec. 7.4, flow rates calculated using Eq. (7.3) will be only slightly larger than those using Eq. (7.2). Furthermore , the remarks of Sec. 7.4 about error analysis apply equally to Eq. (7.3).

The external pressure p_e in Eq. (7.3) is taken as the measured or estimated pressure at the start of blowout. In the absence of water drive, average reservoir pressure will decline during the blowout, and therefore also the external pressure. Where the pressure decline is small, i.e., where the volume of vented gas is small in relation to the initial gas in place in the reservoir, continued use of the initial pressure will cause only a small overestimate on the blowout rates, and in view of the other uncertainties, continued use of the initial pressure may be justified.

Where the pressure decline is appreciable, another semi-steady state formula is applicable, Eq. (6.82) of Ref. 7.3, or

$$q_{sc} = \frac{703\ kh(p_{avg}^2 - p_w^2)}{\mu Tz\ \ln(0.472\ r_e/r_w)} \qquad (7.4)$$

In this equation, the external pressure is replaced by the average reservoir pressure, p_{avg}. Use of this equation requires a good estimate of the reservoir's hydrocarbon pore volume, calculated by Eq. (2.1) or Eq. (2.2) of Sec. 2 and then the use of Eq. (2.1) to calculate the average reservoir pressure, using for the cumulative produced gas G_p a summation of the daily blowout volumes. Example 7.2 illustrates this procedure using the data of Example 7.1 and a value for the hydrocarbon pore volume calculated as shown in Example 2.1

Example 7.2

p_e = 4500 psia; k = 0.064 darcy h = 15 feet

r_e = 6000 ft; r_w = 0.333 ft; T = 600°R

μ = 0.025cp & z = 1.100 at 4500 psia & 600°R

μ = 0.025cp & z = 1.095 at 4461 psia & 600^0R

$V_{HCPV} = 340 \times 10^6 ft^3$

From Fig. 7.1 the initial blowout rate is determined as 55 MMSCF/D from the intersection of the formation and flow string resistance curves. Assuming this rate for 5 days, the cumulative vented gas after 5 days of blowout is 275 MMSCF. Placing this value in Eq. (2.1)

$$\frac{14.7 \times 275 \times 10^6}{520} = \frac{4500 \times 340 \times 10^6}{1.10 \times 600} - \frac{340 \times 10^6}{600} \times \left(\frac{p}{z}\right)_{av}$$

$$\left(\frac{p}{z}\right)_{avg} = 4074 \text{ psia}$$

From a plot of z vs $\frac{p}{z}$ for this reservoir gas, z = 1.095 and

$$p_{avg} = 1.095 \times 4074 = 4461 \text{ psia}$$

This value of p_{avg} may now be used in Eq. (7.4) to find a new reservoir resistance curve, the dashed curve of Fig. 7.3. The intersection of this curve and the flow string resistance curve provides a new and lower value of the blowout rate, approximately 53 MMSCF/D as shown in Fig. 7.3. This value may then be assumed to hold for the next five days, or another selected interval, and the procedure continued.

Where the pressure decline is sufficient for using the material balance method described in Section 2, the cumulative vented volumes calculated by both methods may be compared. The method described by Example 7.2 includes, in addition to the errors discussed in Sec. 7.4, the error in estimating the hydrocarbon pore volume and those introduced in calculating the flow string resistance curve. The latter will be discussed in Section 8.

In many cases the reservoir drive mechanism is not known. It may be active water drive, partial water drive or volumetric expansion. In this event, the procedures described in both Secs. 7.3 and 7.4 should be followed, the results of which bracket the best estimate of the vented gas volumes, and include the possibility of partial water drive.

7.6 Transient Flow

The methods described in Secs. 7.3 and 7.5 assume

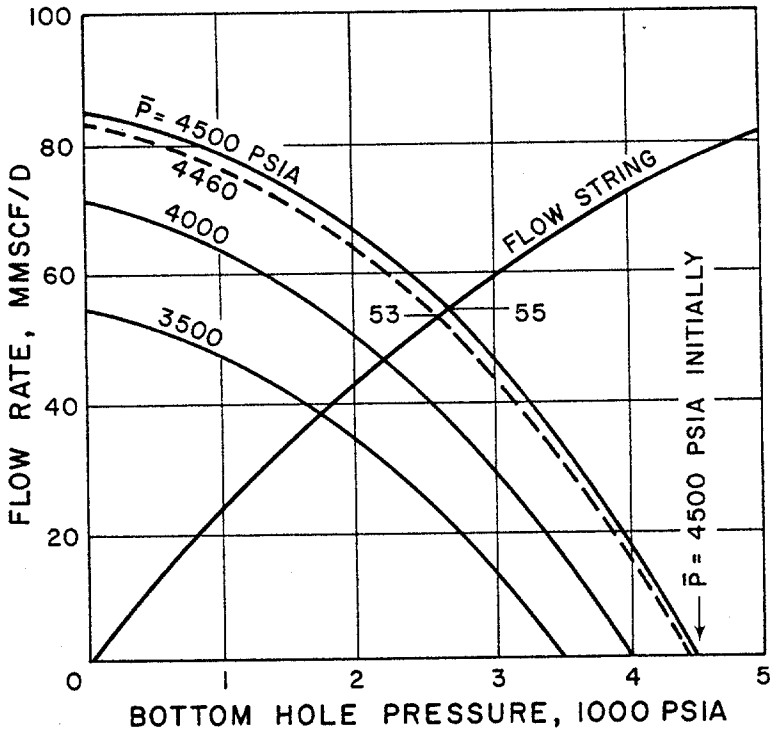

Fig.7.3. Formation resistance curves as calculated in Example 7.2.

that the steady-state or semi-steady state pressure distributions are established in the reservoir in a small and negligible period of time. The approximate time to establish these distributions is expressed by Eq. (6.29) of Ref. 7.4 in which the time referred to is called the readjustment time, or the time for a reservoir to adjust to steady-state or semi-steady state conditions following a sudden change in flow rate, e.g., a blowout.

$$t_R = \frac{0.04\ r_e^2}{\eta} = \frac{0.04\mu c\phi r_e^2}{k} \qquad (7.5)$$

in which

t_R = time, days
μ = gas viscosity, centipoise
c = gas compressibility, psi^{-1}
ϕ = formation porosity, fraction
k = permeability, darcies
r_e = reservoir radius, ft

The gas compressibility may be calculated by methods explained in Ref. 7.5. For the conditions of Example 7.1, and a gas compressibility of $100 \times 10^{-6}\ psi^{-1}$ and

a hydrocarbon porosity of 20 per cent,

$$t_R = \frac{0.04 \times 0.025 \times 100 \times 10^{-6} \times 0.20 \times 6000^2}{0.064}$$

$$t_R = 11 \text{ days}$$

For an external radius of 12,000 feet, the corresponding readjustment time is 44 days. The important variables affecting the readjustment time for gas reservoirs are permeability, gas compressibility, and reservoir size, i.e., r_e. Gas compressibility decreases with pressure and therefore also generally with depth. Thus large readjustment times are to be expected for larger, shallower (lower pressure) reservoirs and those having lower permeability.

Equation (7.5) may be also used to calculate the transient drainage radius at any time, i.e., the radius beyond which reservoir pressure has not been appreciably changed up to that time by the blowout or other rate changes. Inverting Eq. (7.5)

$$r_e = \left[\frac{kt}{0.04\mu c\phi}\right]^{0.5} \qquad (7.6)$$

This value may then be substituted for r_e in Eq. (7.2) to yield

$$q_{sc} = \frac{703\ kh(p_e^2 - p_w^2)}{\mu Tz(0.5)\ln(kt/0.04\mu c\phi r_w^2)} \qquad (7.7)$$

Equation (7.7) may be used to calculate reservoir resistance curves at any time t by procedures illustrated by Example 7.3.

Example 7.3

p_e = 4500 psia; k = 0.064 darcy; μ = 0.025 cp
$c_g = 100 \times 10^{-6}\ psi^{-1}$; ϕ = 0.20; r_w = 0.333 ft
r_e = 6000 ft; h = 15 ft; T = 600°R
For p_w = 3000 psia:

In Eq. (7.7),

$$\frac{703\ kh}{\mu Tz(0.5)} = \frac{703 \times 0.064 \times 15}{0.025 \times 600 \times 1.10 \times 0.5} = \underline{81.8 \times 10^6}$$

and

$$k/0.04\mu c\phi r_w^2 = 0.064/0.04x0.025x0.20x0.333^2$$

$$= \underline{28.8}$$

Therefore:

$$q_{sc} = \frac{81.8x10^6(4500^2-p_w^2)}{\ln 28.8\ t}$$

For p_w = 2500 psia, after 1 day of flow

$$q_{sc} = \frac{81.8x10^6(4500^2-2500^2)}{\ln(28.8x1)}$$

$$q_{sc} = 66.6 \text{ MMSCF/D}$$

After 5, 11, 50 and 100 days for p_w = 2500 psia, q_{sc} = 60.0, 58.4, 54.3 and 52.5 MMSCF/D, respectively. Other values of p_w are assumed to provide data points for the curves of Fig. 7.4.

Figure 7.4 shows the formation resistance or pressure distribution curves for the reservoir of Example 7.3 at 1, 5, 11, 50 and 100 days. It is to be noted that the 11 day curve is the same as the reservoir resistance curve of Fig. 7.1 and essentially the same as the upper curve of Fig. 7.3, the slight difference being caused by the use of $\ln(r_e/r_w)$ in Fig. 7.1 and $\ln(0.65\ r_e/r_w)$ in Fig. 7.3. If the reservoir has an effective external radius of 6,000 feet as used in Example 7.1, 7.2, and 7.3, and an active water drive to maintain pressure at its initial value, then the 11 day curve of Fig. 7.4 may be used for the duration of the blowout. The effect of an error in the estimated effective external radius may be investigated by considering, for example, a value of 12,000 feet, i.e., a reservoir four-times as large. For this larger reservoir the readjustment time will be 44 days, and yield a steady-state formation resistance curves slightly above the 50 day curve of Fig. 7.4.

If on the other hand, the reservoir is of 6,000 feet in radius and has no water drive, then, after reaching the 11 day curve, the reservoir resistance curves will begin to change as shown in Fig. 7.3. As with the water drive reservoir, the effect of a larger external

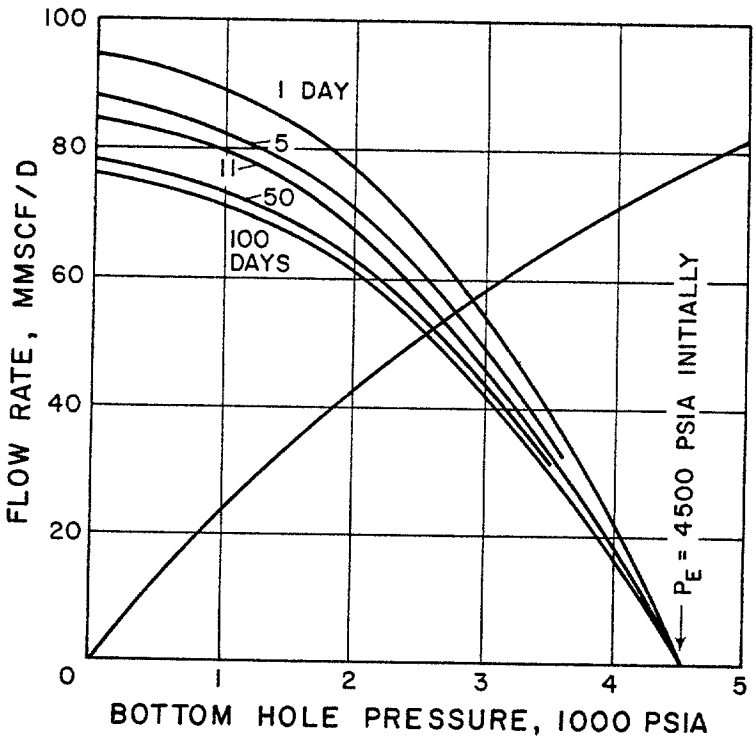

Fig.7.4. Transient formation resistance curves for Example 7.3.

radius, may be investigated. For an effective external radius of 12,000 feet, as this would be a reservoir fourtimes as large as the one of 6,000 feet, upon reaching semi-steady state performance at 44 days, the rates of pressure decline would be only one-fourth those calculated in Example 7.2 and shown in Fig. 7.3.

The intersections of the formation resistance curves with the flow string resistance curve of Fig. 7.4 give the blowout rates during the transient period, varying from 57.2 MMSCF/D at one day after start of blowout to 51.6 MMSCF/D after 100 days. For the latter figure it is assumed that the effective reservoir radius is at least as large as 18,000 feet which would allow a transient flow period of 100 days before entering into steady state or semi-steady state flow.

A plot of the intersections of the curves of Fig. 7.4 yields the lower curve of Fig. 7.5, from which the cumulative vented gas during the transient period is represented by the area under the curve. For an 11 day transient period the vented gas amounts to about 610 MMSCF, which includes an estimated 60 MMSCF during the first day. The flatness of the lower curve of Fig. 7.5 may be somewhat surprising to those familiar with flow rate changes for constant bottom hole pressure.

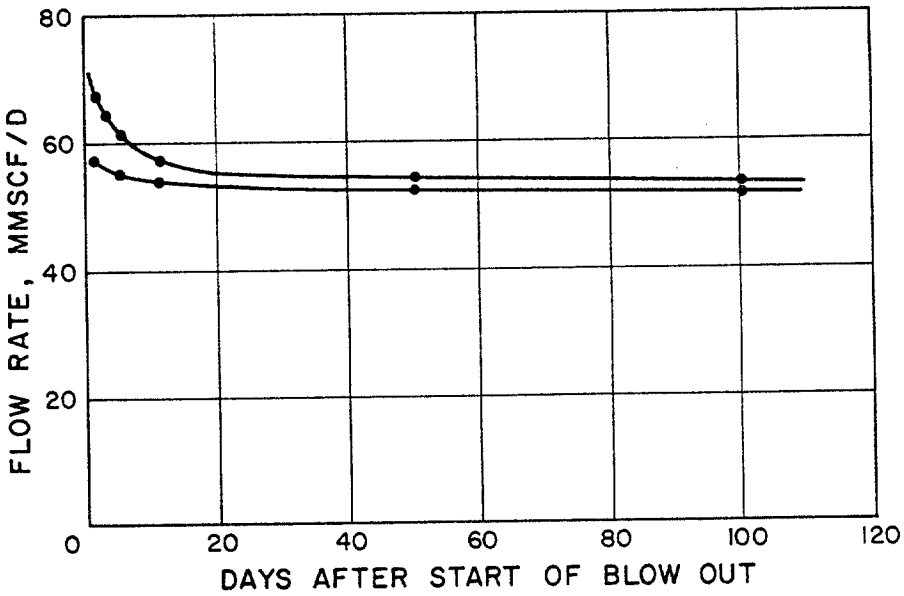

Fig.7.5. Calculated transient blowout rates for a constant bottom hole pressure of 2500 psia (upper curve) and for declining bottom hole pressure (lower curve).

The upper curve of Fig. 7.5 shows the flow rate at a constant bottom hole pressure of 2500 psia, showing rates much higher, particularly in the early blowout period, than for the case of declining bottom hole pressure, which prevails during blowouts.

7.7 Summary and Commentary

Methods have been presented in the foregoing by which the formation resistance curves may be calculated. Where there is doubt whether the reservoir has active, partial or no water drive, calculations should be made for cases of both active and no water drive. Similarly, the effect of effective reservoir radius and initial pressures should be investigated to help bracket the formation resistance curves. Use of computer programs is recommended to facilitate the investigation of different cases and variable sensitivity.

Reservoir permeability and thickness were cited as parameters in the formulas to which the calculated formation resistance curves are most sensitive. These parameters are unfortunately also the ones whose values are known with the least certainty. They are often used as one variable, the kh product to which the term capacity has been given. The effect of a wide range of possible formation capacities on the formation resistance

curves, and therefore on the blowout rates, is treated in Section 9.

The formulas used in the foregoing section are well established in reservoir engineering practice. They do not, however, include the effect of such things as turbulent or non-Darcy flow in the formation, partial well penetration of the formation, zonal damage, wellbore erosion, and perforation efficiency. They have not been included in the calculations because there is no way to evaluate them for blowout wells, and as a matter of fact, their evaluation is often difficult with normal producing wells. The effect of the first three is always to increase formation resistance, that is to reduce the flow rates below those calculated without their consideration. Their individual or combined effects may increase the formation resistance appreciably. Wellbore erosion, on the other hand will decrease the formation resistance by increasing the effective wellbore radius. As explained earlier, because the well radius occurs in a logarithm term, its effect on the calculated resistance curves is greatly attenuated. Perforation efficiencies are believed more usually to increase formation resistances, i.e., have the effect of a well bore radius smaller than the inside diameter of the casing. Even in the best of cases however, perforation does not reduce formation resistance appreciably, i.e., increase the effective well bore radius.

A discussion of the factors mentioned in the preceding paragraph is found in Ref. 7.6. In the estimation of well blowout rates it is recommended that consideration of these factors be included as part of the effect of formation capacity, to be discussed in Section 9.

SECTION 8
FLOW STRING RESISTANCE

8.1 Introduction

The computation of formation and flow string resistances was outlined in Sec. 7.1 along with a brief description of their use to estimate gas blowout rates. Section 7 covered the calculation of formation resistance curves for a variety of reservoir conditions, and this section will cover the calculation of flow string resistance curves.

Flow string resistance curves are calculated using appropriate formulas for the flow of gas through pipes, annuli, etc. by assuming a flow rate and a surface flowing pressure, usually atmospheric for most blowouts. The flowing bottom hole pressure is then calculated for this flow rate and for a range of other assumed flow rates. A plot of the flow rates versus the flowing bottom hole pressures is the flow string resistance curve.

Calculation of the bottom hole pressure required to achieve a given flow rate in a gas well is accomplished by applying the general energy equation over the flow path. For a flowing gas well the bottom hole pressure can be expressed as the sum of the surface pressure and three integrals evaluated over the flow path, or

$$p_w = p_s + \frac{1}{144} \int \rho dZ + \int dp_f + \frac{1}{144g} \int \rho v dv \qquad (8.1)$$

where:

p_w = bottom hole pressure, psia
p_s = surface pressure, psia
p_f = pressure loss due to friction, psia
ρ = gas density, lbs/ft^3
Z = elevation above reference level, feet
v = velocity of gas, ft/sec
g = acceleration due to gravity, ft/sec^2

The first integral term in Eq. (8.1) accounts for changes in pressure due to changes in potential energy along the flow path. The second is the change in pressure over the flow path due to friction. The third accounts for changes in pressure due to changes in kinetic energy along the flow path.

Numerous equations have been developed by integrating the general energy equation over flow paths of constant cross-section. The forms of these equations differ significantly because of various simplifying assumptions that were necessary in order to perform the integrations. Two of the integrated forms of the general energy equation in common use are those presented by Poettmann, (Ref. 8.1) and by Cullender and Smith (Ref. 8.2). However, with the use of modern, high-speed computers numerical integration of the basic terms in the general energy equation can be easily accomplished. This approach is recommended because it is more readily understood and offers greater flexibility than the integrated forms of the general energy equation.

8.2 Potential Energy Term

The change in pressure due to the change in potential energy over a flow path is:

$$(\Delta p)_g = \frac{1}{144}\int \rho dZ \qquad (8.2)$$

If Eq. (8.2) is evaluated over a flow path length short enough to assume that the gas density remains constant, it can be shown that:

$$(\Delta p)_g = \frac{0.0188\ G \cos \phi\ \Delta L}{T} \frac{p}{z} \qquad (8.3)$$

where:

G = gas specific gravity (Air = 1) dimensionless

ϕ = deviation of the flow path from the vertical, degrees

ΔL = flow path length, feet

p = average pressure in length ΔL, psia

T = average temperature in length ΔL, degrees Rankine

z = gas deviation factor at p & T, dimensionless

8.3 Friction Term

The change in pressure due to viscous effects is a measure of the mechanical energy transformed into

heat by frictional resistance. This change due to frictional resistance over the flow path is:

$$(\Delta p)_f = \int dp_f \tag{8.4}$$

If Eq. (8.4) is integrated over a flow path length short enough to assume that the gas density remains constant, it can be shown that:

$$(\Delta p)_f = 0.0000316\ F\ \frac{GTz}{p}\ \frac{Q^2}{A^2} \tag{8.5}$$

where:

F = a dimensionless factor that is dependent on the flow geometry.

Q = the flow rate in MMSCF/D at standard conditions of 14.7 psia and 60^0F.

A = cross-sectional area, sq ft.

In the use of Eq. (8.5) the flow path should be divided into segments such that the pressure drop across a segment does not exceed ten percent of the upstream pressure with a minimum value of 10 psi. The determination of the dimensionless factor F is discussed below for a variety of flow geometries.

Circular Pipe Flow

For flow, through a circular pipe the factor F can be expressed as

$$F = f(\Delta L/D) \tag{8.6}$$

where f is a dimensionless friction factor and D is the internal pipe diameter in feet. For completely turbulent flow or in the transition zone between turbulent and laminar flow, the friction factor f can be computed using the Colebrook equation (Ref. 8.3).

$$\frac{1}{\sqrt{f}} = -2\ \log_{10}\left[0.269\ \frac{\varepsilon}{D} + \frac{2.51}{R_e\ \sqrt{f}}\right] \tag{8.7}$$

where ε is the absolute roughness in feet and R_e is Reynold's Number, dimensionless. The Reynolds Number can be computed from

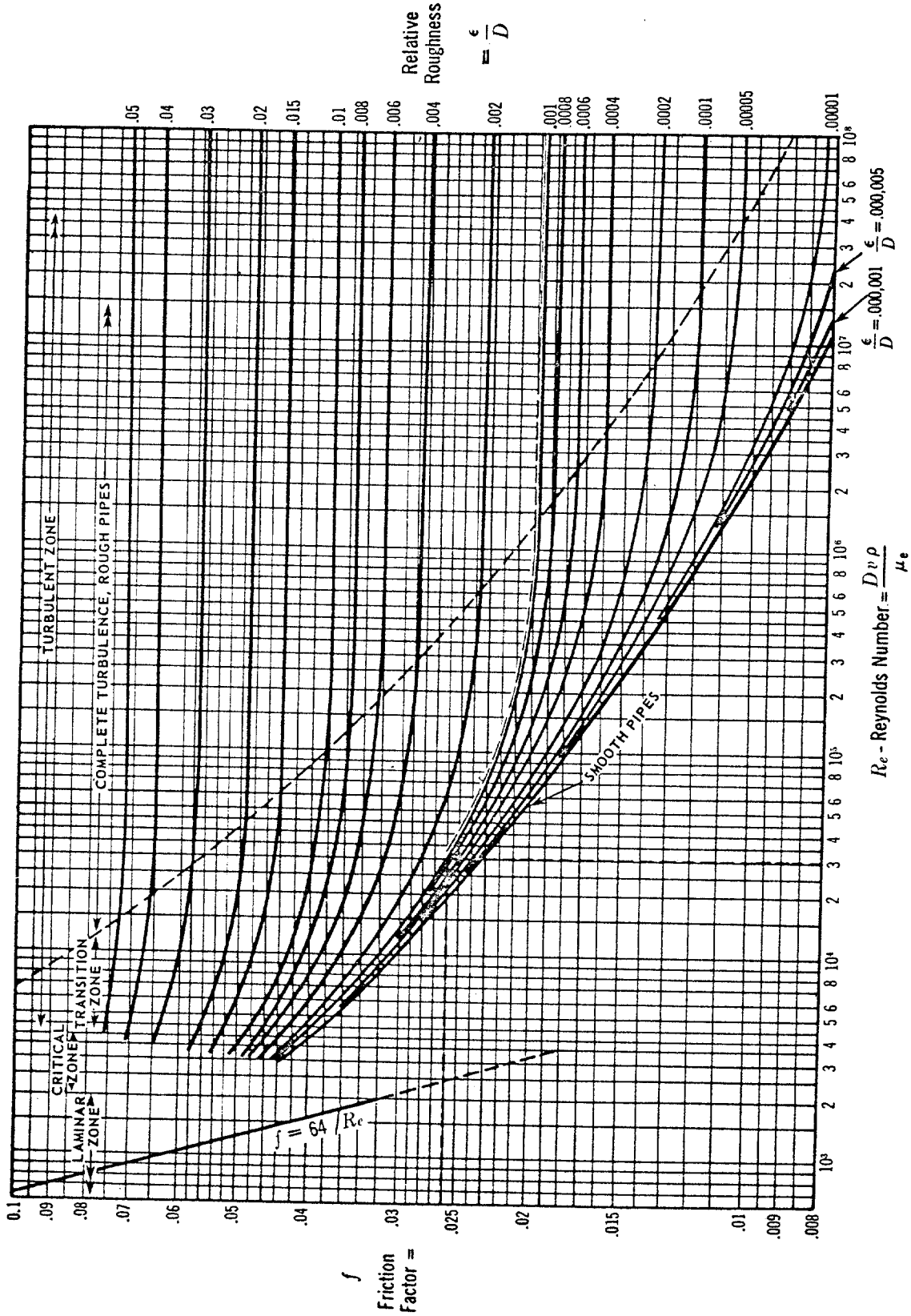

Fig. 8.1. Friction factors for pipe flow. (After Crane, Ref. 8.4.)

$$R_e = 1684 \frac{G\ Q}{\mu\ D} \qquad (8.8)$$

where μ is the gas viscosity in centipoises at prevailing temperature and pressure and Q is the flow rate in MMSCF/D. Equation (8.7) has been solved for the friction factor f over a wide range of the parameters. The results have been plotted and are shown in Fig. 8.1 which can be used to determine the friction factor for any set of flow parameters.

Annular Flow

For flow through an annulus an equivalent diameter is computed for the annulus using the "hydraulic radius" concept. The equivalent diameter for an annulus is:

$$D_e = D_o - D_i \qquad (8.9)$$

where D_e, D_o and D_i are the equivalent, outer and inner diameters, respectively, expressed in feet. Equation (8.5) can be used to compute pressure changes that occur during annular flow. The factor, F, is:

$$F = f\ (\Delta L/D_e) \qquad (8.10)$$

The cross sectional area is calculated by:

$$A = \pi(D_o^2 - D_i^2)/4 \qquad (8.11)$$

The absolute roughness of the annulus can be determined from Ref. 8.5,

$$\varepsilon_e = \varepsilon_o \left(\frac{D_o}{D_o + D_i}\right) + \varepsilon_i \left(\frac{D_i}{D_o + D_o}\right) \qquad (8.12)$$

where ε_e, ε_o and ε_i are the absolute roughness in feet for the annulus, outer wall and inner wall, respectively. The relative roughness to be used in Eq. (8.7) or Fig. 8.1 for ε/D for determining the friction factor f for annular flow is:

$$\text{Relative Roughness} = \varepsilon_e/D_e \qquad (8.13)$$

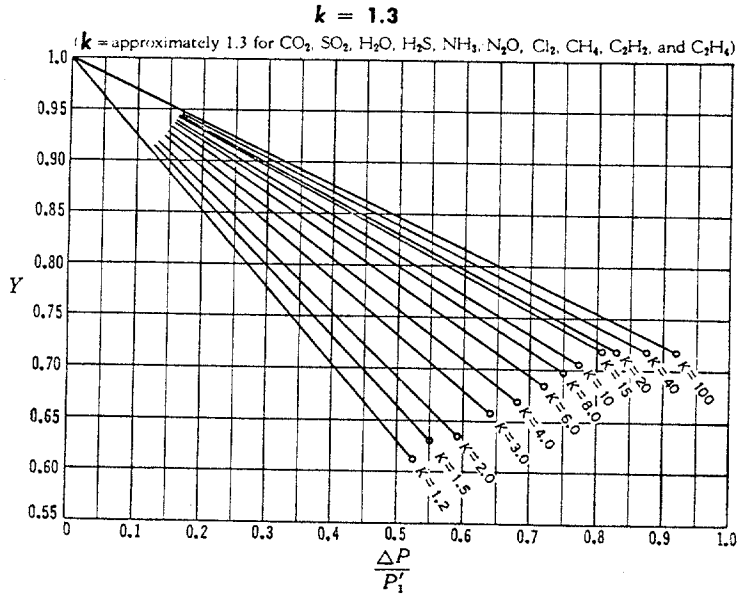

Limiting Factors For Sonic Velocity
$k = 1.3$

K	$\frac{\Delta P}{P'_1}$	Y
1.2	.525	.612
1.5	.550	.631
2.0	.593	.635
3	.642	.658
4	.678	.670
6	.722	.685
8	.750	.698
10	.773	.705
15	.807	.718
20	.831	.718
40	.877	.718
100	.920	.718

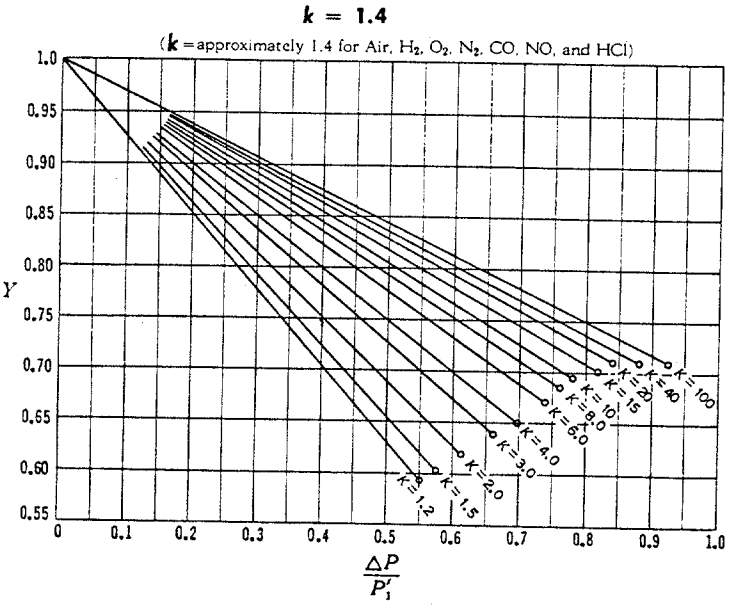

Limiting Factors For Sonic Velocity
$k = 1.4$

K	$\frac{\Delta P}{P'_1}$	Y
1.2	.552	.588
1.5	.576	.606
2.0	.612	.622
3	.662	.639
4	.697	.649
6	.737	.671
8	.762	.685
10	.784	.695
15	.818	.702
20	.839	.710
40	.883	.710
100	.926	.710

Fig. 8.2. Net expansion factors for flow of gases to large flow areas. (After Crane, Ref. 8.4.)

Flow Through Valves and Fittings

For flow through valves and fittings the factor, F, is:

$$F = K/Y^2 \qquad (8.14)$$

where K is a dimensionless resistance coefficient for a specific valve or fitting and Y a net expansion factor, also dimensionless.

The resistance coefficient, K, for valves and fittings must be determined from flow tests. This information is usually available from the manufacturer of the valve or fitting. The net expansion factor, Y, compensates for the changes in fluid properties due to expansion of the fluid caused by a sudden change in pressure. Net expansion factors can be obtained from Fig. 8.2.

Other Resistances to Flow

In addition to the resistances of valves and fittings, discussed above, there are changes in pressure due to sudden enlargement and sudden contraction. Also, when a fluid enters or leaves an open end pipe, there are entrance and exit resistances. The changes in pressure for these conditions can be computed using Eqs. (8.5) and (8.14). Expansion factors Y can be obtained from Fig. 8.2 and resistance coefficients K can be obtained from Fig. 8.3. Note that the values for the resistance coefficient K given in Fig. 8.3 for sudden enlargement or sudden contraction are based on velocity in the smaller pipe.

8.4 Kinetic Energy Term

Ordinarily, in problems involving flow of compressible fluids in a pipe, the change in pressure due to changes in kinetic energy are neglected. The justification for this is that the kinetic energy term is usually small compared to the viscous effects term. The exception is when flow is taking place through a nozzle or orifice. The equation for computing changes in pressure due to flow through a nozzle or orifice is:

$$(\Delta p)_j = 1.049 \frac{GT}{d_o^4} \frac{1}{Y^2 C^2} \frac{1}{p_1} Q^2 \qquad (8.15)$$

where $(\Delta p)_j$ is the difference in psi between the upstream and downstream pressures, p_1 is the upstream pressure, d_o is the throat diameter of the nozzle or orifice in inches and C is a dimensionless nozzle or orifice coefficient. Q as elsewhere in this section is in MMSCF/D. Values for flow coefficients, C, can be obtained from Fig. 8.4 and values for net expansion factors can be obtained from Fig. 8.5. The solution of Eq. (8.15) requires an iterative procedure as will be illustrated in the example calculation.

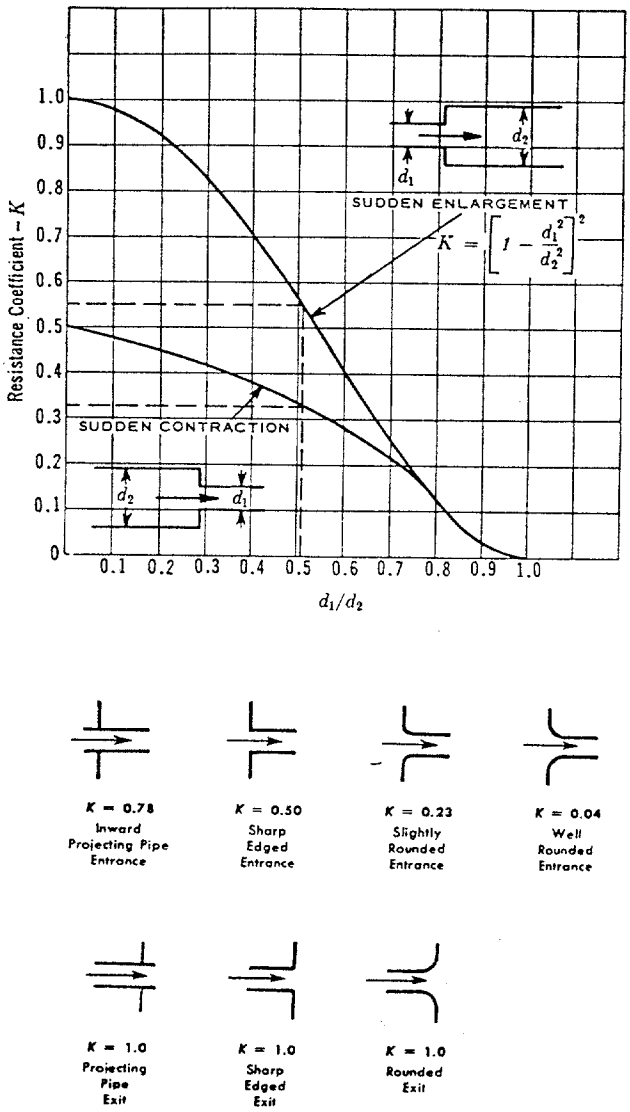

Fig. 8.3. Resistance coefficients for sudden enlargements and contractions (upper) and for exit and entrance effects (lower). (After Crane, Ref. 8.4).

8.5 Limiting Flow of Compressible Fluids

Implicit in Eq. (8.5) and (8.15) for computing pressure changes due to viscous effects and kinetic energy changes is the gas velocity v. The gas velocity can be related to the gas flow rate Q in MMSCF/D at standard conditions of 14.7 psia and 60°F by:

$$v = 0.329 \frac{QT}{A} \frac{z}{p} \qquad (8.16)$$

However, the velocity cannot exceed the sonic velocity v_s of the fluid, which is given by:

$$v_s = 41.43 \left[\frac{kTz}{G}\right]^{0.5} \qquad (8.17)$$

where k is the ratio of the specific heat at constant pressure to that at constant volume, dimensionless. The pressure P_s at the point in the flow path where sonic velocity is reached can be computed by equating Eqs. (8.16) and (8.17). This equality can be solved to obtain a formula for p_s, or:

$$p_s = \frac{0.00789\ Q}{A} \left[\frac{GTz}{k}\right]^{0.5} \qquad (8.18)$$

The point at which sonic velocity occurs in a flow system is usually in a nozzle, an orifice, a valve or fitting, a sudden contraction, or where the system exits to a much larger flow area, e.g., to the atmosphere. Ratios of pressure drop to upstream pressure above which sonic velocity is reached are tabulated in Fig. 8.2. These apply to valves, fittings sudden contractions and exits to much larger areas. Limiting values of the ratios of downstream pressure to upstream pressure for nozzles and Venturi tubes are given in Fig. 8.6.

8.6 Calculation Procedure

The geometry of the flow path in an uncontrolled gas well can be extremely complex. Flow may be occurring through the drill string, the annulus, or both. Several changes in cross sectional area may be present, and a portion of the well may be inclined significantly from the vertical. Multiple valves and restrictions may be present and sonic choking is possible at these restrictions as well as at the surface. The best calculation procedure to use depends upon the flow geometry involved. However, the recommended basic approach is as follows:

1. Assume a gas flow rate, Q.
2. Starting with a known pressure P_o at location L_o, select a pressure increment Δp. Take $\Delta p \leq 10\%$ of P_o, with a minimum value of 10 psi.
3. Calculate the average pressure and average temperature for the increment.

Flow Coefficient C for Nozzles[7]

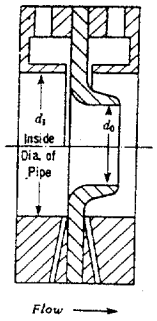

Data from *Regeln fuer die Durchflussmessung mit genormten Duesen und Blenden.* VDI-Verlag G. m.b. H., Berlin, SNW, 7, 1937. Published as Technical Memorandum 952 by the NACA.

$$C = \frac{C_d}{\sqrt{1 - \left(\frac{d_0}{d_1}\right)^4}}$$

Example: The flow coefficient C for a diameter ratio d_0/d_1 of 0.60 at a Reynolds number of 20,000 (2×10^4) equals 1.01.

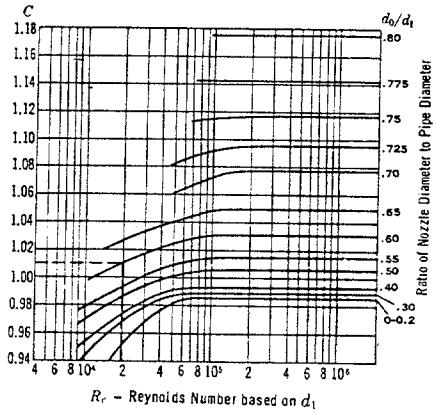

Flow Coefficient C for Square Edged Orifices[7, 17]

$$C = \frac{C_d}{\sqrt{1 - \left(\frac{d_0}{d_1}\right)^4}}$$

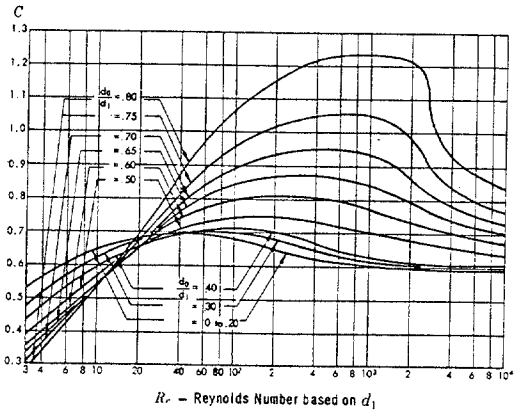

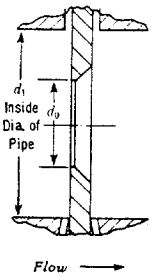

$$C = \frac{C_d}{\sqrt{1 - \left(\frac{d_0}{d_1}\right)^4}}$$

Lower chart data from *Regeln fuer die Durchflussmessung mit genormtem Duesen und Blenden.* VDI-Verlag G. m.b.H., Berlin, SNW, 7, 1937. Published as Technical Memorandum 952 by the NACA.

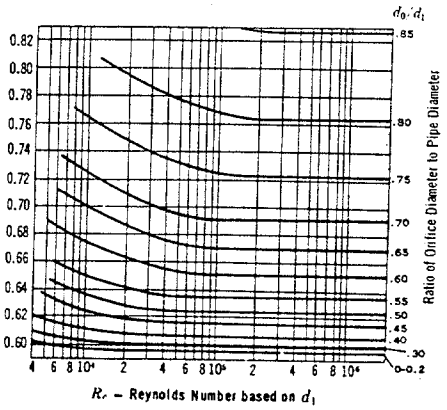

Fig. 8.4. Flow coefficients for nozzles and orifices. (After Crane, Ref. 8.4.)

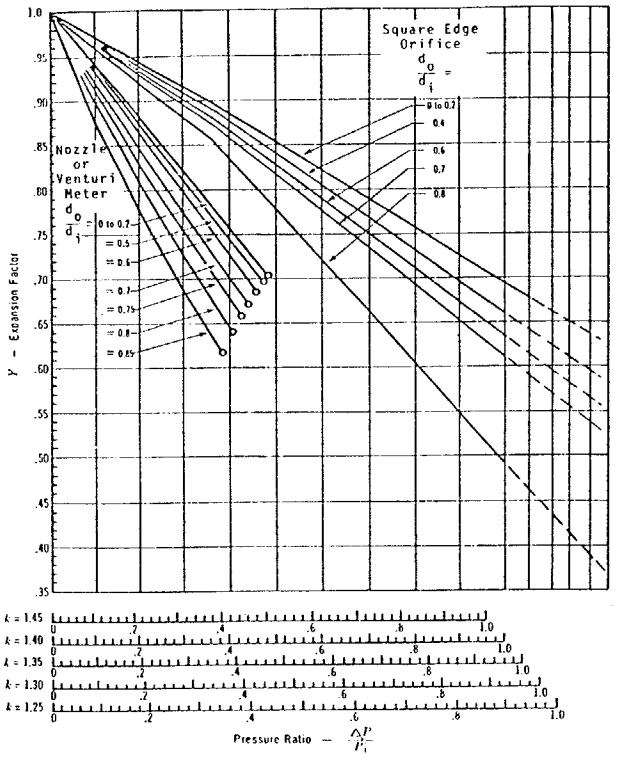

Fig. 8.5. Net expansion factors for compressible flow through orifices and nozzles. (After Crane, Ref. 8.4).

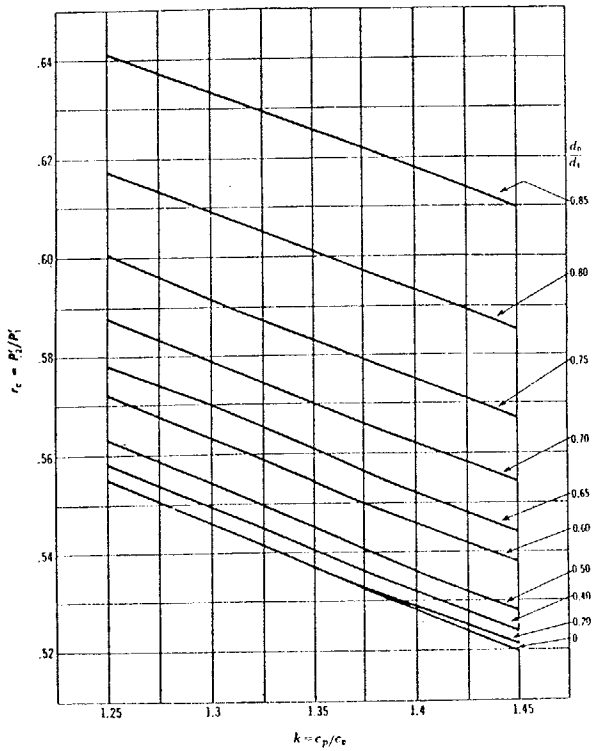

Fig. 8.6. Critical pressure ratios for sonic flow through Venturi tubes and orifices. (After Crane, Ref. 8.4).

4. Determine the gas deviation factor, z, and the gas viscosity, μ, at conditions of average pressure and temperature.

5. Calculate the flowing pressure gradient, dp/dL, for the increment using Eqs. (8.3) and (8.5).

6. Calculate the length increment corresponding to the selected pressure increment, $\Delta L = \Delta p/(dp/dL)$.

7. Set $p = p_o + \Sigma\Delta p$ and $L = L_o + \Sigma\Delta L$.

8. If $\Sigma\Delta L$ is less than the total flow path length repeat the procedure from step 2 using p and L as the starting pressure and location and taking $\Delta p \leq 10\%$ of p with a minimum value of 10 psi. If $\Sigma\Delta L$ is greater than the total flow path length, interpolate between the last two values of L to obtain the pressure at the end of the flow path.

9. Assume a new value for the flow rate and repeat the calculations. Continue until sufficient data is obtained to define the flow string resistance curve, i.e., a plot of flow rate versus flowing bottom hole pressure.

Pressure drops across valves, fittings, or restrictions must be accounted for in the calculation procedure. Also, it will be necessary to check each exit, valve, fitting or restriction to see if sonic velocity has been reached. Once the flow rate is high enough for sonic flow to be achieved at some point, the starting point for the calculation procedure can be moved from the surface to that point. The pressure at the point where sonic velocity has been reached can be computed using Eq. (8.17).

8.7 Illustrative Example

As an illustrative example consider a gas blowout which occurred during drilling operations. The blowout occurred when a drill pipe safety valve failed after the well had kicked. When attempts to stab the Kelly into the safety valve were not successful, the rig personnel evacuated the rig floor, and the well blew out.

The well geometry associated with the blowout is shown in Fig. 8.7. Based on the ball position of the drill pipe safety valve, the area of the opening through which the gas was blowing was computed to be 1.2 sq in.

The valve body had a diameter of 3.25 inches. The bit at the bottom of the drill string contained three 13/32 inch nozzles.

The estimated formation pressure at the time of the blowout was 8000 psia, based on the mud density while drilling and an assumed 750 psia underbalance. The estimated formation temperature is 250°F (710°R), which is also assumed to be the gas temperature throughout the flow string. Figure 8.8 provides values for the gas deviation factor and viscosity of methane at 250°F, as functions of pressure. The ratio of the specific heats k is taken as 1.3.

8.8 Solution of Illustrative Example

The flowing bottom hole pressure will be computed at flow rate increments of 10 MMSCF/D, starting with 10 MMSCF/D, until the bottom hole pressure exceeds the estimated formation pressure, 8000 psia. The gas temperature is assumed constant over the flow path and equal to the estimated bottom hole temperature of 250°F. Completely turbulent flow is assumed for the start of all calculations and is verified by computing Reynolds Numbers where appropriate.

The calculations are made in five steps, to find the following:

1. Pressure at the downstream side of the safety valve.

2. Pressure at the upstream side of the safety valve, also the pressure at the top of the drill pipe.

3. Pressure at the bottom of the drill pipe.

4. Pressure at the bottom of the drill collars.

5. Pressure drop across the bit nozzles, and then the flowing bottom hole pressure.

Step 1. Surface Pressure

The first step is to obtain a starting pressure, in this case the downstream pressure at the safety valve. If flow through the safety valve is subsonic the exit pressure will be atmospheric. If the flow is sonic the pressure will be greater than atmospheric. As the resistance coefficient K for the valve is unknown, the

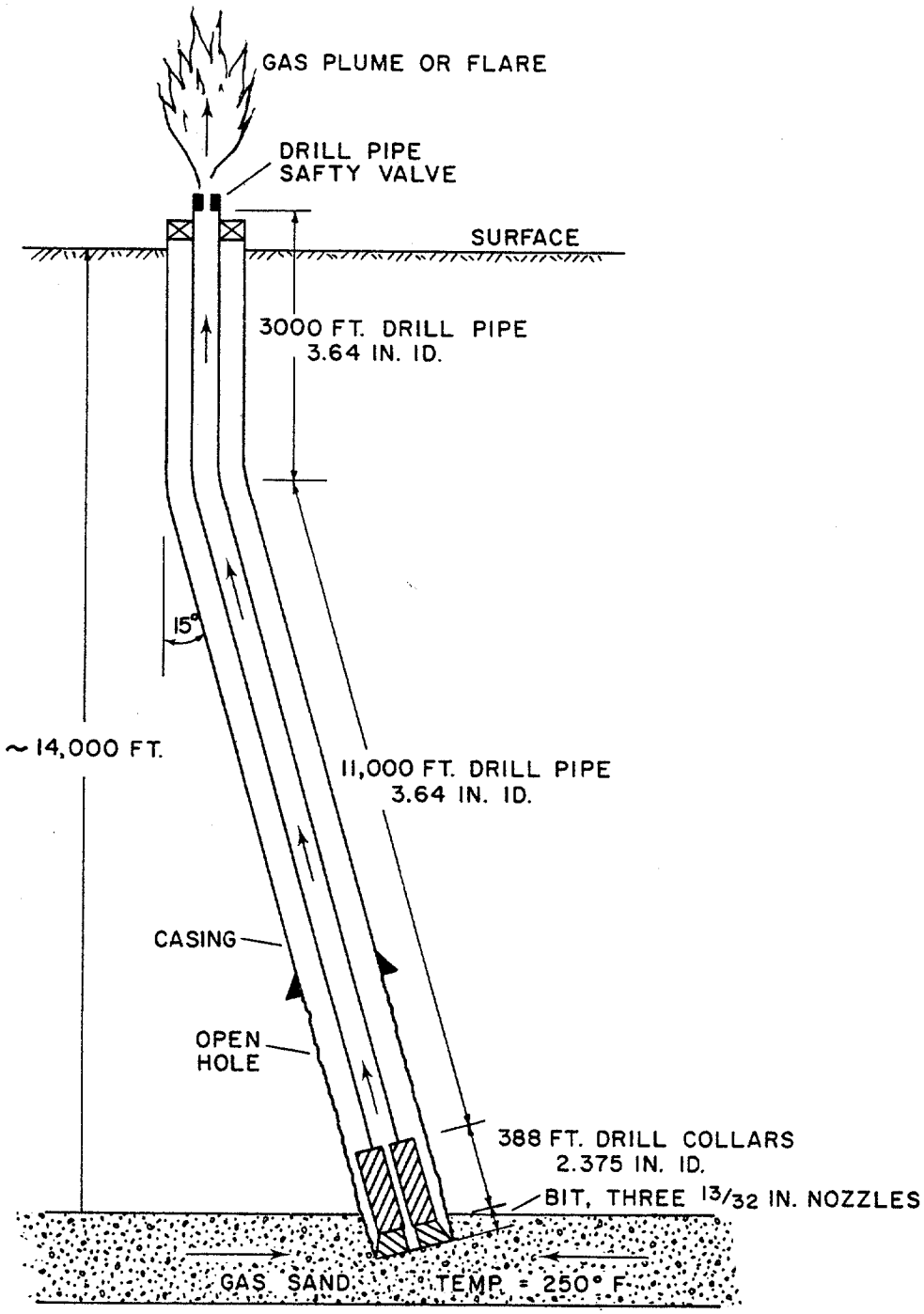

Fig. 8.7. Sketch showing the well geometry for the example of Sec. 8.7.

valve is treated as a square edged crifice whose area is 1.2 square inches whose equivalent throat diameter is

$$d_o = \sqrt{(4)(1.2)/\pi} = 1.24 \text{ inches}$$

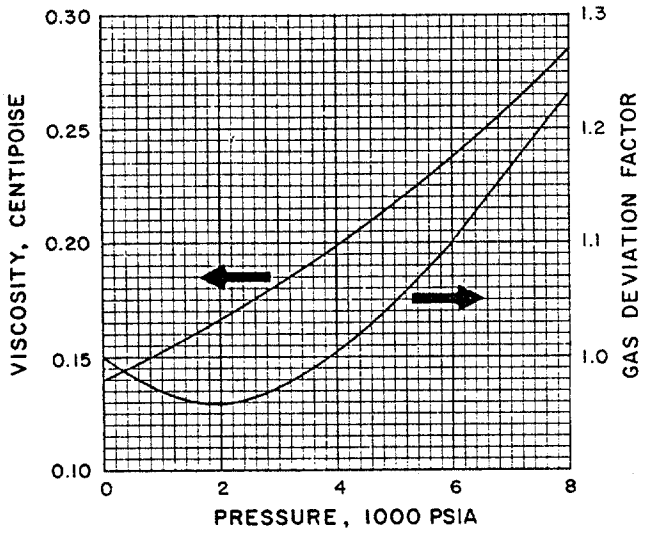

Fig. 8.8. Gas deviation factors and viscosities for methane (G = 0.55) at 250°F.

Assuming subsonic flow for which the well head pressure is atmospheric, taken as 14.7 psia, the theoretical velocity computed by Eq. (8.16) is

$$v = \frac{(0.329)(10)(250+460)}{1.2/144} \frac{1}{14.7} = 19{,}069 \text{ ft/sec}$$

But by Eq. (8.17) sonic velocity for methane gas in the valve is:

$$v_s = 41.43 \left[\frac{(1.3)(710)z}{0.55}\right]^{0.5} = 1697 \left[z\right]^{0.5} \text{ ft/sec}$$

As $z \leq 1.0$ the maximum velocity through the valve is less than 1697 ft/sec, and as the calculated subsonic value is much larger, 19,069 ft/sec, flow through the valve is sonic. The pressure at the valve exit can be estimated using Eq. (8.18).

$$p_s = \frac{0.00789x10}{1.2/144} \left[\frac{(0.55)(710)(z)}{1.3}\right]^{0.5} = 164 \; z^{0.5} \text{ psia}$$

Table I shows the solution by iteration using Fig. 8.8 for values of z, to obtain a downstream pressure at the safety valve of 164 psia.

Table I

Trial	p_s	z(Fig.8.8)	$164\sqrt{z}$
1	14.7	1	164
2	164	1	164

Step 2. Upstream Pressure at the Safety Valve

Using a downstream pressure of 164 psia the upstream pressure at the safety valve is next computed. To do this, first calculate the ratio of the orifice diameter to the pipe diameter as

$$d_0/d_1 = 1.24/3.64 = 0.341$$

From Fig. 8.4 the flow coefficient C of the orifice is 0.603, and using this value in Eq. (8.15) the pressure drop across the valve is

$$(\Delta p)_j = (p_1 - 164)$$

$$= \frac{(1.049)(0.55)(710)}{(1.24)^4} \cdot \frac{1}{(0.603)^2 Y^2} \cdot \frac{1}{p_1} \cdot 10^2$$

$$(p_1 - 164)p_1 = \frac{47651}{Y^2}$$

This quadratic equation is solved by iteration as shown in Table II, using Fig. 8.5 to obtain values for Y. This gives a value of 360 psia for p_1, the pressure just upstream of the valve, at the top of the drill pipe.

Table II

Trial	Y(Fig.8.5)	p_1	Δp	$\Delta p/p_1$
1	1	315	151	0.48
2	0.84	354	190	0.54
3	0.82	360	196	0.54
4	0.82	360		

Step 3. Pressure at the Bottom of the Drill Pipe

Next total flowing pressure gradient at any point in the drill string is determined by combining Eqs. (8.3), (8.5), and (8.6)

$$\frac{\Delta p}{\Delta L} = \frac{0.0188\ G\ \cos\phi}{T}\ \frac{p}{z} + 0.0000316\ \frac{f}{D}\ \frac{GTz}{p}\ \frac{Q^2}{A^2}$$

From 0 to 3000 feet, the hole is vertical, $\cos\phi = 1$ and the total gradient is

$$\frac{\Delta p}{\Delta L} = \frac{(0.0188)(0.55)(1)}{710}\ \frac{p}{z}$$

$$+ \frac{(0.0000316)(0.55)(710)(10)^2}{[3.64/12][(\pi)(3.64)^2/(4)(144)]^2}\ \frac{fz}{p}$$

$$= 1.45\times10^{-5}\ \frac{p}{z} + 778.982\ \frac{fz}{p}$$

An absolute roughness of 0.00065 inches is commonly used for drill pipe. This yields a relative roughness of

$$e/d = 0.00065/3.64 = 0.000179$$

The Reynolds Number calculated using Eq. (8.8) is

$$R_e = \frac{(1684)(0.55)(10)}{\mu\ (3.64/12)} = \frac{30534}{\mu}$$

The pressure at 3000 feet (measured depth) can be determined by starting with a surface pressure of 360 psia and numerically integrating down to 3000 feet. The numerical integration is shown in Table III.

Table III

p	$\Delta p \leq 0.1p$	p_{avg}	z	μ	R_e	f	$\Delta p/\Delta L$	ΔL	Depth
360	30	375	0.99	0.014	2,181,000	0.0138	0.034	882	0
390	30	405	0.99	0.014	2,181,000	0.0138	0.032	938	882
420	40	440	0.99	0.014	2,181,000	0.0138	0.031	1290	1820
460									3110

Interpolating to find the pressure at 3000 ft,

$$p_{3000} = 460 - \frac{40}{1290}(3110-3000) = \underline{456 \text{ psia}}$$

From 3000 to 14,000 feet (measured depth) the hole deviates 15 degrees from the vertical and the flowing pressure gradient at any point is given by

$$\frac{\Delta p}{\Delta L} = (1.456\text{x}10^{-5})(\cos 15^0)\frac{p}{z} + 778.982\,\frac{fz}{p}$$

$$= 1.406\text{x}10^{-5}\,\frac{p}{z} + 778.982\,\frac{fz}{p}$$

The pressure at 14,000 feet (measured depth) can be determined by starting with a pressure of 456 psia at 3000 feet, and numerically integrating down to 14,000 feet. The numerical integration is shown in Table IV. Interpolating to find the pressure at 14,000 ft,

$$p_{14,000} = 750 - \frac{20}{800}(14,051-14,000) = \underline{749 \text{ psia}}$$

The pressure drop due to the sudden enlargement at the top of the collars is computed using Eqs. (8.5) and (8.15) and Figs. 8.2, 8.3, and 8.8.

$$\Delta p = p_1 - p_2 = 0.0000316\,\frac{K}{Y^2}\,\frac{GTz}{p_1}\,\frac{Q^2}{A^2}$$

Table IV

p	$p \leq 0.1p$	p_{avg}	z	μ	R_e	f	$\Delta p/\Delta L$	ΔL	Depth
456	44	478	0.99	0.014	2,181,000	0.0138	0.029	1517	3,000
500	50	525	0.99	0.014	2,181,000	0.0138	0.028	1786	4,517
550	54	577	0.99	0.014	2,181,000	0.0138	0.027	2000	6,303
604	60	634	0.99	0.014	2,181,000	0.0138	0.026	2308	8,303
664	66	697	0.98	0.014	2,181,000	0.0138	0.025	2640	10,611
730	20	740	0.98	0.014	2,181,000	0.0138	0.025	800	13,251
750									14,051

$$(p_1-749)p_1 = \frac{(0.0000316)(0.55)(710)(10)^2}{[(\pi)(2.375)^2/(4)(144)]^2}\ \frac{Kz}{Y^2}$$

$$= 1304\ Kz/Y^2$$

The diameter ratio is

$$d_1/d_2 = 2.375/3.64 = 0.652$$

From Fig. 8.3 the resistance coefficient K is 0.32, so the expression becomes

$$(p_1-749)p_1 = (1304)(0.32)\ \frac{z}{Y^2} = 417\ \frac{z}{Y^2}$$

This expression is solved by iteration using Figs. 8.2 and 8.8 as shown in Table V to give a value of 749.55 psia, say 750 psia for p .

Table V

Trial	z(Fig.8.8)	Y(Fig.8.2)	p_1	Δp	$\Delta p/p_1$
1	1	1	749.56	0.56	0.0007
2	0.98	1	749.55	0.55	0.0007

Step 4. Pressure at the Bottom of the Drill Collars

Proceeding with the pressure change calculations in the drill collars, the Reynolds Number by Eq. (8.8) is

$$R_e = \frac{(1684)(0.55)(10)}{\mu(2.375/12)} = \frac{46797}{\mu}$$

For an absolute roughness of 0.00065 in and 2.375 in I.D. for the drill collars, the relative roughness is 0.000274. From 14,000 to 14,388 feet (measured depth) the flowing pressure gradient in the drill collars is calculated using Eq. (8.3), (8.5) and (8.6)

$$\frac{\Delta p}{\Delta L} = 1.406\text{x}10^{-5}\ \frac{p}{z} + 6587.438\ \frac{fz}{p}$$

The pressure at 14,388 feet (measured depth) is determined by starting with a pressure of 750 psia at 14,000 feet and numerically integrating down to 14,388 feet. The results of these numerical integrations are shown in Table VI.

Table VI

p	$\Delta p \leq 0.1p$	p_{avg}	z	μ	R_e	f	$\Delta p/\Delta L$	ΔL	Depth
750	20	760	0.98	0.015	3,119,800	0.0145	0.134	149	14,000
770	20	780	0.98	0.015	3,119,800	0.0145	0.131	153	14,149
790	20	800	0.98	0.015	3,119,800	0.0145	0.128	156	14,302
810									14,458

Interpolating, the pressure at the bottom of the drill collars is

$$p_{14,388} = 810 - \frac{(14,458-14,388)}{156}20 = \underline{801 \text{ psia}}$$

Step 5. Pressure Drop Through the Bit Nozzles

The final step is to compute the pressure drop across the bit. If sonic flow is taking place through the three 13/32 inch nozzles the downstream pressure can be computed using Eq. (8.18). The area A of the three bit nozzles is

$$A = \frac{(3)(3.14)(13/32)^2}{(4)(144)} = 0.0027 \text{ ft}^2$$

and the downstream pressure for 10 MMSCF/D is

$$p_s = \frac{(0.00789)(10)}{(0.0027)} \left[\frac{(0.55)(710)z}{(1.3)}\right]^{0.5}$$

$$p_s = 506\, z^{0.5}$$

Solving for p_s by iteration p_s = 501 psia.

Because this pressure is less than the actual downstream pressure (801 psia) the flow through the nozzles is subsonic. Since the flow through the nozzles is sub-

sonic the assumption that sonic flow occurred only at the safety valve is correct. The pressure drop across the bit can be computed using Eq. (8.15) and Figs. 8.4 and 8.5, assuming the flow rate through each nozzle is 10/3 MMSCF/D, or

$$(\Delta p)_j = (p_{bh}-801) = \frac{(1.049)(0.55)(710)}{(13/32)^4} \frac{1}{Y^2C^2} \frac{1}{p_{bh}} (10/3)^2$$

from which,

$$(p_{bh}-801)p_{bh} = \frac{167102}{Y^2C^2}$$

The diameter ratio

$$d_0/d_1 \simeq 0$$

From Fig. 8.4 the flow coefficient C for the nozzles is 0.985, hence

$$(p_{bh}-801)p_{bh} = \frac{172230}{Y^2}$$

This equation is solved by iteration as shown in Table VII using Fig. 8.5 for values of Y and gives a value of 1028 psia for pressure below the bit, i.e., the flowing bottom hole pressure.

Bottom Hole Pressures for Other Flow Rates

In order to determine the flow string resistance curve, the five step calculation procedure is repeated at incremental values of assumed flow rates and the

Table VII

Trial	Y(Fig.8.5)	p_{bh}	Δp	$\Delta p/p_{bh}$
1	1	977	176	0.18
2	0.89	1015	214	0.21
3	0.87	1023	222	0.22
4	0.86	1028	227	0.22

flowing bottom hole pressure calculated for each flow rate. Table VIII gives the calculated pressures on the upstream side of the safety valve, on the downstream side of the bit and finally the bottom hole pressure. Figure 8.9 is a plot of the flow string resistance curve for this example. It indicates a maximum possible flow rate of 79 MMSCF/D, i.e. when the flowing bottom hole pressure is equal to the estimated static formation pressure (8000 psia). There is, of course, a pressure drop in the formation as the gas flows to the bore hole. If, for example, the formation pressure drop is 2000 psi, the blowout rate is about 60 MMSCF/D.

Table VIII

Q MMSCF/D	Pressure Upstream of Safety Valve (psia)	Pressure Downstream of Bit (psia)	Bottom Hole Pressure (psia)
10	360	798	1028
20	725	1505	1984
30	1087	2207	2944
40	1450	3010	3969
50	1790	3710	4933
60	2130	4490	5950
70	2497	5277	6953
80	2860	6340	8156

8.9 Critique of Computational Procedure

The three parameters that are not known accurately in the calculation procedure are the absolute roughness of the drill pipe, the mean temperature of the flowing gas, and the gas gravity. To determine the sensitivity of the computational procedure to changes in these parameters, an error analysis was made at a flow rate of 60 MMSCF/D.

If the absolute roughness is taken as 0.0065 inches instead of 0.00065 inches (a 900% increase) the computed bottom hole pressure is 6844 psia instead of 5950 psia. This is a 15 per cent increase in bottom hole pressure.

If the mean temperature is taken as 150°F instead of 250°F (a 40% decrease) the computed bottom hole pressure is 5657 psia instead of 5950 psia. This is a 5 percent decrease in bottom hole pressure.

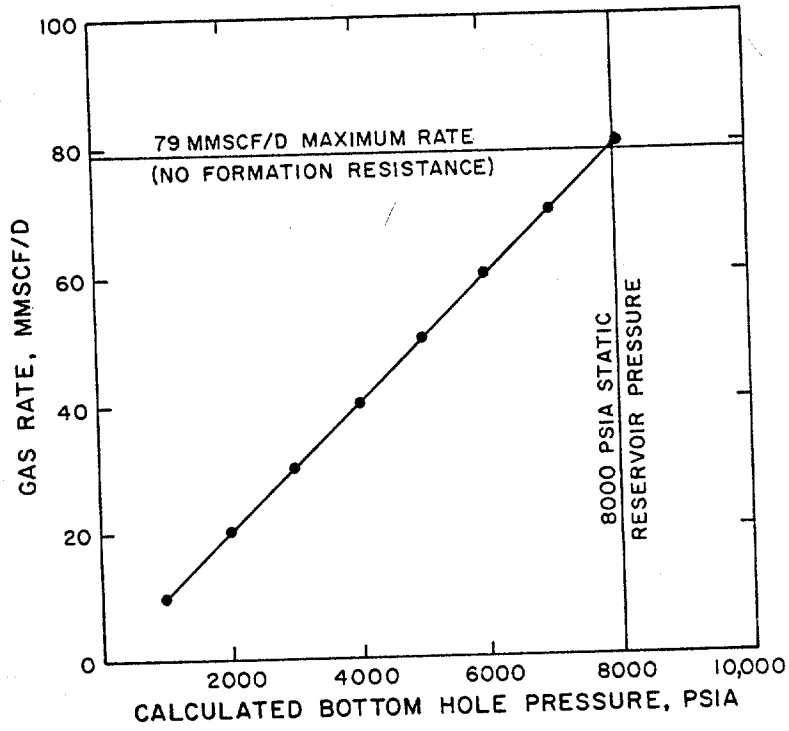

Fig. 8.9. Flow string resistance curve for the example of Secs. 8.7 and 8.8.

If the gas gravity is taken as 0.7 instead of 0.55 (a 27% increase) the computed bottom hole pressure is 6964 psia instead of 5950 psia. This is a 15 percent increase in bottom hole pressure.

The above analysis indicates the importance of an accurate determination of gas gravity. Though not as important as gas gravity, a reasonably accurate estimate of the mean temperature is needed. The least important parameter is the absolute roughness. Any reasonable estimate of absolute roughness should suffice.

Other factors that can affect the accuracy of the computational procedure are the presence of water and/or consensate. The presence of liquid will cause the bottom hole pressure determined using the computational procedure for a given flow rate to be too low. This means that the flow string resistance curve of Fig. 7.1 would shift to the right. Hence, for a given bottom hole pressure, the two-phase flow rate will be less than that for the case of dry gas.

The difficulty in determining an accurate geometry of the gas flow path can have a major effect on the accuracy of the computational procedure. This is

especially troublesome when flow is in the annulus or downhole tubulars have failed. Every effort should be made to make an accurate determination of the gas flow path.

8.10 Conclusions and Recommendations

If an accurate determination of the gas flow path has been made and reasonably accurate values of absolute roughness, mean temperature of the flowing gas, and the gas gravity are available, the computational procedure presented in this chapter should yield a flow string resistance that is within 20 percent of the actual value for a given flow rate. The procedure is very tedious and time consuming and should be programmed for use on a high-speed digital computer.

SECTION 9
CROSS PLOTS OF FORMATION AND FLOW STRING RESISTANCES

9.1 Introduction

The methods for calculating formation and flow string resistances have been discussed in Sections 7 and 8, respectively, where it was shown that crossplots of these two curves can be used to estimate blowout rates. It was pointed out in Sec. 7.4 that in most cases the major cause for uncertainty in the formation resistance curves was caused by uncertainties in formation permeability and thickness. The product of permeability and formation thickness is called formation capacity, or simply capacity. It is usually expressed in units of millidarcy-feet (md-ft). In this section special consideration is given to the effect of uncertainty in formation capacity on estimated blowout rates.

The theories and calculations of Sections 7 and 8 also provide the insight for the generalizations

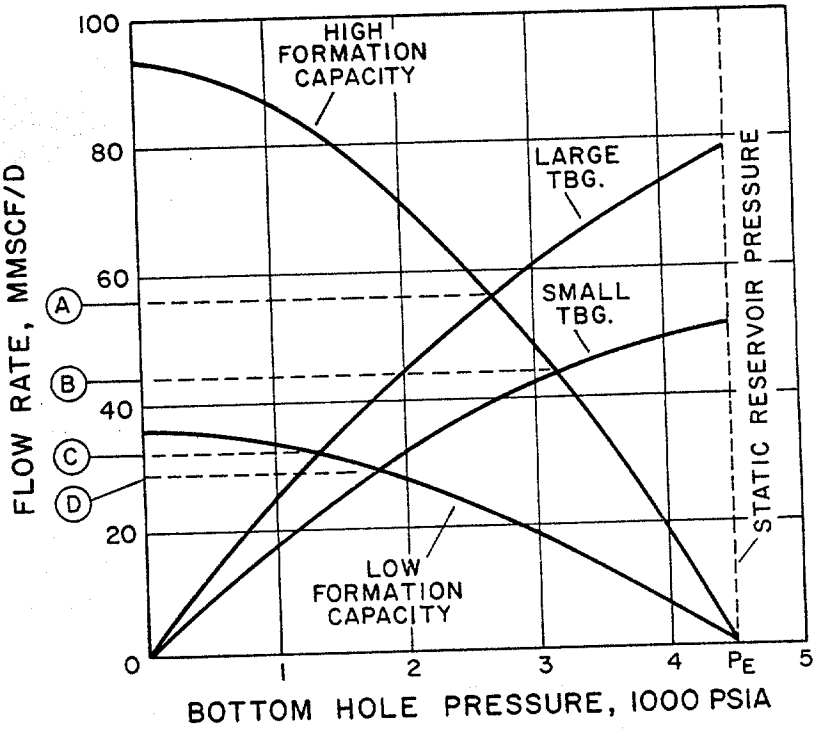

Fig. 9.1. Generalized formation and flow string resistance curves showing the effects of formation capacity and effective flow string diameter.

expressed by Fig. 9.1. As would be expected, maximum blowout rates occur for higher formation capacities and larger effective flow string diameters, point A. Conversely, also to be expected, low formation capacities and small effective flow string diameters cause lower blowout rates, as at point D.

Figure 9.1 should not be used except for generalization as indicated above. Instead, for each blowout similar curves should be calculated as shown in Sections 7 and 8.

9.2 Effect of Formation Capacity

The formation resistance curves of Fig. 9.2 are based on Eq. (7.2), the steady-state formula for gas flow. Equations (7.3), (7.4) and (7.7) may also be used, as appropriate. Example 9.1 shows the calculation of a point on the 2000 md-ft formation resistance curve, i.e., 233 MMSCF/D for a flowing bottom hole

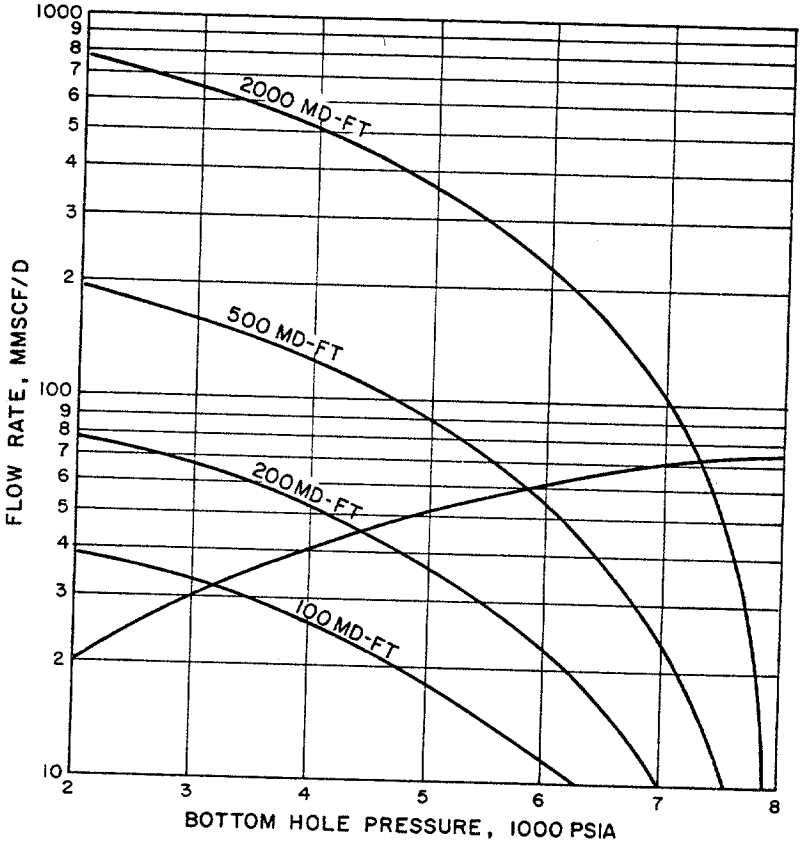

Fig. 9.2. Formation resistance curves for capacities of 100, 200, 500 and 2000 md-ft.

pressure of 6000 psia.

Example 9.1

Data:

8000 psia----------static reservoir pressure

6000 psia----------flowing BHP, assumed

0.024 cps----------gas viscosity at 6000 psia & 710°R

710°R----------reservoir temperature

1.11----------gas deviation factor at 6000 psia & 710°R

9.0----------$\ln r_e/r_w$

2000 md-ft----------formation capacity, assumed (2.0 darcy-ft)

$$q_{sc} = \frac{703\ kh(p_e^2-p_w^2)}{\mu T z\ \ln(r_e/r_w)}$$

$$q_{sc} = \frac{703x2.0x(8000^2-6000^2)}{0.024x710x1.11x9}$$

$$q_{sc} = \underline{233\ MMSCF/D}$$

The flow string resistance curve of fig. 9.2 is the one calculated for the base condition of the example of Secs. (8.7) and (8.8) and shown in Fig. 8.9. Because of the small uncertainty in the flow string resistance curve, at least with respect to the large uncertainty in the formation resistance curve, only one flow string resistance curve is shown in Fig. 9.2.

Figure 9.2 shows the uncertainty in the estimated blowout rate caused by uncertainty in the formation capacity. However, it is noted in this example that a twenty-fold range in formation capacity (100 to 2000 md-ft) causes only a little more than a two-fold change in the blowout rate, i.e., from 72 MMSCF/D for 2000 md-ft to 32 MMSCF/D for 100 md-ft. In many, if not most cases, the uncertainty in the formation capacity should be considerably less than a twenty-fold range, certainly where there are producing wells in the reservoir, drilled either prior to or after the blowout.

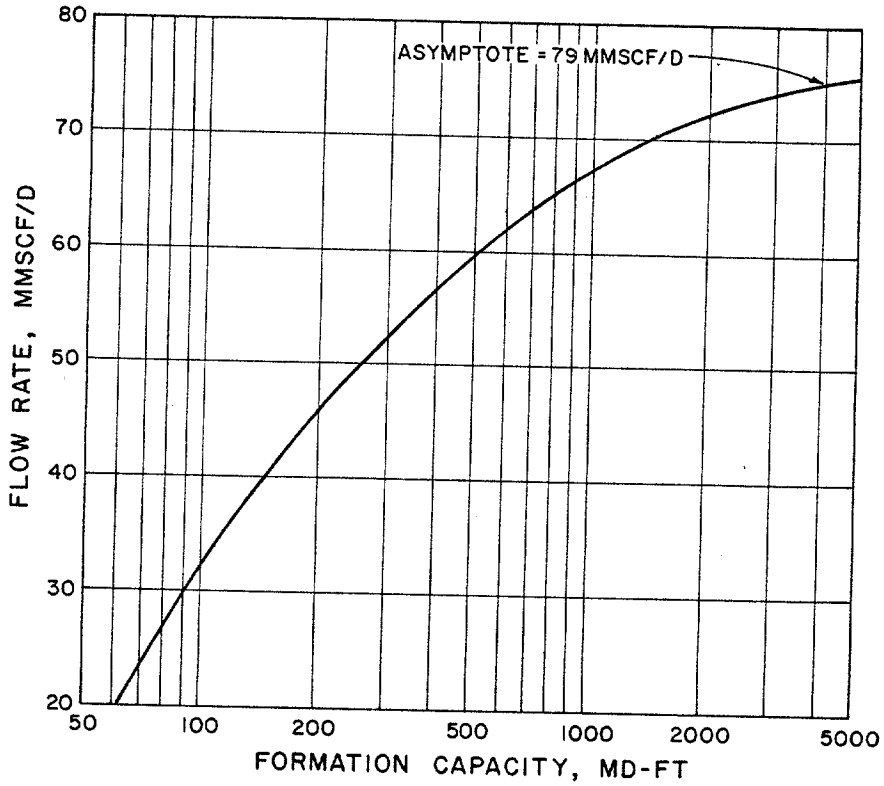

Fig. 9.3. Blowout rate as a function of formation capacity.

Figure 9.3 is a cross-plot of the data of Fig. 9.2, and further illustrates the effect of formation capacity in the estimated blowout rate, for a particular flow string resistance curve.

9.3 Cratered Wells and Underwater Blowouts

Of the several methods presented only that of cross-plotting calculated formation and flow string resistances does not depend upon some sort(s) of measurement(s). This method is therefore applicable to cratered wells and underwater blowouts but with the additional uncertainty in the pressure at the outlet end of the flow string, now no longer atmospheric. Use of the method assuming atmospheric pressure at the outlet will provide estimates of the maximum flow rate. Also, as explained below, considerable increases in outlet pressure above atmospheric pressure cause relatively small reductions in the flow rates.

For gas flow in vertical pipes Smith's formula (Ref. 9.1) may be expressed as

$$q_{sc} = C[p_w^2 - e^S p_o^2]^{0.5} \quad \ldots\ldots\ldots\ldots\ldots\ldots\ldots\ldots (9.1)$$

The following application of Eq. (9.1) will serve to define its terms and units.

Data:

X = 8000 feet, elevation difference between pressure points p_w and p_o.

p_e = 4000 psia, external reservoir pressure

T = 620^0 Rankine, average temperature in the flow string.

z = 1.00, average gas deviation factor for gas in the flow string.

G = 0.70, gas specific gravity (air = 1).

$S = 0.0375\ G\ X/T\ z$

$S = 0.0375 \times 0.70 \times 8000/620 \times 1.00$

$S = 0.34$ and $e^S = 2.718^{0.34} = 1.40$

Case I

p_e = 4000 psia

p_w = 3000 psia, flowing bottom hole pressure

p_o = 14.7 psia, flow string outlet pressure

$q_{sc} = C[3000^2 - 1.40 \times 14.7^2]^{0.5}$

$q_{sc} = 3000\ C$

and for p_o = 1,000 psia

$q_{sc} = C[3000^2 - 1.40 \times 1000^2]^{0.5}$

$q_{sc} = 2757\ C$

Flow Reduction $= \frac{3000 - 2757}{3000} \times 100 = 8\%$

Case II

p_e = 4000 psia

p_w = 2000 psia

p_o = 14.7 psia

$q_{sc} = C[2000^2 - 1.40 \times 14.7^2]^{0.5}$

$q_{sc} = 2000\ C$

and for p_o = 700 psia

$q_{sc} = C[2000^2 - 1.40 \times 700^2]^{0.5}$

$q_{sc} = 1820\ C$

Flow Reduction $= \frac{2000 - 1820}{2000} = 9\%$

The above example illustrates the relatively small effect a substantial increase in outlet pressure has on the flow rate. It is noted that a blowout from a sea floor assembly at a depth of 1500 feet has an outlet pressure near 700 psia. For a more precise evaluation of the effect of outlet pressure on flow rate, the method of Section 8 should be used.

SECTION 10
SUGGESTIONS FOR FURTHER INVESTIGATION

10.1 Introduction

The foregoing sections have presented the state of the art for determining gas flow rates and vented volumes during blowouts. Such presentations naturally evoke thought on further work which might improve the determinations. Suggestions for further work are of two kinds: those which seek to improve or refine current technology and those which propose new technology, either innovative or adapted from other areas of technology.

All of the methods presented in this report have been developed for calculations on engineering problems other than the blowout problem, and have therefore received periodic improvement and refinement. In any event the precision of these methods as applicable to the gas well blowout problem is more than adequate because of the complex nature of the problem and because of the unavailability and/or imprecision of some of the data. Therefore, improvement in the determination of vented gas volumes lies in the development of new technology.

10.2 Suggestions for New Technology

Among the suggestions received or conceived during these investigations there are four which appear to merit further consideration. No claim is made for an in-depth look into the feasibility of these suggested methods, which are briefly discussed in the following.

10.2.1 Heat Flux

Where blowing gas wells have been ignited, assuming complete combustion, the heat flux from the well is the product of the gas flow rate and the heating value of the gas. If the heat flux can be measured, in BTU/day for example, then by dividing into it the measured or estimated heating value of the gas, in BTU/SCF, the flow rate in SCF/day is obtained.

The heat flux is a combination of radiation and convection. It is possible that aerial surveys above and around the burning plume using suitable measuring devices could provide data for determining the total heat flux. To handle the problem of incomplete

combustion it is suggested that suitably taken samples can be analyzed for carbon, carbon monoxide, carbon dioxide and hydrocarbons.

The most attractive feature of this proposed method is that it can be applied to all burning gas wells and, more important, it does not require operations at or near the well location. It is therefore of interest for offshore blowouts where operations at or near the wellhead are usually precluded.

10.2.2 Bullet Trajectory

A suggestion of the possible use of bullet trajectory was received from the Research Program, Branch of Marine Oil and Gas Operations of the Geological Survey. The basic idea is similar to that of estimating the blowout rate from the deflection of a sledge hammer passed through the flow stream (Section 1.2).

In this proposed method, the basic measurement would by the angular deflection of a bullet of known velocity when fired through the center of the flow stream. Although some experimentation might be required to develop this method, it is likely that there is a great deal in the relevant literature which would shed considerable light on this measurement.

This method is also attractive in that it does not require operations at or very near the well head. Although apparently less adaptable to offshore gas blowouts than those on land, innovative technology might prove otherwise.

10.2.3 Other Measurement Technology

Consideration has been given to other measurement technology which involve the reaction of a sensing element placed in the flow stream. This idea envisions, for example, a heavy yoke containing a wire or rod which could be placed in the flow stream on the end of long shaft attached to a piece of heavy equipment such as a bulldozer.

Although this proposed method involves operations near the blowing well, presumably measurements would not take very much time. For offshore blowouts the method would be limited to control measures in which there is a barge or platform from which to operate a bulldozer.

10.2.4 Indirect Measurements

It is suggested that there are more or less precise correlations between the size and shape of a burning gas plume and its rate of flow. Other correlations are believed to exist between the flow rate and the sonic emissions at the well, i.e., the sound level in decibels and/or the frequency distribution of the sound. A third suggestion is a correlation between the flow rate and the air velocity and/or pressure distribution in the vicinity of a blowing well.

Unlike the method suggested in Sec. 10.2.3, these indirect methods do not involve the insertion of a device into the flow stream. However, although suitable measurement equipment (photography, sound meters, anemometers, pressure sensors) exist, considerable effort is anticipated in establishing the necessary correlations, assuming reasonably reliable ones do exist.

10.3 Gas-Condensate and Oil Well Blowouts

It is implicit in this report that the methods presented apply only to dry gas production, i.e., that in which no liquid hydrocarbon phase develops prior to entering the atmosphere. Neither does it apply to dry gas accompanied by water production. If the methods are used for gas-condensate blowouts or gas and gas-condensate blowouts accompanied by water production, the calculated rates and vented volumes will be larger than actual. Of course, the methods do not apply to oil well blowouts.

It is suggested that these investigations be extended to include gas-condensate and oil well blowouts.

References

2.1 Craft, B.C. and M.F. Hawkins: Applied Petroleum Reservoir Engineering, Prentice-Hall, Inc., Englewood Cliffs, NJ (1959) 16-47.

2.2 Ibid., 47-48.

3.1 Lichty, L.D.: "Measurement, Compression and Transmission of Natural Gas," John Wiley & Sons, Inc. (1924).

3.2 Rawlins, E.L. and M.A. Schellhardt: "Back-Pressure Data on Natural Gas Wells and Their Application to Production Practices," U.S.B.M. Monograph 7.

3.3 Chandler Engineering Company, 7707E 38th Street, Tulsa, Oklahoma, (918) 627-1740.

3.4 Katz, D.L., et al: "Handbook of Natural Gas Engineering," McGraw-Hill (1959).

3.5 The Pacific Coast Gas Association: "Gas Engineering Handbook," McGraw-Hill (1934).

3.6 Rowse, W.C.: "Pitot Tubes for Gas Measurement," Transactions of the ASME, Vol. 35.

4.1 API Recommended Practices for Blowout Prevention, American Petroleum Institute, API RP 53 (February, 1976).

4.2 Shapiro, Asher H.: The Dynamics and Thermodynamics of Compressible Fluid Flow," Vol. I., The Ronald Press Co., New York.

4.3 Katz, D.L., et al: Handbook of Natural Gas Engineering, McGraw-Hill, New York (1959).

4.4 Nisle, R.G. and F.H. Poettmann: "Calculation of Flow and Storage of Natural Gas in Pipe," Petroleum Engineer, 27(1): D14; 27(2): C36; 27(3): D37 (1955).

4.5 Moody, L.F.: "Friction Factors for Pipe Flow," Trans. ASME, Vol. 66 (1944).

4.6 Crane Company: "Flow of Fluids Through Valves, Fittings and Pipe," Technical Paper No. 410.

4.7 Standing, M.B. and D.L. Katz: "Density of Natural Gases," Trans. AIME (1942) 146.

4.8 Brown, G.B., D.L. Katz, G.B. Oberfell and R.C. Alden: Natural Gasoline and Volatile

Hydrocarbons, Natural Gasoline Association of American, Tulsa, Oklahoma (1948) 44.

4.9 Edmister, W.C.: "Application of Thermodynamics to Hydrocarbon Processing," Petroleum Engineer, (1948-49).

5.1 Newendorp, P.D.: Decision Analysis for Petroleum Exploration, Petroleum Publishing Co., Tulsa, Oklahoma (1975) 651.

6.1 Rawlins, E.L. and M.A. Schellhardt: Back Pressure Data on Natural Gas Wells and Their Application to Production Practices, U.S. Bureau of Mines, Monograph 7.

6.2 Craft, B.C. and M.F. Hawkins: Applied Petroleum Reservoir Engineering, Prentice Hall, Inc., Englewood Cliffs, NJ (1959).

6.3 Elenbaas, J.R. and D.L. Katz: "A Radial Turbulent Flow Formula," Trans. AIME (1948) 186, 36.

6.4 Graham, J.R. and W.E. Boyd: "An Analysis of Changing Backpressure Test Curves from Some Gulf Coast Area Gas Wells," J. Pet. Tech., (Dec., 1967).

6.5 Interstate Oil Compact Commission: Manual of Back Pressure Testing of Gas Wells.

6.6 Cullender, M.H.: "The Isochronal Performance Method of Determining Flow Characteristics of Gas Wells," Trans. AIME, Vol. 204, (1955) 137.

6.7 Alberta Oil and Gas Conservation Board: Theory and Practice of Testing Gas Wells (1955).

7.1 Craft, B.C. and M.F. Hawkins: Applied Petroleum Reservoir Engineering, Prentice-Hall, Inc., Englewood Cliffs, NJ (1959) 326.

7.2 Ibid., 17-22, 264-266.

7.3 Ibid., 333.

7.4 Ibid., 289.

7.5 Ibid., 269-272.

7.6 Ibid., 295-307.

8.1 Poettman, F.H.: "The Calculation of Pressure Drop in the Flow of Natural Gas Through Pipe," Transactions, AIME, Volume 192 (1951).

8.2 Cullender, M.H. and R.V. Smith: "Practical Solution of Gas-Flow Equations for Wells and Pipelines with Large Temperature Gradients," Transactions, AIME, Volume 207 (1956).

8.3 Colebrook, C.F., "Turbulent Flow in Pipes, with Particular Reference to the Transition Region Between the Smooth and Rough Pipe Laws," J. Inst. Civil Engrs. (London) Volume II (1938-1939).

8.4 Crane Company: "Flow of Fluids Through Valves, Fittings, and Pipe," Technical Paper No. 410 (1967).

8.5 Cornish, R.E.: "The Vertical Multiphase Flow of Oil and Gas at High Rates," J. Pet. Tech. (July, 1976).

9.1 Smith, R.V.: "Determining Friction Factors for Measuring Productivity of Gas Wells," Trans. AIME, 189, 73 (1950).

☆ U.S.GOVERNMENT PRINTING OFFICE:1980-671-115/72